NASA/TM–20250003346

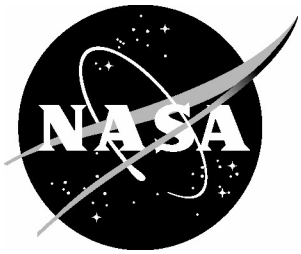

Perceived Level of Sonic Boom Noise: Recommended Computation Methods, Rationale, and a Minor Modification

Jacob Klos
Langley Research Center, Hampton, Virginia

April 2025

NASA STI Program . . . in Profile

Since its founding, NASA has been dedicated to the advancement of aeronautics and space science. The NASA scientific and technical information (STI) program plays a key part in helping NASA maintain this important role.

The NASA STI program operates under the auspices of the Agency Chief Information Officer. It collects, organizes, provides for archiving, and disseminates NASA's STI. The NASA STI program provides access to the NTRS Registered and its public interface, the NASA Technical Reports Server, thus providing one of the largest collections of aeronautical and space science STI in the world. Results are published in both non-NASA channels and by NASA in the NASA STI Report Series, which includes the following report types:

- TECHNICAL PUBLICATION. Reports of completed research or a major significant phase of research that present the results of NASA Programs and include extensive data or theoretical analysis. Includes compilations of significant scientific and technical data and information deemed to be of continuing reference value. NASA counter-part of peer-reviewed formal professional papers but has less stringent limitations on manuscript length and extent of graphic presentations.

- TECHNICAL MEMORANDUM. Scientific and technical findings that are preliminary or of specialized interest, e.g., quick release reports, working papers, and bibliographies that contain minimal annotation. Does not contain extensive analysis.

- CONTRACTOR REPORT. Scientific and technical findings by NASA-sponsored contractors and grantees.

- CONFERENCE PUBLICATION. Collected papers from scientific and technical conferences, symposia, seminars, or other meetings sponsored or co-sponsored by NASA.

- SPECIAL PUBLICATION. Scientific, technical, or historical information from NASA programs, projects, and missions, often concerned with subjects having substantial public interest.

- TECHNICAL TRANSLATION. English-language translations of foreign scientific and technical material pertinent to NASA's mission.

Specialized services also include organizing and publishing research results, distributing specialized research announcements and feeds, providing information desk and personal search support, and enabling data exchange services.

For more information about the NASA STI program, see the following:

- Access the NASA STI program home page at http://www.sti.nasa.gov

- E-mail your question to help@sti.nasa.gov

- Phone the NASA STI Information Desk at 757-864-9658

- Write to:
  NASA STI Information Desk
  Mail Stop 148
  NASA Langley Research Center
  Hampton, VA 23681-2199

NASA/TM–20250003346

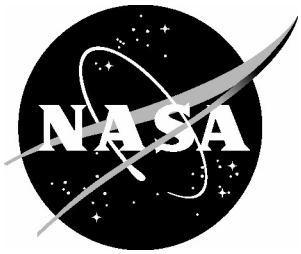

Perceived Level of Sonic Boom Noise: Recommended Computation Methods, Rationale, and a Minor Modification

Jacob Klos
Langley Research Center, Hampton, Virginia

National Aeronautics and
Space Administration

Langley Research Center
Hampton, Virginia 23681-2199

April 2025

Available from:

NASA STI Program / Mail Stop 148
NASA Langley Research Center
Hampton, VA 23681-2199
Fax: 757-864-6500

This page intentionally left blank.

Table of Contents

Table of Figures

Table of Tables

List of acronyms and symbols

dB	Unit, decibels
e_i	Energy of the i^{th} narrow band bin
F	Weighting factor in the total loudness computation
f_i	Frequency of the i^{th} narrow band bin
$f_{i,edges}$	Edge frequencies of the i^{th} narrow band bin
$f_{o,c}$	Center frequency of the o^{th} one-third-octave band
$f_{o,l}$	Lower edge frequency of the o^{th} one-third-octave band
$f_{o,u}$	Upper edge frequency of the o^{th} one-third-octave band
Hz	Unit, hertz
i	An index
LCASB	Loudness Code for Asymmetric Sonic Booms (deprecated software)
L_i	Level of the i^{th} narrow band bin
N	A count
NASA	National Aeronautics and Space Administration
NFFT	Number of points in a discrete-time waveform
NOM	Narrow-band Octave-band Metrics (current metrics software)
OTOB	One-third-octave band
o	An index
P	A variable, level, in decibels
PL	Perceived Level
P5	5^{th} percentile of a dataset
P50	Median (50^{th} percentile) of a dataset
P95	95^{th} percentile of a dataset
P_{ref}	Reference pressure, 4E-10 Pa^2
S	A variable, loudness, in sone
S_i	Loudness in the i^{th} one-third-octave band
S_m	Maximum loudness
S_t	Total loudness
SPL	Sound pressure level
Δ_{P95-P5}	Span between the 5^{th} and 95^{th} percentile of a dataset
Δf	Bin width of a narrow band spectrum

Abstract

Analysts face algorithmic choices when writing software to compute the Perceived Level (PL) noise metric. This document contains algorithmic recommendations for computing the PL of a sonic boom waveform. For the four main computational steps, the recommended algorithm and a less accurate alternative are introduced. Rationale for each recommendation is provided by comparing levels returned by the recommended algorithms versus the alternate algorithms while discussing the expected accuracies of each. Algorithm evaluations are performed using as input predicted shaped sonic boom waveforms for the X-59 aircraft and background noise waveforms measured in a community. A minor addition to a data table used to weight the loudness spectrum while summing to total loudness is also described here; that weighting is a precursor to the Perceived Level value. This table addition, which fills a gap at low sound levels, should increase the accuracy of PL values for quiet background noise and evanescent waves in the Mach cutoff shadow region.

I. INTRODUCTION

Transportation noise regulations are typically based on the loudness of the vehicle noise to which communities are exposed. Perceived Level (PL) [1, 2] is commonly used to quantify the loudness level of sonic boom noise produced by supersonic aircraft. It is also one of several noise metrics [3] that NASA will evaluate during future community testing using the purpose built X-59 aircraft [4, 5, 6]. Dose-response data from those tests may enable regulators to change the current prohibition of commercial supersonic flight to a noise-based certification standard. If so, those dose-response data will inform the noise metric type and the loudness level that is chosen by regulators to regulate shaped sonic boom noise that is produced by future commercial overland supersonic aircraft.

A flow chart of the Perceived Level computation is provided in Figure 1. The algorithms that analysts must use for these computations are more complex than other noise metrics used to characterize perception of sonic boom loudness – like weighted sound exposure level (SEL) – for three reasons:

1) A one-third-octave band sound pressure level (SPL) spectrum is needed as input,
2) The weighting function used to convert the input SPL spectrum to a loudness spectrum varies with both frequency and sound level, and
3) The summation of the loudness spectrum to total loudness is also weighted.

Unfortunately, there are no standardized methods for computing the weighting values used in items 2) and 3), which may lead programmers to choose an algorithm that is less accurate than an alternative. For example, older versions of NASA software to compute PL utilized pre-computed equal loudness contours that are discussed by Stevens [2] as an interpolant to approximate item 2 above. However, all current NASA software uses a closed form, geometry-based method documented by Jackson and Leventhall [7] to determine these weightings since that method is expected to be more accurate than interpolation. Additionally, differences are possible in the SPL spectrum calculation – item 1) above – even if methods used to compute it conform to available standards. For example, a range of filter skirt and pass band gain is typically permissible (see Ref. [8] section 4.4).

Consequently, these and other computational complexities may lead to variations in the computed PL value of a shaped sonic boom that depend on the software implementation. Such variation is undesirable if PL is to be used in future regulations as a standard measure of sonic boom loudness. Additionally, algorithm-induced variation in PL is not quantified within the existing literature for shaped sonic boom noise, so sources, magnitudes, and significances of expected variations are currently not known. Quantifying the sources of variation and identifying the algorithms that are expected to give accurate, well-converged results is the goal of this report.

The next section reviews four main computational steps to compute PL of a discrete-time waveform (Figure 1), where that waveform may be a sonic boom from a field recording, a simulated sonic boom, or background noise from a field recording. Those four main computational steps are:

1) Computing the one-third-octave band sound pressure level spectrum from the discrete-time waveform (in Subsection II.A),
2) Computing the loudness spectrum from the one-third-octave band spectrum (in Subsection II.B),
3) Converting between level and amplitude (in Subsection II.C), and
4) Summation of the loudness spectrum to find total loudness (in Subsection II.D).

Subsection II.D also documents a minor modification to a data table provided by Stevens since the table was determined to be incomplete at very low sound levels. Additionally, the preferred algorithm for each step is identified in each subsection in II. Then, the waveforms and error analyses that inform the rationale for those recommendations are documented in Sections III and IV, respectively. Specifically, the errors in PL values for shaped sonic booms and background noise are compared in Sections IV.A to IV.F for the different algorithms identified in II.

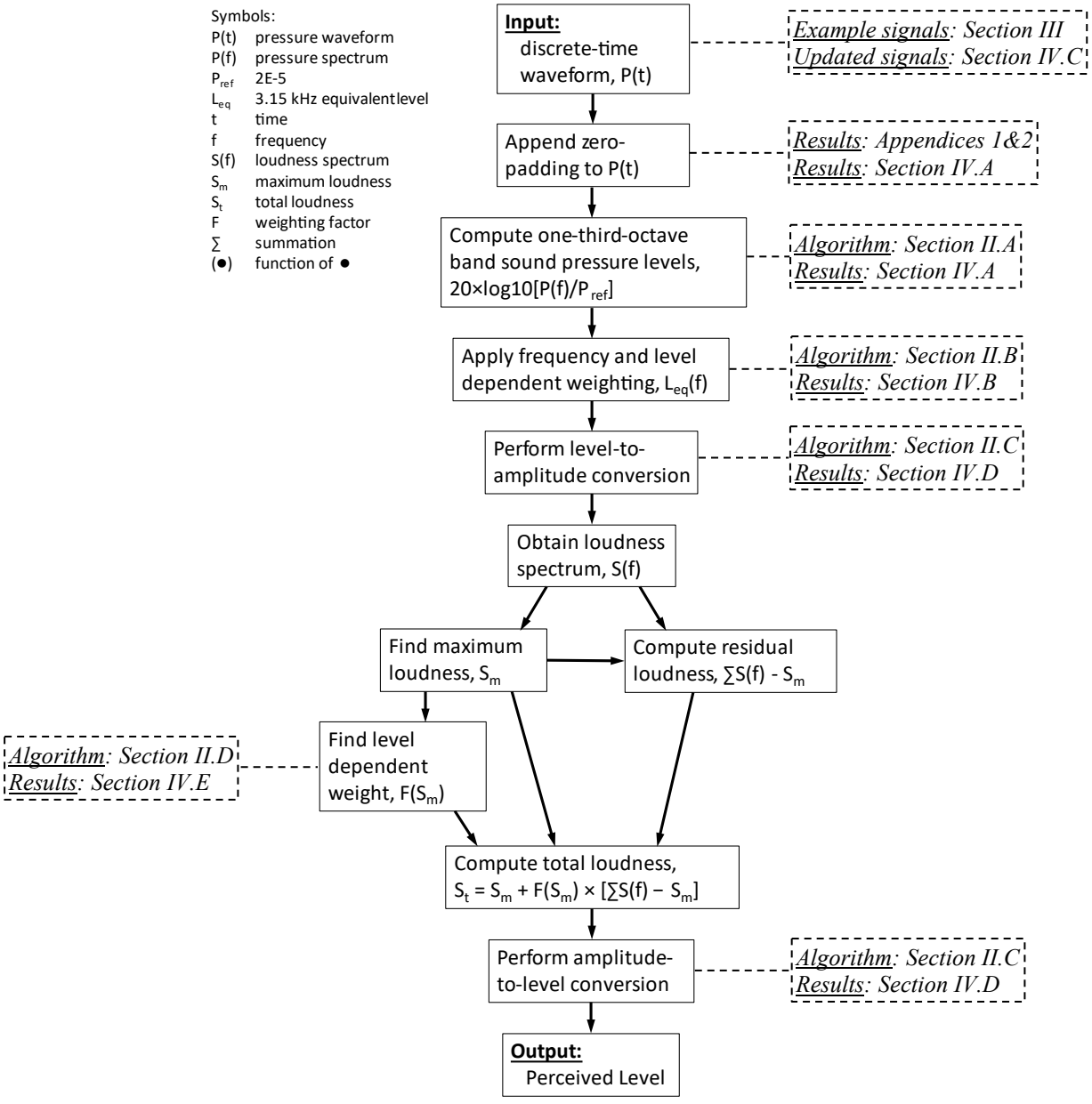

Figure 1: Flow chart of Perceived Level steps and --- [*discussion location*].

II. OVERVIEW OF ALGORITHM OPTIONS AND RECOMMENDATIONS

The subsections below summarize two algorithm choices available for each computational step (Figure 1), based on information from the literature and known software implementations. Each subsection identifies the higher-accuracy method that is recommended for future use. All recommended algorithms are implemented in the sonic boom metrics software named NOM (Narrow-band Octave-band Metrics)[1]. The source code for NOM may be requested at the link provided in footnote 1.

A. Computing the one-third-octave band sound pressure level spectrum

Given a sonic boom waveform, analysts must first compute the one-third-octave band spectrum of the pressure waveform. Two computation methods are considered here:

- Compute the narrow band spectrum using a discrete Fourier transform then sum the narrow band spectral bins while assuming rectangular-shaped one-third-octave bands and proportionally apportioning narrow-band bins that overlap band edges.
- Use discrete-time infinite impulse response one-third-octave band filters that have finite-slope, analog-filter-like skirt behaviors that meet the requirements of Ref. [8] section 4.4 (for example).

While both methods conform to the performance tolerances defined in Ref. [8], rectangular filters well approximated by the first item above are the ideal response that the discrete-time filters attempt to mimic. Thus, it is sensible to recommend the first method since it should more closely match the ideal rectangular filter behavior.

The error observed in computed loudness levels, PL, of shaped sonic booms and background noise signals are discussed in Section IV.A below to contrast the methods listed above. The effects of zero-padding duration and filter order are also discussed in that section, where it is shown that results for a high order filter and long zero padding converge to the narrow band summation results that are less computationally expensive. Thus, the first method – narrow band summation – is recommended when computing one-third-octave band levels and is the method implemented in the NOM metrics codes[1]. The deprecated metrics code LCASB[2] (Loudness Code for Asymmetric Sonic Booms) also uses this method.

The narrow band summation algorithm is described in Appendix 1, including a pictorial example illustrating the bin apportioning approach with example computations. Additionally, convergence behavior of one-third-octave band levels and Perceived Level values across a set of 3,000 shaped boom waveforms is evaluated in Appendix 2 as zero-padding duration is varied while using the narrow band summation method to compute the band levels. Those results demonstrate good convergence across one-third-octave bands from 1.25 Hz to 20 kHz even when using relatively short duration signals. For example, levels for zero-padded signals that are about 2.7 seconds in duration are compared to those of zero-padded signals that are about 22 seconds in duration in Appendix 2. Perceived

[1] Sonic boom metrics software, NOM, can be found by searching for the software case number LAR-20093-1 at the online software catalog website at https://software.nasa.gov/search.

[2] LCASB is deprecated sonic boom metrics software that was released under software case number LAR-16954-1. Use of LCASB is no longer recommended since it is no longer supported and does not include many recent updates that are found in NOM, see footnote 1. End users of LCASB are encouraged to switch to NOM.

Level is also well converged in all cases. The error results presented in Appendix 2 demonstrate convergence to within a few hundredths of a dB in all one-third-octave bands and in the Perceived Level values. This convergence behavior is adequate for the purpose of Section IV.A below, which will use the narrow band summation method to compute true levels that will be used to evaluate discrete-time one-third-octave band filter performance.

B. Computing the loudness spectrum

The loudness spectrum is an intermediate quantity computed from the one-third-octave band SPL spectrum. This computation applies weighting functions to convert from sound pressure to loudness, where the weighting shapes vary with both frequency and sound level. Stevens tabulated the weighting data required for this step in Appendix A of Ref. [2] and plotted those data as equal loudness contours. However, those data are provided at relatively coarse, discrete intervals and with limited precision – generally three or four significant figures. Thus, direct use of Stevens' weighting data requires interpolation within the cited values to find specific loudness values. Such interpolation may lead to inaccuracies given the coarseness and limited precision of the data. As an alternative, Jackson and Leventhall [7] documented geometry-based algorithms to convert an input SPL spectrum to a loudness spectrum. Use of these closed-form, geometric algorithms to apply the frequency and level dependent weighting functions should be more accurate than interpolating Stevens' tabulated data since the geometric method should be exact.

Differences between the interpolation and the geometric methods for computing PL are discussed later in Section IV.B. The Jackson and Leventhall method is implemented in the NOM[1] and LCASB[2] metrics codes and is preferred over the interpolation method when computing the loudness spectrum. Some older, deprecated versions of PCBoom software have instead used interpolation of Stevens' table data, where the algorithm taken from that software is discussed and evaluated in Section IV.B to quantify errors when using interpolation. Importantly, supported software versions of PCBoom [9] and NOM[1] utilize the Jackson and Leventhall method.

C. Converting between level and amplitude

When using the Jackson and Leventhall method to find the loudness spectrum, conversion from level, P in decibels, to loudness amplitude, S in sone, is required prior to the summing the spectrum to find total loudness. The reciprocal equation is also needed when converting the total loudness, in sone, to the Perceived Level value, in decibels. One equation given by Stevens [2] is

$$P = 32 + 9log_2(S), \text{for } S \geq 1 \text{ sone}, \quad (1)$$

and the reciprocal is

$$S = 2^{(P-32)/9}, \text{for } P \geq 32 \text{ dB}. \quad (2)$$

Although these equations have been implemented in some computational codes for conversions at all sound levels, for instance in LCASB[2] and those based on Ref. [10], they are only valid for levels, P, above 32 dB (and for amplitudes, S, above 1 sone). They will

deviate from proper relationship at lower sound levels. Additionally, Stevens [2] suggests using them for conversion between quantities S and P at levels as low as 20 dB. However, these two equations are approximate at all levels between −3 and 32 dB, and this approximation worsens in the lower portion of that range. Consequently, they should only be used for levels above 32 dB (amplitudes above 1 sone).

A closed form equation for conversion between level and amplitude in the lower range, −3 to 32 dB (0 to 1 sone), is

$$P = 10log_{10}\left((10^{3.2} - 10^{-0.3})S^3 + 10^{-0.3}\right), \text{for } 0 < S < 1 \text{ sone}, \quad (3)$$

and the reciprocal equation is

$$S = \left(\frac{10^{P/10} - 10^{-0.3}}{10^{3.2} - 10^{-0.3}}\right)^{1/3}, \text{for } -3 < P < 32 \text{ dB}. \quad (4)$$

These are roughly equivalent to equation (5) in Ref. [2], but the equations above are defined with higher precision. While Eqs. (3) and (4) are exact for P values ranging from −3 to 32 dB (at amplitudes, S, between 0 and 1 sone), Eqs. (1) or (2) should still be used at higher levels and amplitudes – above 32 dB and 1 sone, respectively – since (1) and (2) are exact in that range while Eqs. (3) and (4) are not. Importantly, a level of −3 dB corresponds to a loudness amplitude of 0 sone, and negative loudness amplitude values are nonsensical, so proper application of Eqs. (1) through (4) will cover the entire range of level/amplitude pairs that one may encounter. Section IV.D compares PL values computed using Eqs. (1) and (2) for all levels with PL values found using proper application of Eqs. (1) through (4).

The NOM[1] code implements the level appropriate combination of Eqs. (1) through (4) as described above. Likewise, the PCBoom software implements the above conversions properly. NOM[1] is preferred over LCASB[2] when computing PL since LCASB does not properly convert between level and amplitude, which may affect the PL value returned by LCASB for very quiet sounds. The LCASB[2] software is not actively maintained so it will not be updated to address this inaccuracy.

D. Summation of the loudness spectrum

When computing PL, the loudness spectrum is summed to find the total loudness, S_t, using the summation equation

$$S_t = S_m + \mathrm{F} \times (\sum S_i - S_m), \quad (5)$$

where S_m is the loudness value of the one-third-octave band with the highest loudness, the residual quantity $(\sum S_i - S_m)$ is the sum of the loudness spectrum across all i one-third-octave bands but excluding the band with the highest loudness, S_m, and F is a weighting factor that depends on the value of S_m. Data from the lookup table in Appendix B of Ref. [2] must be interpolated to find the weighting value, F, in Eq. (5) using S_m as the independent variable. However, the data table is incomplete at very low sound levels since the interpolant, F(S), is not tabulated in Ref. [2] for loudness amplitudes, S, below 0.181 sone.

A minor modification has been made to the table found in Appendix B of Ref. [2] for application at low loudness amplitudes. Specifically, points (0.0, 0.0) and (0.113, 0.0) shown in Figure 2 (red circles) are prepended to the existing points in the table (Figure 2, blue triangles). The new point at (0.113, 0.0) was determined by linearly extrapolating the existing first two points in Appendix B of Ref. [2] (triangles) to find their x-intercept. The point at (0.0, 0.0) was chosen as the first point in the updated table since negative loudness values, S, are nonsensical. The weighting factor, F, for loudness amplitudes between these points should be found using interpolation and will fall along the dashed line segments in Figure 2 when using linear interpolation. Thus, the frequency band summation term when the maximum loudness amplitude is between 0 and 0.113 sone will not contribute to the total loudness calculation since the weighting factor, F, will be zero in these cases. The band summation term will contribute to the total loudness only when the maximum loudness amplitude, S_m, is greater than 0.113 sone since F will always be nonzero in that case.

The first five points in the updated interpolation table when summing the loudness spectrum to find total loudness are listed in Table 1. The points following the first two are a concatenation of the list from Appendix B of Ref. [2]. Additionally, F(S) values at loudness amplitudes, S, between 0 and 1 sone are plotted in Figure 3 to illustrate the behavior of the two new points relative to the original points from Appendix B of Ref. [2].

Table 1: List of the first five points in updated weighting table.

Loudness, sone	**Weighting, F**	**Data source**
0.000	0.000	New point from Figure 2
0.113	0.000	New point from Figure 2
0.181	0.100	First point listed in Appendix B of Ref. [2]
0.196	0.122	Second point listed in Appendix B of Ref. [2]
0.212	0.140	Third point listed in Appendix B of Ref. [2]
⋮	⋮	Remaining points listed in Appendix B of Ref. [2]

The Perceived Level value below which the effect of the additional points may become important occurs for a spectrum where the loudness of all one-third-octave bands is 0.181 sone, which corresponds to the PL value of the 0.181 equal loudness contour, or 30.70 dB PL. To demonstrate the effect, the PL value of the 0.180 equal loudness contour – a spectrum where all one-third-octave bands have a constant loudness of 0.180 sone – is computed as 30.47 dB PL when using an F table that includes the two new points discussed above. That is a small, well-behaved change in PL for such a small change in the spectral levels. In contrast, 9.89 dB PL is returned for a 0.180 sone constant loudness spectrum when using the original table data in Ref. [2] while also assuming the terms multiplying F in Eq. (5) do not contribute to S_t below the lowest cited F value. That step change is illustrated in Figure 4 when using the original instead of the updated table data to find F in Eq. (5). The locus of Perceived Level values is plotted in that figure for many different spectra of constant loudness, where that constant loudness value is indicated along the abscissa. The step change in PL values is annotated around the 0.181 sone mark (Figure 4, solid blue line) when using the original table data to find the F value like discussed

above. In contrast, PL values are always well behaved (Figure 4, dashed red line) when using the updated table data instead. For reference, the sound pressure level values corresponding to three different spectra of constant loudness are listed in Table 7. The corresponding PL values are also listed. Similar sound pressure level spectra were used to compute the Perceived Level values near the transition seen at 0.181 sone in Figure 4 and cited above.

Thus, the inclusion of these two new points is only expected to affect PL values of low-level sounds like that of very quiet background noise, evanescent waves that may occur in the Mach cutoff shadow zone, or over-the-top sonic booms[3]. The effect may be large for these types of signals, possibly more than 10 dB PL. Importantly, the PL values for moderate or loud background noise and shaped sonic boom noise in the primary carpet are not likely to be affected by these additional points since the maximum loudness, S_m, for these sounds is generally higher than 0.181 sone. The impact of including these two new points and the sound levels when they begin to affect computed PL values of quiet noises is explored further in Section IV.E.

Importantly, the two new points recommended here for F(S) below 0.181 sone are only approximate since the proper behavior in this loudness range is not documented by Stevens. Additionally, the description given in Ref. [2] for computation of the original F(S) values is vague and difficult to follow, complicating a more accurate derivation of F in this range. The errors in computed PL values are expected to be small when using the table that includes the two approximate points, compared to a new table recomputed from first principles. Thus, a proper derivation of F in this range is left to future work, if desired.

Both NOM[1] and PCBoom were recently updated to use these two new points when computing the factor F. The deprecated, unmaintained loudness code, LCASB[2], does not include these two new points.

When computing total loudness using Eq. (5), the NASA software NOM and LCASB use linear interpolation to find F values that lie between the interpolant values listed in Appendix B of Ref. [2]. Interpolation is required in this step since a closed form expression for F is not currently available. Use of a higher order cubic interpolation method is explored in Section IV.E since the curvature in the tabulated data might affect the accuracy of linear interpolation. However, the effect using cubic interpolation instead of linear interpolation was found to be very small in Section IV.E, so linear interpolation is still used in NASA software.

Finally, using the original table data while extrapolating below the lowest value instead of prepending the two new points is not recommended since that may yield negative F values for S values below 0.181 sone. Explicitly including the two new points, while using linear interpolation, is recommended since it avoids such nonsensical values.

[3] See Chapter 1 and Figures 1.2 and 1.3 and Chapter 2 in Ref. [15] for a discussion of the primary versus secondary boom carpet, Mach cutoff, and over-the-top sonic booms.

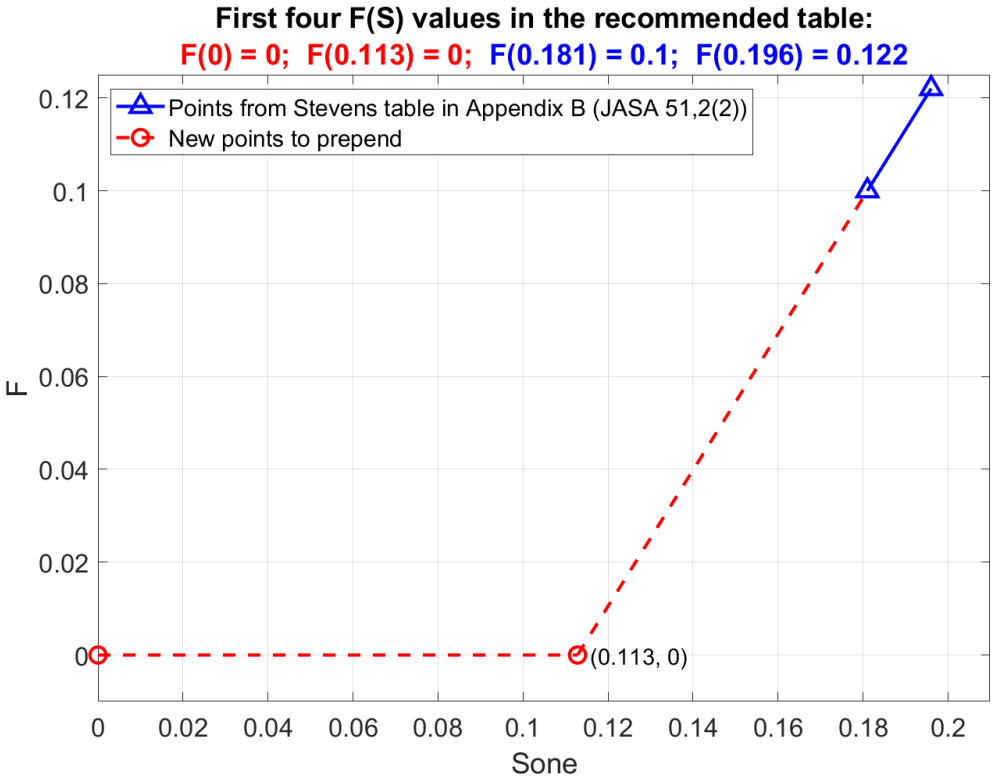

Figure 2: Two new interpolation points (circles) prepended to the table data from Appendix B of Ref. [2], with the first two points from that table also shown (triangles).

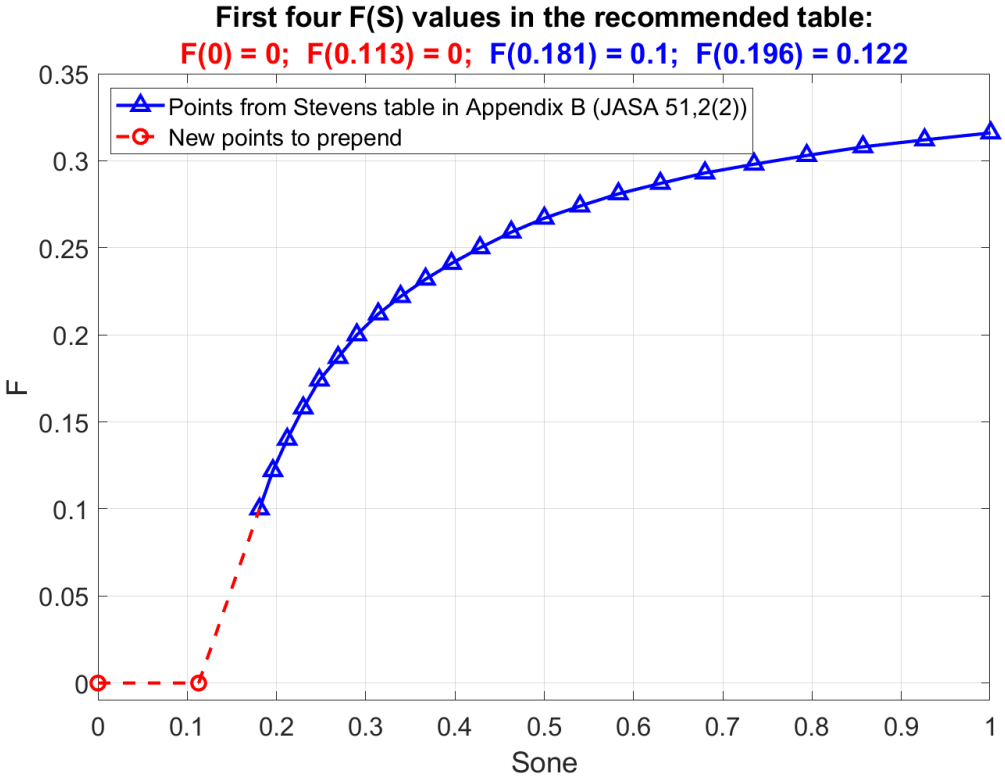

Figure 3: Updated summation weighting factor, F, values for loudness amplitudes of 1 sone and below including the two new points prepended to the list from Ref. [2].

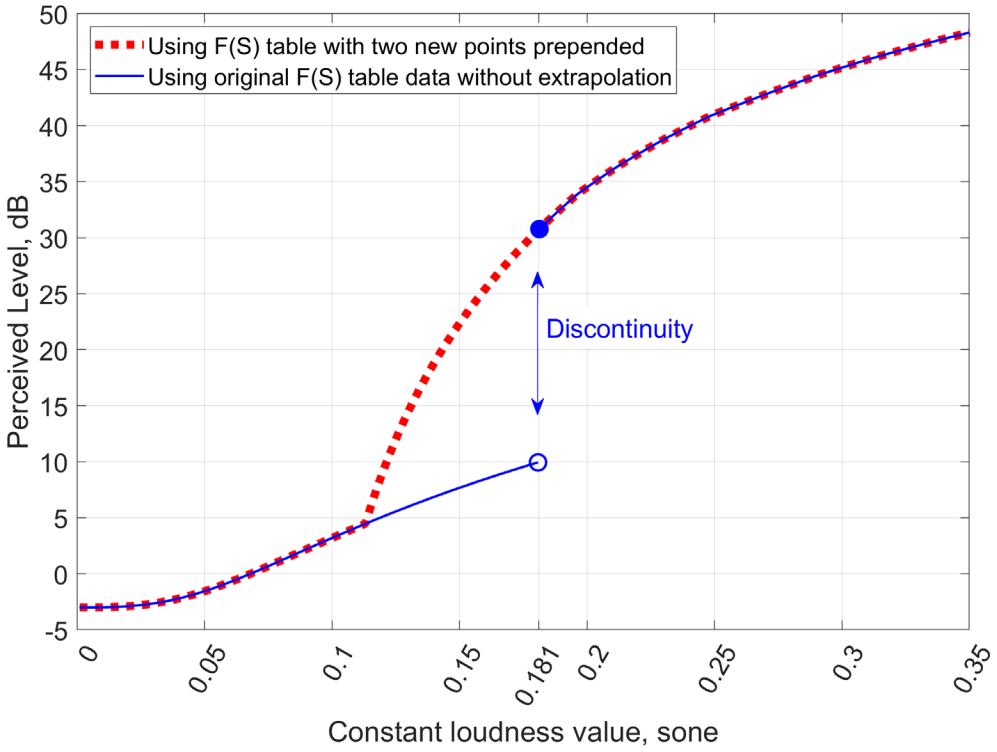

Figure 4: Locus of Perceived Level values for different spectra of constant loudness.

Table 2: Table of sound pressure level values, in decibels, versus one-third-octave band center frequency, in Hz, corresponding to three different spectra of constant loudness; with the loudness values, S in sone, identified in the first column and Perceived Level for each spectrum appended.

	1.259 Hz	**1.585 Hz**	**1.995 Hz**	**2.512 Hz**	**3.162 Hz**	**3.981 Hz**	**5.012 Hz**	**6.310 Hz**	**7.943 Hz**	**10.00 Hz**
S = 0.180	153.8964	147.7928	141.6892	135.5856	129.4821	123.3785	117.2749	111.1713	105.0677	98.96412
S = 0.181	153.8991	147.7981	141.6972	135.5963	129.4954	123.3944	117.2935	111.1926	105.0917	98.99074
S = 0.182	153.9017	147.8033	141.7050	135.6067	129.5083	123.4100	117.3117	111.2134	105.1150	99.01670

	12.59 Hz	**15.85 Hz**	**19.95 Hz**	**25.12 Hz**	**31.62 Hz**	**39.81 Hz**	**50.12 Hz**	**63.10 Hz**	**79.43 Hz**	**100.0 Hz**
S = 0.180	92.86054	86.75695	80.65336	74.54977	68.44619	62.34260	56.23901	50.13542	44.03184	40.29667
S = 0.181	92.88981	86.78888	80.68796	74.58703	68.48610	62.38518	56.28425	50.18332	44.08240	40.34989
S = 0.182	92.91837	86.82004	80.72171	74.62338	68.52505	62.42672	56.32839	50.23006	44.13173	40.40182

	125.9 Hz	**158.5 Hz**	**199.5 Hz**	**251.2 Hz**	**316.2 Hz**	**398.1 Hz**	**501.2 Hz**	**631.0 Hz**	**794.3 Hz**	**1000 Hz**
S = 0.180	36.56150	32.82634	29.09117	25.35600	21.62084	17.88567	17.88567	17.88567	17.88567	17.88567
S = 0.181	36.61739	32.88488	29.15238	25.41987	21.68736	17.95486	17.95486	17.95486	17.95486	17.95486
S = 0.182	36.67191	32.94200	29.21209	25.48218	21.75227	18.02236	18.02236	18.02236	18.02236	18.02236

	1259 Hz	**1585 Hz**	**1995 Hz**	**2512 Hz**	**3162 Hz**	**3981 Hz**	**5012 Hz**	**6310 Hz**	**7943 Hz**	**10000 Hz**
S = 0.180	17.88567	15.88567	13.88567	11.88567	9.88567	9.88567	9.88567	9.88567	9.88567	13.88567
S = 0.181	17.95486	15.95486	13.95486	11.95486	9.95486	9.95486	9.95486	9.95486	9.95486	13.95486
S = 0.182	18.02236	16.02236	14.02236	12.02236	10.02236	10.02236	10.02236	10.02236	10.02236	14.02236

	12589 Hz		**PL[4], dB**	**PL[5], dB**
S = 0.180	17.88567	…	30.472	9.886
S = 0.181	17.95486	…	30.700	30.700
S = 0.182	18.02236	…	30.922	30.922

[4] Perceived Level computed when using the updated F(S) table that includes the two additional points at (0.0, 0.0) and (0.113, 0.0).
[5] Perceived Level computed when using the original F(S) table found in Ref. [2] while assuming factor F = 0.0 for S < 0.181 sone since the original table of F values is undefined below that S value.

III. ERROR ANALYSIS OVERVIEW

Two or more algorithms were discussed in Section II for each of the four main computational steps to compute Perceived Level values. A concise summary of the recommended and the non-recommended algorithms from Section II is provided below in Table 3. In the next section, IV, the error in computed level when using one or more of the non-recommended algorithms to compute PL is characterized for a variety of boom-related noises. The waveforms used for those evaluations and the methods used to compute error in level are documented below in Subsections III.A and III.B, respectively.

A table like Table 3 will be used repeatedly in the subsections that follow to summarize the types of algorithms that are being used for computations in each subsection. However, the adjectival descriptions found in Table 3 will not be included in those tables. Check marks will be placed inside the cells instead to identify when the recommended versus the non-recommended algorithms are being used.

Table 3: Summary of recommended versus non-recommended algorithms for the four main computational steps in the PL calculation.

Computational step	Recommended algorithm	Non-recommended algorithm
1: OTOB sound pressures	Narrow band summation	Discrete-time filters
2: Loudness spectrum	Closed-form method in [7]	Interpolation of contours in [2]
3: Level-amplitude conversions	Eqs. (1), (2), (3), and (4)	Only Eqs. (1) & (2)
4: F(S) table values	Add two new points to table[6]	Unmodified existing table[6]

A. Signals and methods used for error evaluations

The loudness levels of sounds in two categories are of specific interest here: 1) shaped sonic boom noise, and 2) background noise. These two categories of waveforms are also likely of interest to the wider supersonics community since field recordings will likely be required in the future for both certification of future supersonic commercial aircraft and studies of community noise. Specifically, future noise regulations will likely require documentation of the loudness level of shaped sonic booms from future vehicles while also documenting the background noise levels that were present when the booms were recorded. Similarly, the loudness levels of shaped sonic booms that are simulated within software will also need to be computed since those data will be integral to the evaluation of future shaped boom aircraft designs. Thus, waveforms that are representative of these two categories of signals are discussed in the next two subsections, and are used later in Subsection IV to quantify the error when using the non-recommended relative to the recommended algorithms (Table 3 above). All waveforms are at a sample rate of 24,000 Hz unless stated otherwise.

[6] Unmodified existing table is found in Appendix B of Ref. [2]; the two new points NASA recommends adding are documented above in Section II.D.

1. Predicted X-59 sonic boom waveforms

The waveforms used for the error analysis should have a range of acoustical properties (e.g., loudness level and spectral shape) since the error behavior may change with acoustical properties. Consequently, the waveforms for the first category of signals used here are a random subset chosen from a large, numerical, country-wide study of X-59 exposure in which the effects of variable weather on these sonic boom waveforms were characterized [11, 12]. Specifically, a set of 3,000 simulated "on-design" X-59 waveforms is used as a surrogate for shaped sonic boom noise from both the real X-59 aircraft and future commercial aircraft. The acoustical properties of waveforms from that study are expected to vary modestly since different weather conditions will affect the absorption and propagation to cause modest changes in the rise time, duration, and overall amplitude of the shaped boom waveform that is received at ground level. The term "on-design" refers to a computer-based simulation case where the X-59 aircraft is cruising at optimal conditions – e.g., trim, speed, and altitude. These optimal conditions correspond to settings where the aircraft was designed to produce a quiet, shaped sonic boom at ground level within the primary boom carpet[7]. While "off-design" sonic boom waveforms, which are louder than on-design booms since the aircraft is flown at non-optimal conditions, are also available, only on-design waveforms are used in the current study since the algorithm-based effects are more impactful for the quieter on-design shaped sonic booms.

The acoustical characteristics of the 3,000 shaped sonic boom waveforms in the set used here are summarized in Figures 5 to 8. Eight example X-59 sonic boom waveforms are shown in Figure 5 below illustrating typical variations in the amplitude, duration, and rise time. These variations affect the spectral levels and shape, and so the loudness level of the sonic booms. Even modest changes in amplitude, like the doubling when comparing waveform A and B in Figure 5, can result in higher than expected changes in loudness level. For example, a 9.4 dB change in loudness level is observed when comparing those two example waveforms (see PL values listed in the Figure 5 legend), instead of 6 dB that might be expected from amplitude doubling. The variation in loudness level across the full set of 3,000 waveform is summarized in the histogram of Figure 6. A range of about 20 dB PL is observed across the set. For reference, the loudness levels of example waveforms A and B are annotated in Figure 6 (the cyan circle and the magenta triangle).

Sound pressure and loudness spectra for 100 example waveforms are shown in Figures 7 and 8 (gray lines). The two spectra corresponding to example waveforms A and B in Figure 5 are highlighted in Figures 7 and 8 (cyan and magenta lines). A large variation in the spectral level is observed within each one-third-octave band in both Figures 7 and 8, which is a result of varying amplitude and rise time of the waveform (e.g., Figure 5). Such variation in spectral levels causes the variation in loudness level shown in Figure 6. Importantly, the slope of the sound pressure level spectrum is very steep as frequency increases for shapes booms (Figure 7). For example, the slope of the spectrum of waveform B (Figure 7, magenta line) is roughly −42 dB/octave at frequencies above 160 Hz (see right-hand annotation). A similarly steep slope can also occur at low frequencies at around 16 Hz (left annotated), which is near a null in the narrow band spectrum and causes the dip in level observed in that one-third-octave band. Such behavior may affect the accuracy of one-third-octave band levels computed from discrete-time filters since the skirt behavior of discrete-time filters may interact with the steep spectral slope. Specifically, energy from

[7] See Chapter 1 and Figure 1.2 in Ref. [15] for a discussion of the primary versus secondary boom carpet.

low frequencies may interact with the skirts to increase one-third-octave band levels computed using filters. This effect will be discussed later in Section IV.A where the frequency responses of discrete-time filters and the errors associated with using those filters are documented.

Finally, the loudness spectra (Figure 8) help identify the frequency range that contributes significantly to the Perceived Level value. Recall that the total loudness is the maximum loudness plus the weighted sum of all other bands, see e.g., Eq. (5). For the X-59 on-design sonic booms considered here, the loudness spectrum is typically non-zero in the frequency range from about 20 Hz to about 1 kHz and is maximal in the range from about 40 Hz to about 400 Hz (Figure 8). Thus, PL is expected to be most sensitive to errors in computed spectral levels between 40 and 400 Hz, which is important to consider when discussing error in level in Section IV.

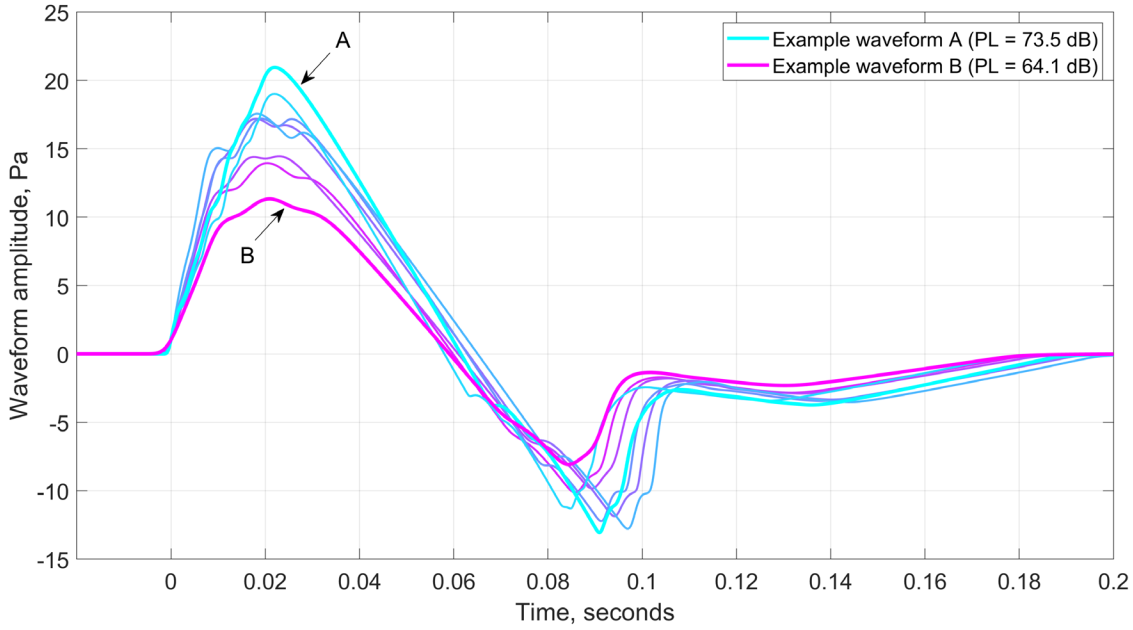

Figure 5: Eight example shaped sonic boom waveforms from the set of 3,000 waveforms that were used here to study computational effects on level error; where the loudness level of two select waveforms, A and B, are annotated in the legend.

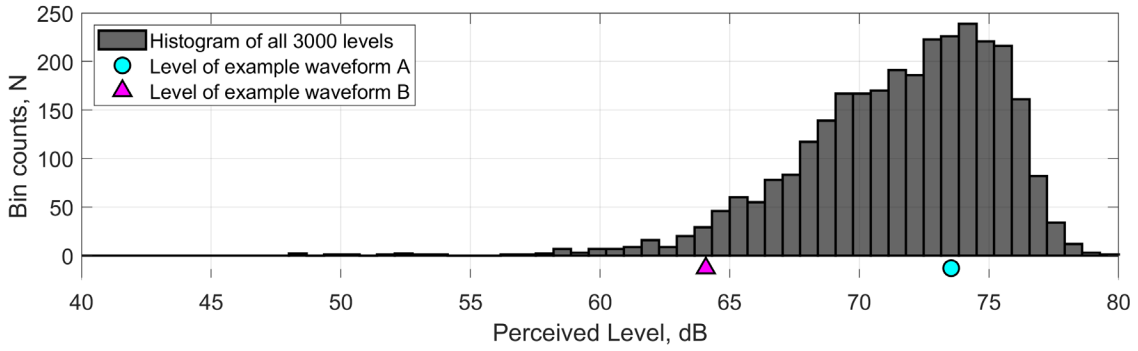

Figure 6: Range of PL observed across the 3,000 predicted X-59 waveforms; where two markers annotate the loudness level of example waveforms A and B from Figure 5.

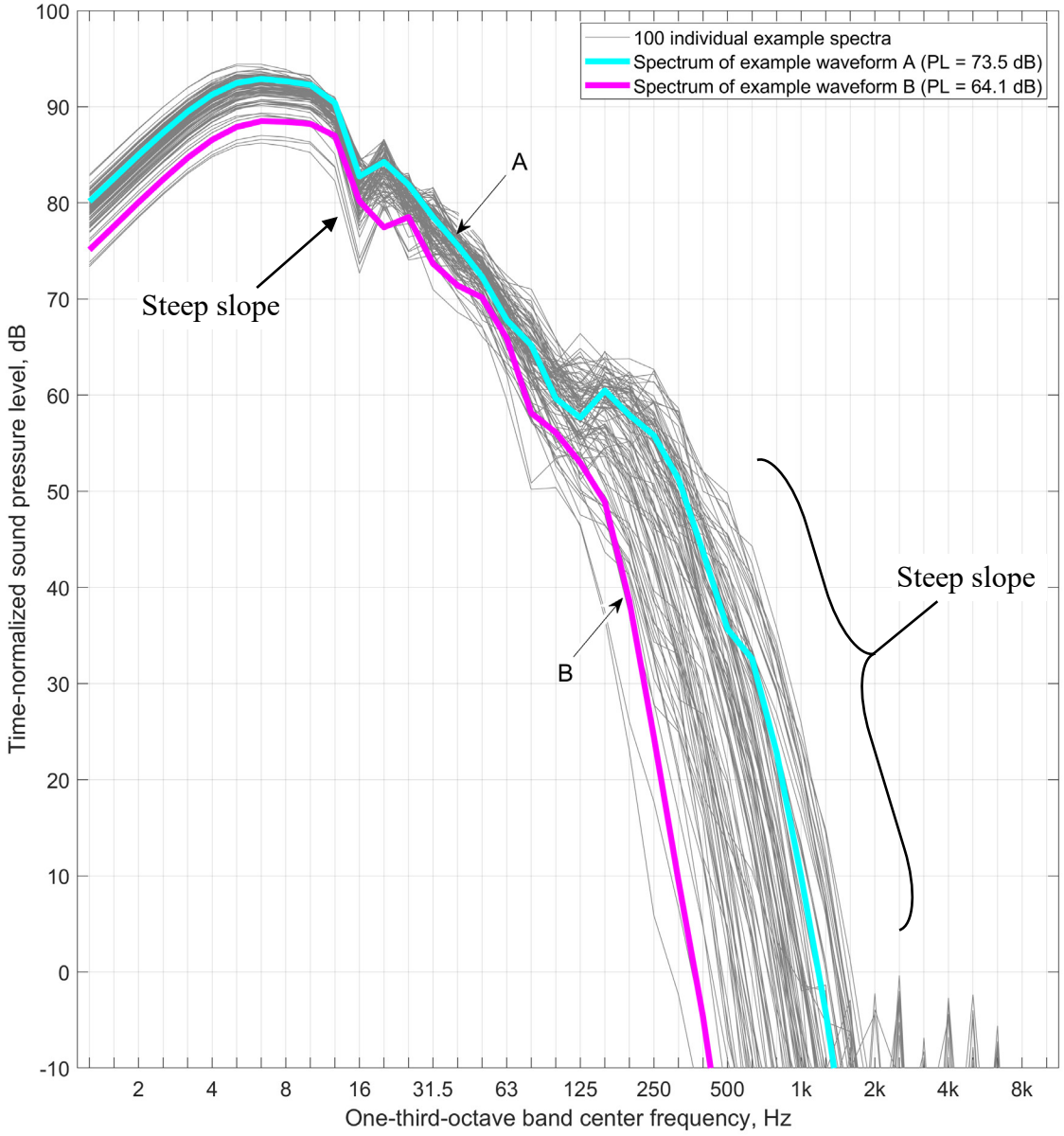

Figure 7: One hundred example shaped sonic boom spectra (sound pressure level) from the set of 3,000 waveforms that were used to study computational effects on level error, with the spectra of example waveforms A and B from Figure 5 highlighted.

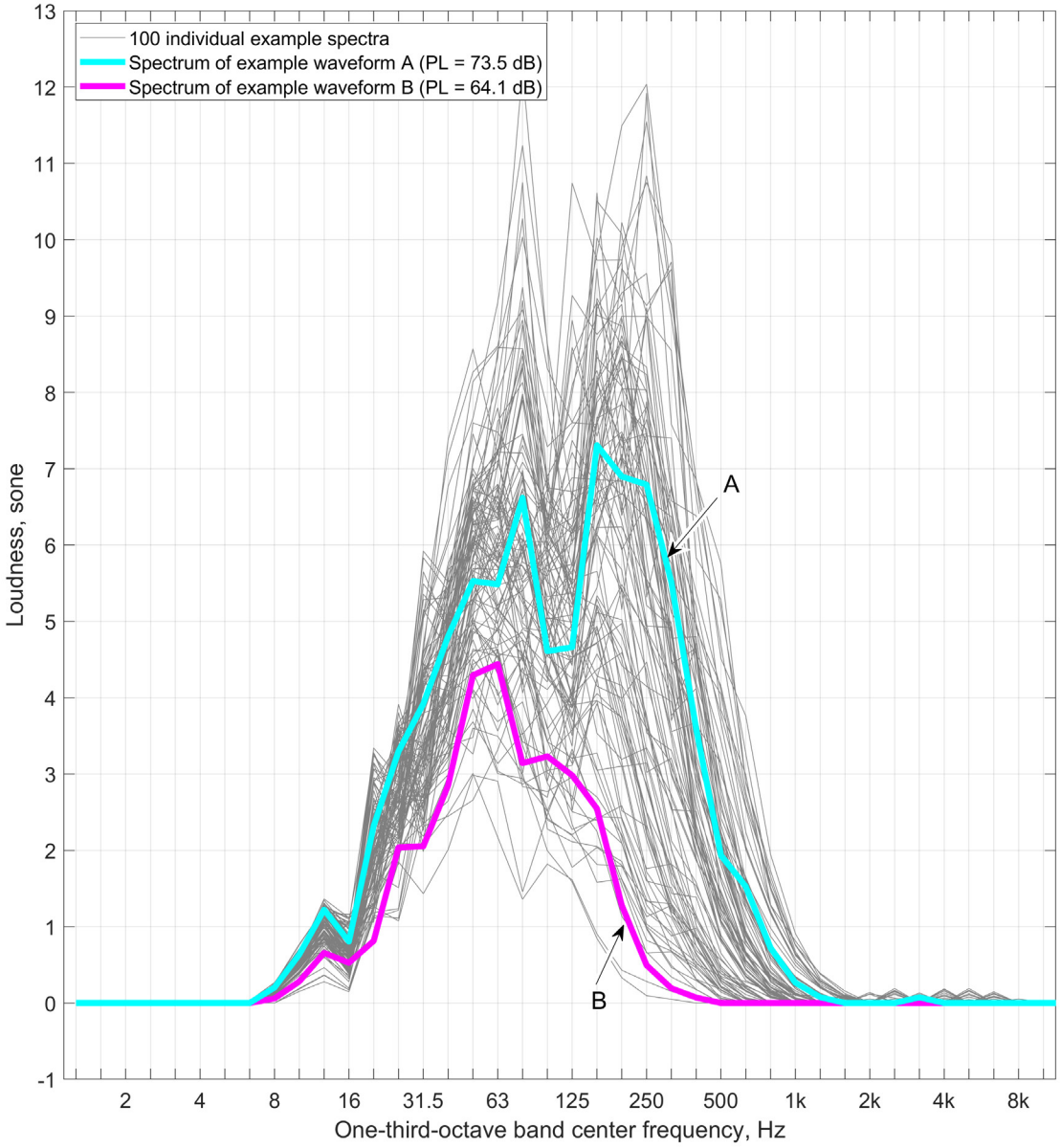

Figure 8: One hundred example shaped sonic boom spectra (loudness) from the set of 3,000 waveforms that were used to study computational effects on level error, with the spectra of example waveforms A and B from Figure 5 highlighted.

2. Background noise waveforms from the QSF18 test in Galveston, TX

The second set of waveforms is taken from background noise that was recorded during the NASA QSF18 community response test that was conducted in Galveston, TX. The background noise data from QSF18 was chosen since it contains 42.25 total hours of noise that was recorded across several days, times of day, and locations within a populated community during a community annoyance experiment. Thus, it is a diverse set of background noise data that exemplifies what NASA may observe at noise monitors during future X-59 community tests. However, this dataset may overestimate the background levels in quiet environments like those of future certification tests of commercial supersonic aircraft since such test sites may be unpopulated. Even so, these QSF18 data are the best available background noise dataset for these evaluations.

Importantly, error in level observed for the background noise waveforms discussed in this subsection and the sonic boom waveforms discussed in the prior subsection are always analyzed separately. The waveforms are never combined in this report to study the error in PL for cases where a shaped sonic boom is contaminated by background noise, like might be present in an field recording. That analysis is left for future work, if desired.

The acoustical characteristics of the background noise waveforms used here are documented in Figures 9 to 12. There is a wide range of acoustical characteristics (e.g., level) for the background noise, like was documented above for sonic booms. Two example waveforms are shown in Figure 9, where the loudness levels of each are annotated in the legend. Importantly, a taper window is applied to the background noise waveforms used here prior to passing the waveforms as input to the PL computation (Figure 1). This windowing avoids spectral contamination associated with non-zero discontinuous steps that would otherwise occur at the edges of the time window. The taper window was taken from Ref. [13] and is shown in Figure 9 (lower subplot). The fade-in cosine taper is 0.1 seconds long; the fade-out cosine taper is 0.3 seconds long; and the pass portion of the window is 0.3 seconds long. That window function was chosen since it will be used when analyzing X-59 acoustical recordings of both shaped booms and background noise.

The range of loudness levels across the 3,000 background noise waveforms is shown in Figure 10, where levels vary from about 50 to about 75 PL dB. This is a result of the spectral variations shown in Figures 11 and 12. The slope of the background noise spectra as frequency increases (Figure 11) is not as steep as for the sonic boom spectra (Figure 7). For example, the slope of the spectrum of example waveform B is only about −4 dB/octave, on average, across the frequency range from about 4 Hz to about 5 kHz (Figure 11, magenta line). That compares to a high-frequency slope of about −42 dB/octave for the shaped sonic booms (e.g., Figure 7). Thus, the error when using discrete-time filters to compute one-third-octave bands levels may differ for background noise as compared to shaped sonic boom noise if the interaction of the finite skirts and the spectral slope is important.

Additionally, the frequency range where the loudness spectrum is maximal is much broader but lower in amplitude for background noise (Figure 12) than for shaped booms (Figure 8). Thus, this change may impact the frequency range where the PL computation is sensitive to spectral errors.

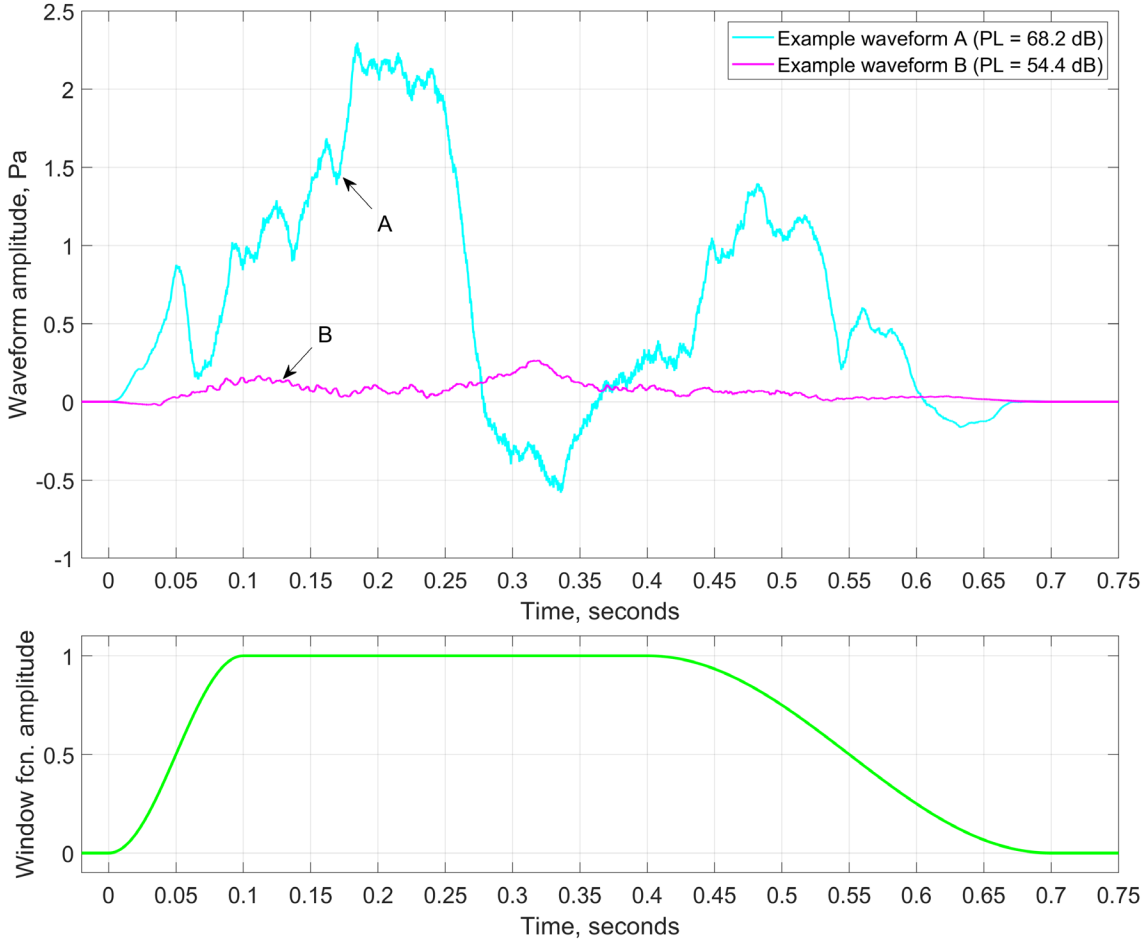

Figure 9: Two example windowed background noise waveforms from the set of 3,000 waveforms that were used here to study computational effects on level error; where the loudness level of two select waveforms are annotated in the legend, and where the window function is shown in the lower subplot.

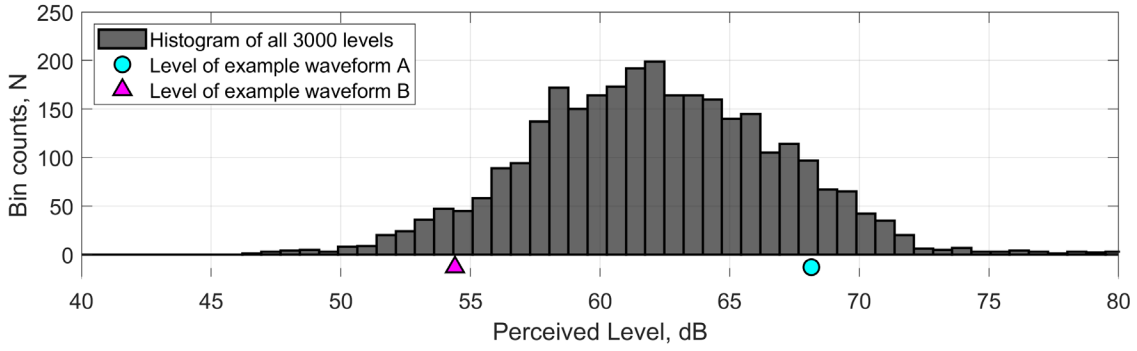

Figure 10: Range of PL observed across the 3,000 background noise waveforms; where two markers annotate the loudness level of example waveforms A and B from Figure 9.

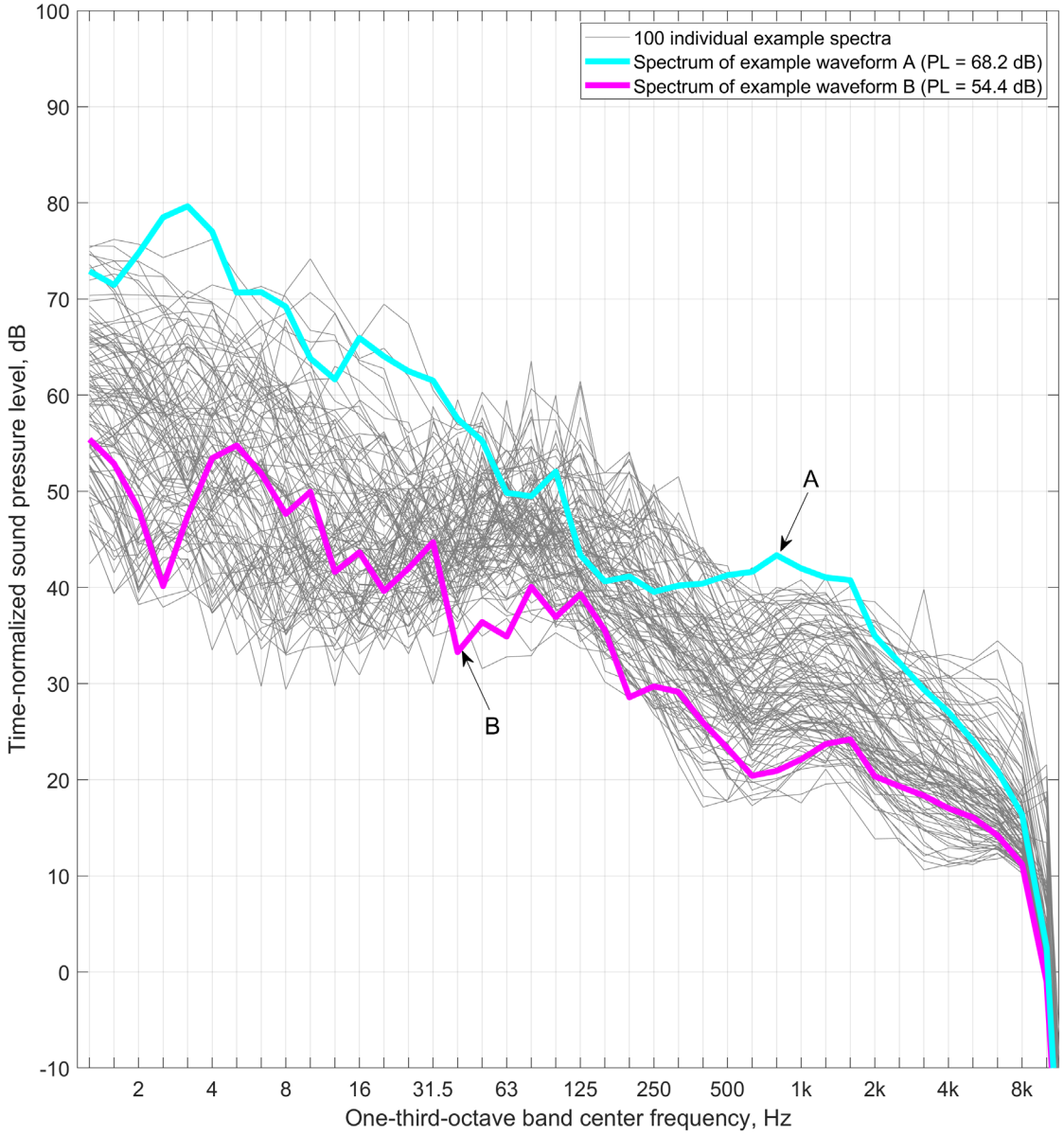

Figure 11: One hundred example background noise spectra (sound pressure level) from the set of 3,000 waveforms that were used to study computational effects on level error, with the spectra of example waveforms A and B from Figure 9 highlighted.

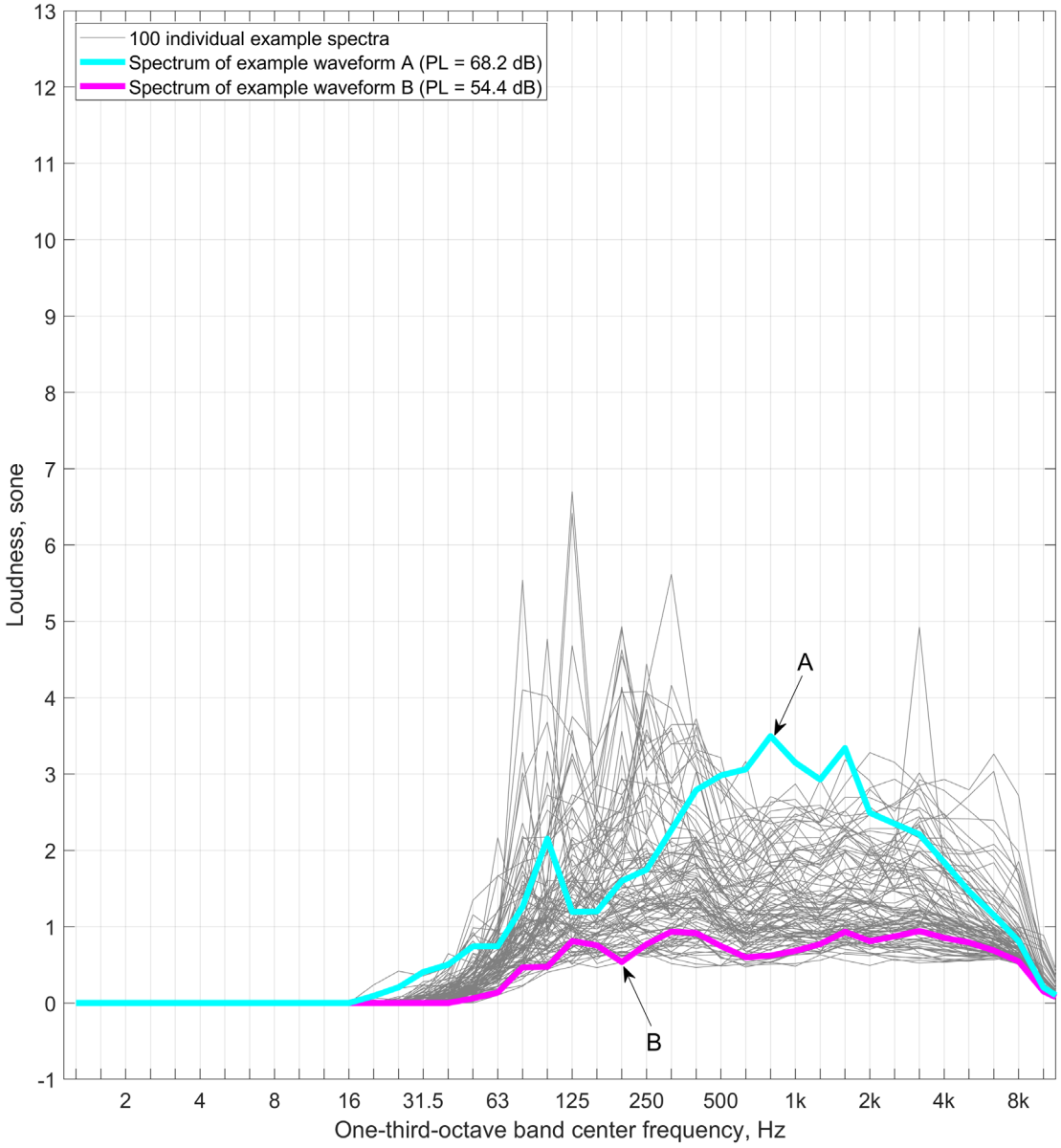

Figure 12: One hundred example background noise spectra (loudness) from the set of 3,000 waveforms that were used to study computational effects on level error, with the spectra of example waveforms A and B from Figure 9 highlighted.

B. Loudness level error computation

For each waveform in the two categories of waveforms discuss above, the error in the sound pressure level spectrum and/or Perceived Level is computed for five different combinations of the non-recommended and recommended algorithms. The five combinations are documented in the following five subsections of Section IV below:

- Errors resulting from algorithm used to compute one-third-octave band sound pressure levels (Subsection IV.A)
- Errors resulting from algorithm used to compute loudness spectrum (Subsection IV.B)
- Errors related to the equations used to convert between level and amplitude (Subsection IV.D)
- Errors related to the weighting table used to compute total loudness (Subsection IV.E)
- Errors when combining all non-recommended algorithms (Subsection IV.F)

The errors documented in each of those subsections are computed from the difference between "inexact" levels minus "true" levels, where error distributions across the 3,000 waveforms in each set are presented. True levels are always computed using all the recommended methods, as indicated by the check marks in the second column in Table 4 below. The inexact levels in each subsection are computed using a different combination of non-recommended and recommended methods, where the combinations used in each subsection are identified by the check marks in Table 5. Studying these different combinations of non-recommended methods and recommended methods (Table 5) will help identify which steps of the PL calculation (Figure 1) are most sensitive to the choice of algorithm. For example, using the non-recommended F(s) table values – a version of the table without the two new values – may be less impactful than using the non-recommended method to compute one-third-octave band levels. For clarity, Table 4 and the applicable portion of Table 5 will be repeated in each of the five subsections below so readers can easily identify which non-recommended methods are being evaluated in the subsection, and each subsection will include a discussion of the methods used.

All true spectra and loudness levels are computed using the NOM software[1] that is available publicly as MATLAB® source code. All inexact spectra and loudness levels are computed using a modified version of the NOM subroutines using MATLAB® R2019a. Specifically, the function named *OctaveBandSPL_Matrix.m* is used to compute one-third-octave band levels using (non-recommended) discrete-time filters. The discrete-time filters are designed using the *fdesign.octave* command in MATLAB®. The function *pl_matrix_NonRecommededMethods_rev2.m* is used to compute PL using the different combinations of non-recommended and recommended methods, where analysis choices are made using Boolean inputs. These two scripts are identified for documentation purposes only. They are not available for public distribution.

Table 4: Algorithms used to compute true levels in all subsections that follow.

Computational step	Recommended algorithm	Non-recommended algorithm
1: OTOB sound pressures	✓	
2: Loudness spectrum	✓	
3: Level-amplitude conversions	✓	
4: F(S) table values	✓	

Table 5: Check mark indicates algorithms used to compute inexact levels in all subsections that follow.

Subsection	Computational step	Recommended algorithm	Non-recommended algorithm
IV.A	**1:** OTOB sound pressures		✓
	2: Loudness spectrum	✓	
	3: Level-amplitude conversions	✓	
	4: F(S) table values	✓	
IV.B	**1:** OTOB sound pressures	✓	
	2: Loudness spectrum		✓
	3: Level-amplitude conversions	✓	
	4: F(S) table values	✓	
IV.D	**1:** OTOB sound pressures	✓	
	2: Loudness spectrum	✓	
	3: Level-amplitude conversions		✓
	4: F(S) table values	✓	
IV.E	**1:** OTOB sound pressures	✓	
	2: Loudness spectrum	✓	
	3: Level-amplitude conversions	✓	
	4: F(S) table values		✓
IV.F	**1:** OTOB sound pressures		✓
	2: Loudness spectrum		✓
	3: Level-amplitude conversions		✓
	4: F(S) table values		✓

IV. RESULTS

The discussions in this section document the rationale for the algorithm recommendations that were provided in Section II. In Subsections IV.A, IV.B, IV.D, IV.E, and IV.F, the true levels (Table 4) are compared to those of the inexact levels (Table 5) to quantify the error in level that is expected if programmers were to utilize the non-recommended algorithms in software. Generally, the Perceived Level error documented in Subsections IV.A and IV.B is larger than in IV.D and IV.E. Importantly, Subsection IV.C describes a minor modification to the input waveforms that are used for error evaluations in Subsections IV.D and IV.E only. Specifically, the amplitudes of the sonic boom and the background noise waveforms from Subsection III.A are reduced in amplitude since the algorithm changes that are evaluated in Subsections IV.D and IV.E tend to only introduce error for noises that are very low in level.

A. Errors resulting from algorithm used to compute one-third-octave band sound pressure levels

1. Subsection overview

In this subsection, the errors in the one-third-octave sound pressure levels from 1.25 Hz to 8 kHz, and the errors that propagate through to the Perceived Level values, are studied. Table 6 summarizes the algorithms that are used in this subsection for each of the four main computational steps when computing both the true levels and the inexact levels (see also Table 3). Distributions of the error in level across the 3,000 X-59 shaped sonic booms (from Subsection III.A.1) and the 3,000 background noise waveforms (Subsection III.A.2) are summarized in separate tables and figures below. Errors in level are always presented as the difference of the inexact levels minus the true levels, so a positive error indicates the non-recommended algorithm – the discrete-time one-third-octave band filters in this subsection – overestimates the true level.

Table 6: Algorithms used to compute true levels and inexact levels in subsection IV.A.

	True levels:		***Inexact levels:***	
Computational step	**Rec. algorithm**	**Non-rec. algorithm**	**Rec. algorithm**	**Non-rec. algorithm**
1: OTOB sound pressures	✓			✓
2: Loudness spectrum	✓		✓	
3: Level-amplitude conversions	✓		✓	
4: F(S) table values	✓		✓	

In all cases in this subsection, the true levels are computed using the narrow band summation method to find the one-third-octave band levels – the initial step in the computation of PL (Table 6 and Figure 1). Inexact levels are always found using discrete-time filters for that initial step (Table 6 and Figure 1). Then, the recommended algorithms are used for the final three steps in both cases. However, before proceeding to discuss the error results for discrete-time filters, the convergence behavior of true levels is first summarized in the next subsection.

2. Summary of a narrow band summation method convergence study

A tutorial for the narrow band summation method is provided in Appendix 1 and an evaluation of the convergence behavior of that method as the zero-padding duration changes is provided in Appendix 2. The results from Appendix 2 are briefly repeated here to provide context for the discrete-time filter error analysis results that appear in subsections that follow.

In Appendix 2, errors in one-third-octave band levels and Perceived Level are studied across 3,000 sonic boom waveforms. The assumed true levels used a total waveform duration, including zero padding, of 21.85 seconds. Those true levels are differenced with levels computed when the waveform total duration is either 2.731, 5.461, or 10.92 seconds to identify how less zero padding affects the levels. Levels for all four durations were always computed using narrow band summation to find the one-third-octave band levels since identifying the convergence behavior of that method is desired. Discrete-time filter performance was not evaluated in this subsection but will be in subsequent subsections. Errors across the 3,000 shaped sonic boom waveforms are summarized visually as box plots in Figure 13. The percentiles associated with box plot features are identified in the legend. Errors in the one-third-octave band levels are shown in the left-hand subplots and the error in the PL noise metric is shown in the right-hand subplots. The total signal durations are noted in the figure caption. Because the error in Perceived Level is very small in all three cases, those error results are also summarized in Table 7, where the 5^{th}, median, and 95^{th} percentile error values are cited.

The largest error in one-third-octave band levels observed here is roughly −0.023 dB in the 2.5 Hz band for the analysis case with the shortest total signal duration (Figure 13a). All other one-third-octave bands have less error. For example, the one-third-octave band level error is typically only a few thousandths of a dB at frequencies above 50 Hz for all three total waveform duration cases (Figure 13, subplots a, b, and c). Additionally, Perceived Level is well behaved in all three cases, where the largest median error is only 0.00034 dB PL, and the 95^{th} percentile is only 0.00107 dB PL for the case when the total signal duration is 2.731 seconds (Table 7). Additionally, errors in the one-third-octave band levels and Perceived Level decreases as signal duration increases from 2.731 to 10.92 seconds (Figure 13 and Table 7).

It will be shown in the next subsections that the errors observed when using discrete-time filters to compute one-third-octave band levels are more than an order of magnitude larger than any of the errors that were observed in this convergence study (Figure 13 and Table 7 and documented in Appendix 2). It will also be shown that the design parameters of the discrete-time filters can be refined so their output converges to the narrow band summation results. However, the computational expense of using the refined filters and the modest error that is present even after that refinement suggests that there is no benefit to using filters instead of narrow band summation.

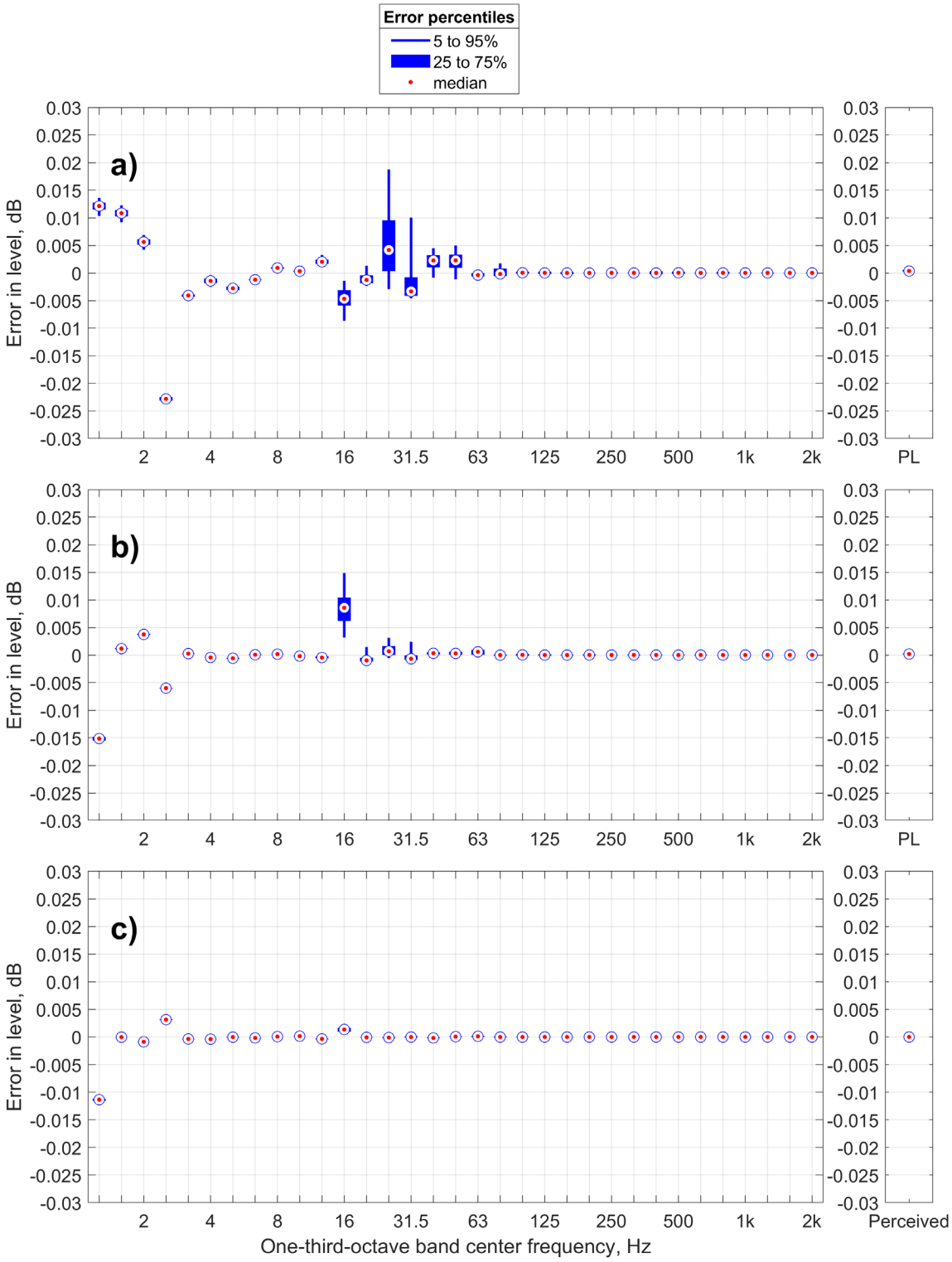

Figure 13: Error distributions for one-third-octave band levels (left-hand subplots) and the PL noise metric (right-hand subplots) across 3,000 X-59 waveforms when using the narrow band summation method; for waveform durations (zero padded) of a) 2.731 s, b) 5.461 s, and c) 10.92 s; and relative to values with a duration of 21.85 s.

Table 7: Tabulated 5th, 50th, and 95th percentiles of error in PL for the data shown in Figure 13 (the right-hand subplots) when using the narrow band summation method.

Total signal duration, s	**Number of signals**	**5th percentile error PL, dB**	**50th percentile error PL, dB**	**95th percentile error PL, dB**
2.731	3000	0.00017	0.00034	0.00107
5.461	3000	9.16E-05	0.00018	0.00040
10.92	3000	-3.05E-05	7.63E-06	3.81E-05

3. Discussion of the properties and application of discrete-time filters

There are several design parameters that influence the frequency response of the discrete-time filters, which may affect the error in level when using filters to compute one-third-octave band levels. The shape of the frequency response is primarily determined by two parameters: 1) the filter order, and 2) the number of bands per octave. The latter item is always set to three here since one-third-octave band levels are needed (e.g., see Figure 1). The discrete-time filter order is varied here to identify whether the shape of the filter skirts has an impact on the error that is observed relative to the true levels computed using narrow band summation. The filter orders considered here are listed in Table 8 for the X-59 waveform set and in Table 9 for the background noise waveform set. Figures containing error analysis results are also indicated in those tables (right-most column). Filter orders are 6, 10, 18, and 34. When filtering waveforms, the discrete-time filters are always applied using a cascaded second-order sections format to avoid problems with numerical stability that can sometimes occur with other filter formats (e.g., see discussions in Ref. [14] Annex B Sections B.6 and B.7). In addition, the waveforms filtered by the 1.25 to 20 Hz bands are resampled by a factor of 1/100, to a sample rate of 240 Hz, before applying the filters to improve stability [14].

Table 8: Discrete-time filter error analysis parameters and corresponding results figures for X-59 sonic boom waveforms.

Filter order	Total waveform duration, s (1.25 to 20 Hz)	Total waveform duration, s (25 Hz to 20 kHz)	Number of waveforms	Error results summarized in figure(s)
6	2.733	2.731	3000	Figure 17a
6	5.467	2.731	3000	Figure 17b
6	10.93	2.731	3000	Figure 17c & Figure 18a
10	10.93	2.731	3000	Figure 18b
18	10.93	2.731	3000	Figure 18c & Figure 19a
18	21.85	5.461	3000	Figure 19b
34	21.85	5.461	3000	Figure 19c

Table 9: Discrete-time filter error analysis parameters and corresponding results figures for background noise waveforms.

Filter order	Total waveform duration, s (1.25 to 20 Hz)	Total waveform duration, s (25 Hz to 20 kHz)	Number of waveforms	Error results summarized in figure
6	10.93	2.731	3000	Figure 20a
10	10.93	2.731	3000	Figure 20b
18	21.85	5.461	3000	Figure 20c

In addition to the filter order, the total duration of the waveforms, which includes zero padding appended to the waveforms from Section III.A, was varied since this may affect one-third-octave band levels. For example, the impulse responses of low-frequency one-third-octave bands will ring down slowly since the filter passband width is quite narrow with respect to the center frequency. This will manifest as a slow impulse response

decay rate. For example, the impulse response decay rate for a few combinations of one-third-octave band center frequency and filter order are shown in Table 10 for class 1 filters designed in MATLAB® R2019a using the *fdesign.octave* command. The impulse response decay rate of the 1.25 Hz band is very slow in comparison to higher bands: about −2.18 and −1.22 dB/second for 6th and 18th order filters, respectively (Table 10). Thus, applying those filters to short duration signals – e.g., signals that are only a few seconds long – may result in temporal truncation error in the estimated level of those bands if: 1) the waveform to be filtered does not have sufficient zero-padding appended to it, or 2) some other compensation is not applied to correct for truncation of the filter ring down. Truncation effects are expected to become particularly problematic when the filter order is high since decay rate is inversely proportional to the order; higher filter orders reduce the decay rate (Table 10). Additionally, this effect has greater impact at very low frequencies since the decay rate is proportional to center frequency (Table 10). Thus, the high frequency bands decay quickly and are not as susceptible to truncation error. Such truncation errors are demonstrated below by varying the total (zero-padded) duration of the waveform that is used to compute the band levels for the 1.25 to 20 Hz bands when using 6th and 18th order filters (Table 8, first and second column).

Table 10: Calculated impulse response decay rate, dB/second, for some combinations of one-third-octave band center frequency and filter order.

One-third-octave band center frequency, Hz	**6th order filter decay rate, dB/second**	**10th order filter decay rate, dB/second**	**18th order filter decay rate, dB/second**
1.25	−3.55	−2.21	−1.23
2.50	−7.10	−4.34	−2.43
5.00	−14.2	−8.67	−4.85
25.0	−71.0	−44.2	−24.5
250	−712.0	−435.4	−243.6
2500	−7120	−4355	−2437

For context, the frequency response magnitude (filter gain) of a typical one-third-octave band (the 1 kHz band) discrete-time filter is compared in Figure 14 for a 6th order, a 10th order, and an 18th order design (blue lines). Also included in Figure 14 are vertical lines representing the upper and lower edges of the 1 kHz one-third-octave band (the dot-dash magenta lines), which provide a visual indication of the extent of the ideal rectangular passband width. The ideal response would be 0 dB within the passband and −∞ dB in the stopbands. The change in stopband gain as filter order increases is evident in Figure 14, where the gain at 860 Hz is annotated for the 6th and 18th order discrete-time filters. The stopband attenuation changes from about −7.8 dB to about −21.2 dB for these two orders. Then in Figure 15, the frequency response for three adjacent one-third-octave bands is shown for 6th order filters to highlight the skirt overlap for adjacent, low-order filters.

Importantly, these two figures help to illustrate how the steep slope of a shaped sonic boom spectrum at high frequencies might interact with the filter skirts to produce errors in the estimated one-third-octave band levels. The slow roll-off of low order filters outside the passband could allow energy outside the passband to increase the filter output, causing the filter to overestimate the band level. For example, the response of a 1 kHz

filter to a signal with spectral slope of −42 dB/octave (like that of a shaped sonic boom) is shown in Figure 16 for discrete-time filter orders of both 6 (top subplot) and 18 (bottom subplot). The computed filter responses (blue lines) are compared to the ideal response of the band to such a signal (magenta lines). The magnitude of the filter response for the 6^{th} order filter (Figure 16a) is much high than the ideal response in the lower stopband region (to the left of the passband) but the 18^{th} order filter better matches the ideal response both above, below, and within the passband (Figure 16b). Importantly, the level of a band is computed as the total energy in the filtered signal, in contrast to the data in Figure 16 that shows how the energy in the filtered signal varies with frequency. In effect, the band level is the area under a curve shown in Figure 16. Thus, 6^{th} order filters are expected to overestimate the band levels when the narrow band spectral slope is large due to the high stopband response (e.g., Figure 16a, dotted blue line), while 18^{th} order filters (e.g., Figure 16b, solid blue line) are expected to produce a better estimate. These types of behaviors are investigated here by studying the error in one-third-octave band level as filter order changes (see Tables 8 and 9 for filter orders used when analyzing boom and background noise waveforms, respectively).

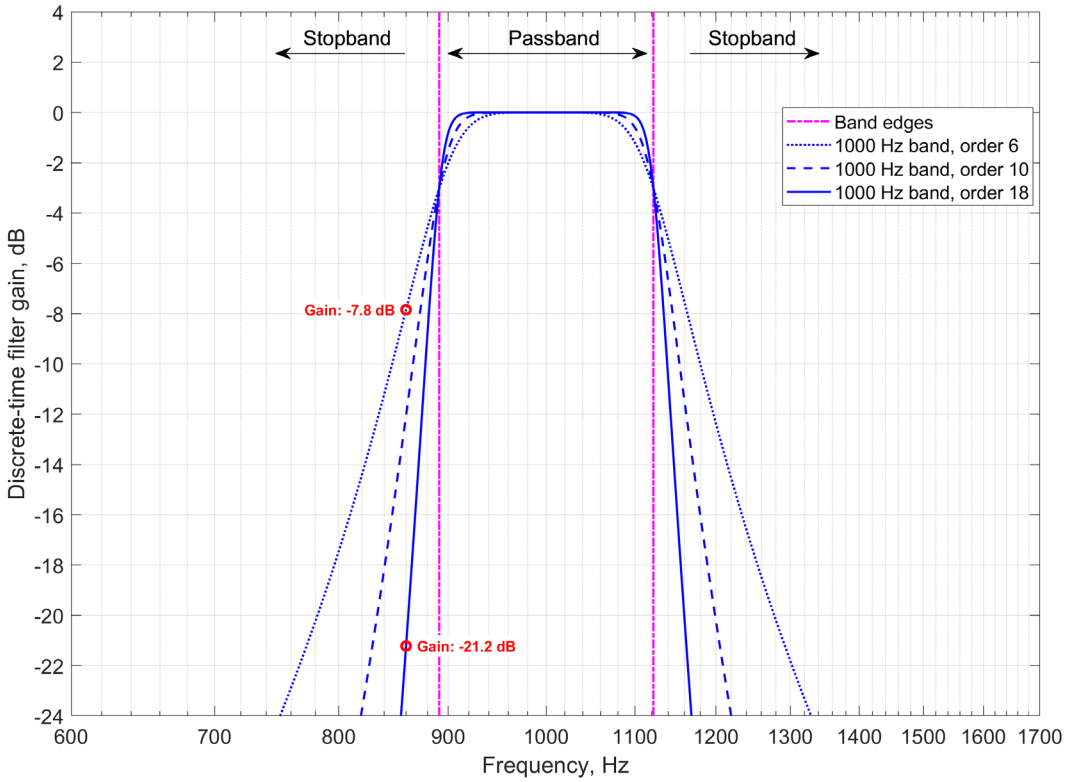

Figure 14: Class 1 discrete-time filter gain for three different filter orders identified in the legend, and the band edges for the 1 kHz one-third-octave band; gains at 860 Hz annotated in red text for the 6th and 18th order filters.

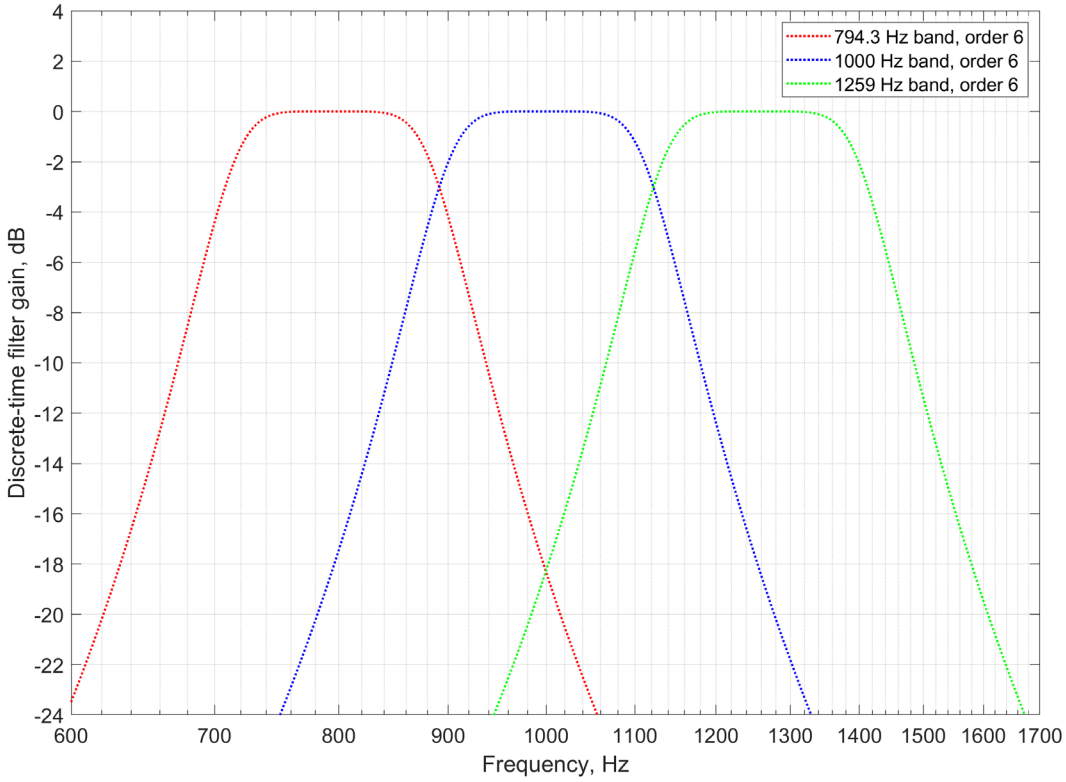

Figure 15: Illustration of skirt overlap for three neighboring 6th order, class 1 filters.

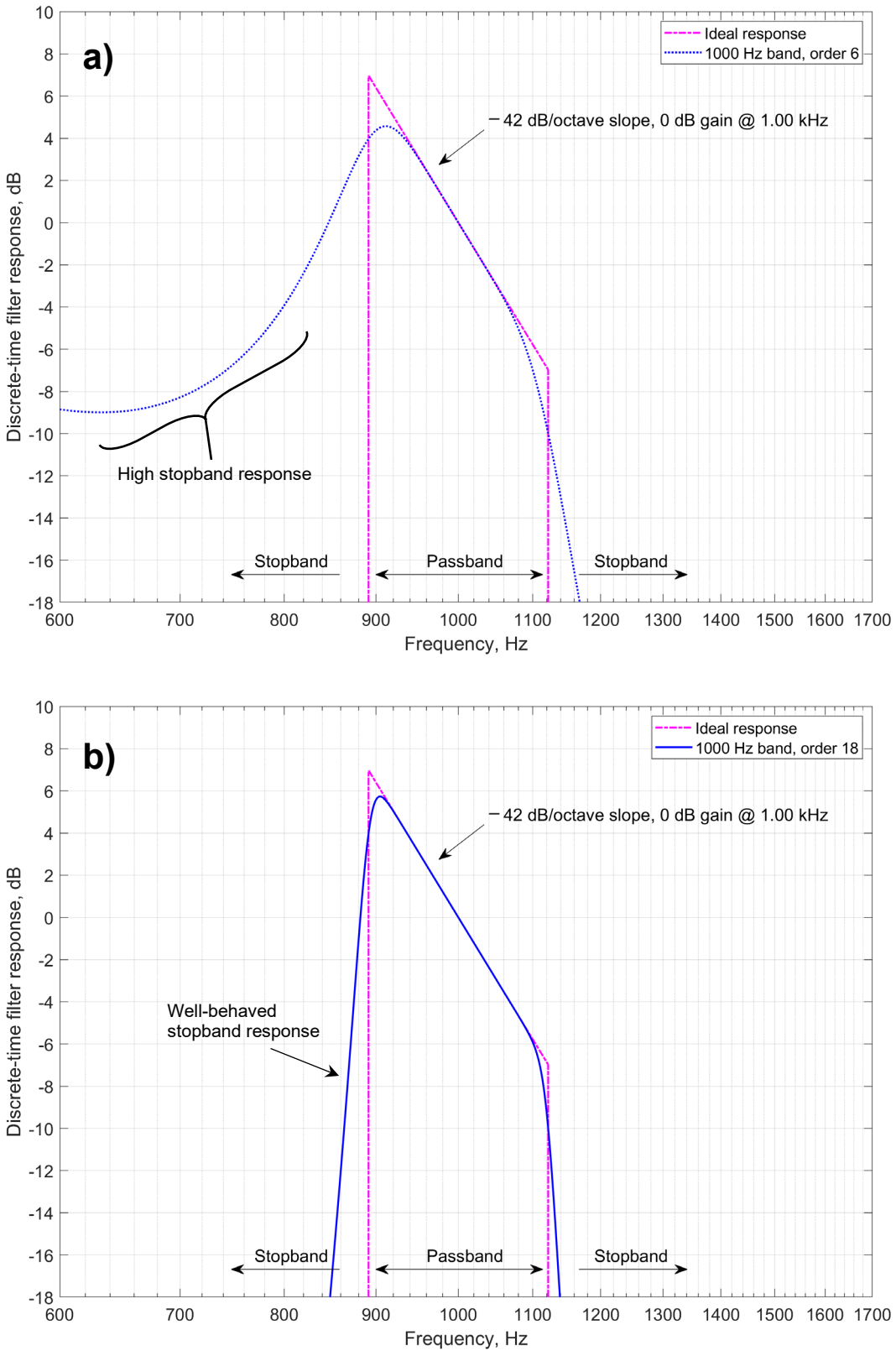

Figure 16: Frequency response of the 1 kHz one-third-octave band to a signal with a narrow band spectral slope of −42 dB/octave and gain that passes through 0 dB at 1 kHz; ideal response (magenta lines) compared to: a) that of a 6th order discrete-time filter (blue dotted line), and b) that of an 18th order discrete-time filter (blue solid line).

4. Error results

The distributions of errors in one-third-octave band levels are summarized in Figure 17 for the first three analysis cases listed in Table 8. All three subplots in Figure 17 correspond to using 6th order discrete-time one-third-octave band filters to compute levels of shaped sonic boom waveforms that are compared with true levels found using the narrow band summation method (Appendices 1 and 2). The total waveform duration increases from 2.73 to 10.93 seconds moving from the top to the bottom subplot. The errors in one-third-octave band levels (along the ordinate) are summarized as individual box plots for each one-third-octave frequency band (along the abscissa). The features and corresponding error percentiles across the 3,000 waveforms are shown in the legend, where box plot features for the 5th, 25th, median, 75th, and 95th error percentiles are indicated. In some frequency bands, some box plot features may exceed the displayed ordinate range. In those cases, annotations are included around the edge of the subplot to indicate the numeric values for some out-of-range percentiles. An annotation is also included alongside the ordinate label to indicate when use of the non-recommended method either overestimated or underestimated the true level. Similarly formatted figures are discussed below for all the analysis cases and figures identified in Tables 8 and 9 above.

The data in Figure 17a indicate the band levels are underestimated for the lowest frequency one-third octave bands, shown at the left side of the figure. For example, the error in the 1.25 Hz band across all 3,000 waveforms is about −3.8 dB for the shortest duration case (Figure 17a). As more zero-padding is appended to the waveform to increase the total waveform duration, the errors observed within the low frequency bands are reduced (moving from Figure 17a to 17b then to 17c). This demonstrates both the effect and mitigation of the first type of error discussed above: truncation of the discrete-time filter ring down. Caution must be used when utilizing discrete-time filters to ensure that the zero-padded signal duration is long enough to avoid this type of error.

In all three subplots of Figure 17, significant error (several tenths of a dB to several dB) is present in the frequency bands above about 16 Hz (right-hand side of the subplots). This mid- and high-frequency error is not affected by changes to the zero-padding duration. However, increasing the filter order, as shown in Figure 18, significantly reduces the error in those bands. Specifically, the error when using filter orders of 6, 10, and 18 are shown in Figure 18a, 18b, and 18c, respectively. See Table 8 for a list of analysis parameters corresponding to these subplots. The top subplot, Figure 18a, is the same analysis case shown in Figure 17c, the error when using 6th order filters, but with a reduced ordinate range. Figure 18b and 18c correspond to 10th and 18th order filters. Inspecting the 63 Hz one-third-octave band, for example, the median error is about 0.55 dB when using 6th order filters (Figure 18a). This median error reduces to about 0.22 dB when using 10th order filters (Figure 18b) and about 0.07 dB when using 18th order filters (Figure 18c). Also, the ranges in the error – e.g., the spans between the 5th and 95th percentile (thin blue lines) – at frequencies above the 16 Hz band are also reduced when moving from subplot 18a to 18c. This suggests that the discrete-time filters converge to the true levels (computed using narrow band summation) as order increases. However, an increase in error in the lowest-frequency bands when using the 18th order filters is observed (Figure 18c, right-hand side). This behavior is due to a slower decay rate of the discrete-time filters as the filter order is increased (e.g., Table 10). Thus, an increase in truncation errors occurs as filter order increases for a fixed signal duration, and additional zero padding is needed to counter the effects of the decreased filter decay rate.

The balance between low- and high-frequency error is further demonstrated in Figure 19, where the error when using 18th order filters is summarized in subplots 19a and 19b for different zero-padded signal durations: 10.93 and 21.85 seconds, respectively. The low frequency error observed in Figure 19a is mitigated in Figure 19b by doubling the total waveform duration with additional zero-padding. However, the high frequency error (above about 16 Hz) is unchanged in those two subplots (Figure 19a and 19b). Figure 19c illustrates the impact of applying a 34th order filter to further reduce high frequency error relative to the true levels, but at the expense of increased low frequency error, which would require additional zero padding to mitigate.

In addition to the error in one-third-octave band levels, a boxplot showing the range of error in PL is shown in the right-hand subplots of Figures 18 and 19. Additionally, the 5th, median, and 95th percentile of error in PL values across the 3,000 waveforms are tabulated in Table 11 for the boxplots shown in Figures 18 and 19. Modest error is observed in PL when filter order is low. For example, the median error in PL for 6th order filters is about +0.33 dB (overestimate) and the 95th percentile error is +0.45 dB (Table 11). Errors in PL of those magnitudes are undesirable if PL is to be used for regulatory purposes. Overall, the PL error decreases as both filter order and zero-padded signal duration increase (Table 11). However, the error in PL is significantly higher when using discrete time filters (Table 11) compared to the narrow band summation method when the signal duration is only about 2 seconds (Section IV.A.2: Table 7 and Appendix 2: Table A2.1).

Finally, results for similar analyses to those above but when processing background noise waveforms instead of shaped sonic booms are summarized in Figure 20 and Table 12. The filter orders and signal durations used for Figure 20 (background noise results) are like those of Figure 18 (shaped boom results). The frequency (abscissa) range is slightly larger in Figure 20 than in Figure 18 since the signal bandwidth is higher for background noise than shaped booms. Importantly, the median errors in level (red dots) of one-third-octave bands above about 16 Hz are much better behaved when using low order filters – e.g., 6th order – to process background noise waveforms (Figure 20a) than when processing shaped sonic boom waveforms (Figure 18a). This supports the supposition that the steep slopes of the shaped sonic boom spectra at high frequency can interact with the filter skirts in the stopband to cause the increase in level error observed in Figure 17 and 18a.

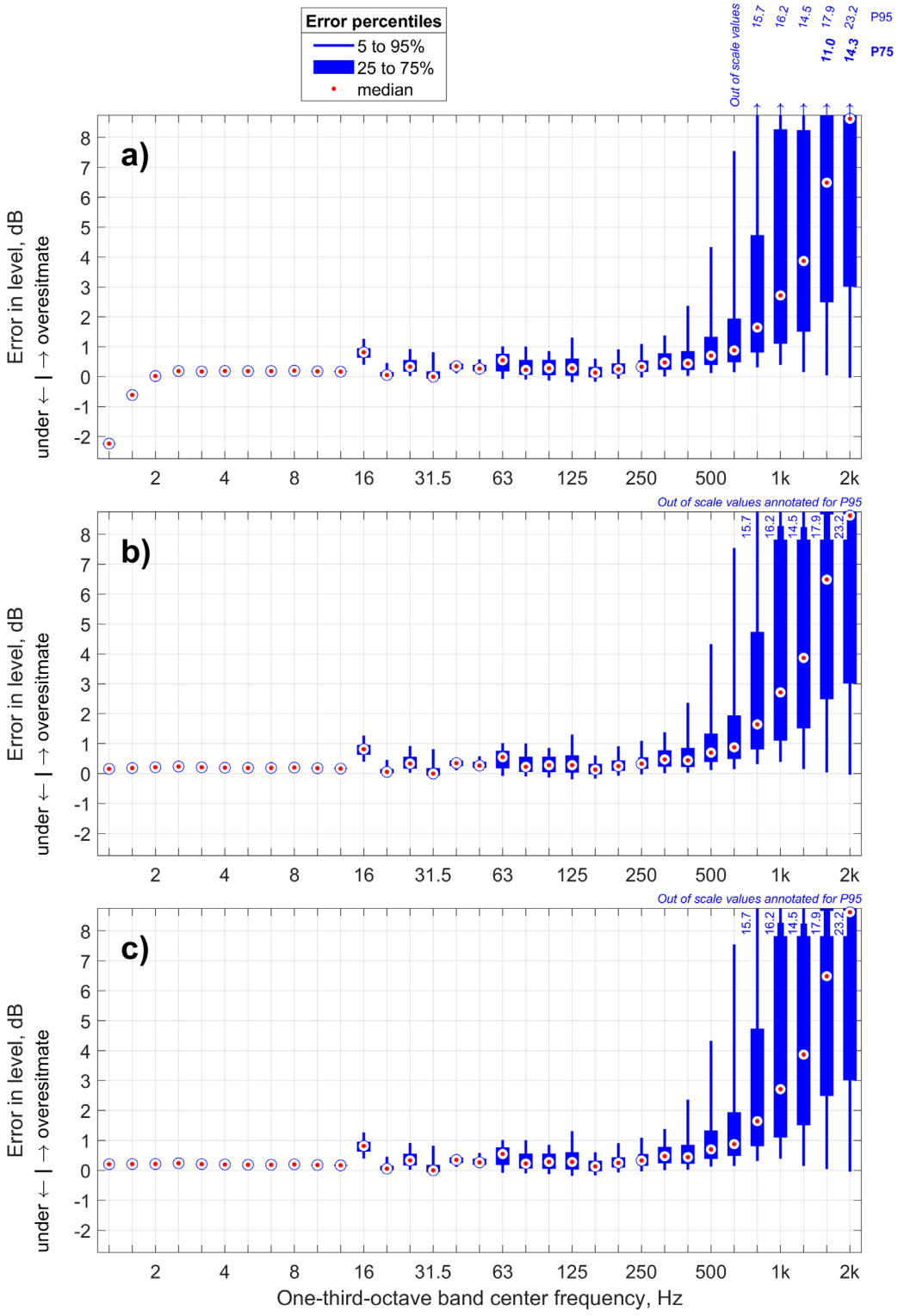

Figure 17: Spectral error observed across 3,000 X-59 sonic boom waveforms using discrete-time filters to compute OTOB levels as compared to using narrow-band summation; for 6th order filters and varying zero-padding when computing the low frequency bands: a) 2.733 s, b) 5.467 s, and c) 10.93 s.

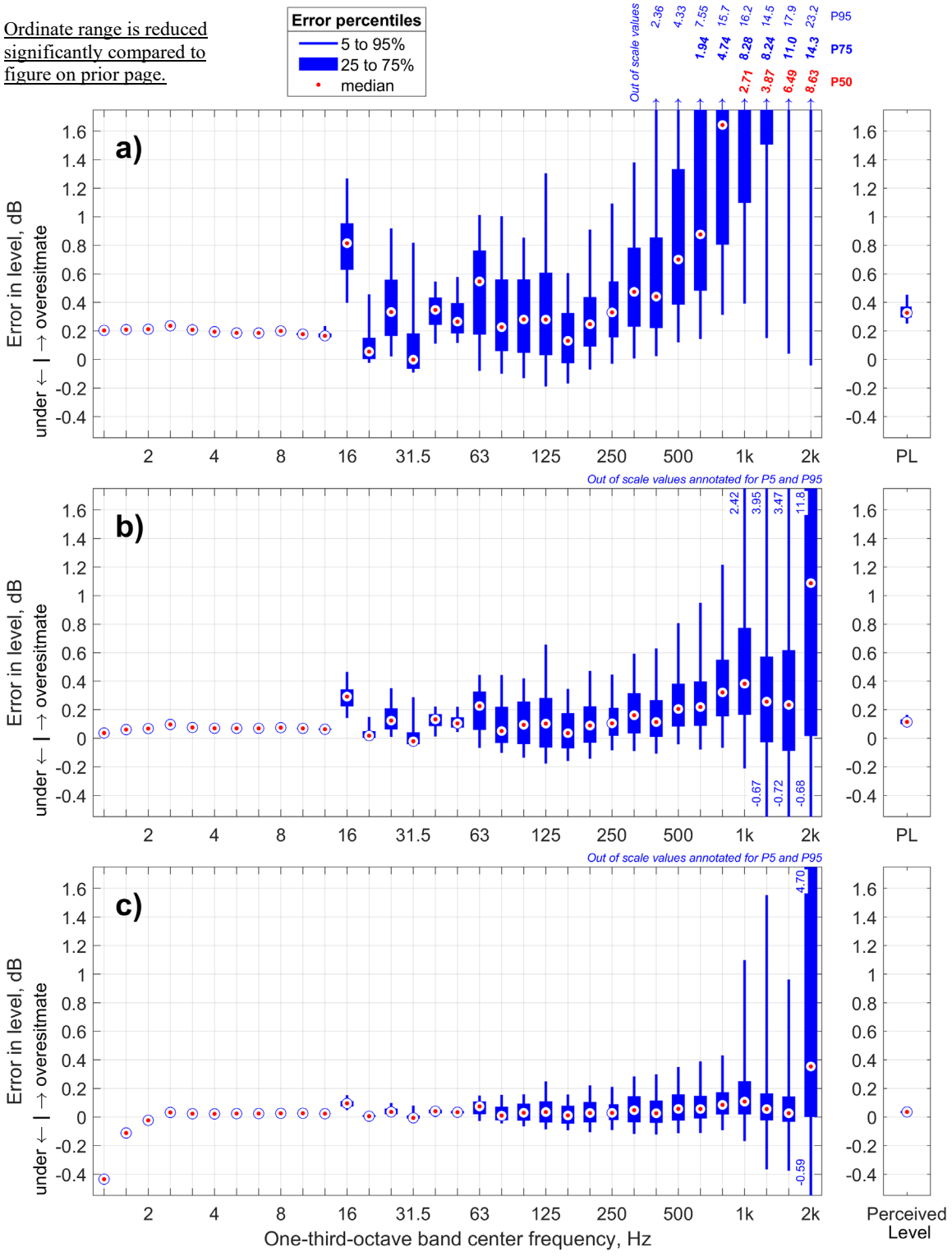

Figure 18: Spectral error (left) and error in PL (right) observed across 3,000 X-59 sonic boom waveforms using discrete-time filters to compute OTOB levels as compared to using narrow-band summation; where discrete-time filter are a) 6th order, b) 10th order, and c) 18th order.

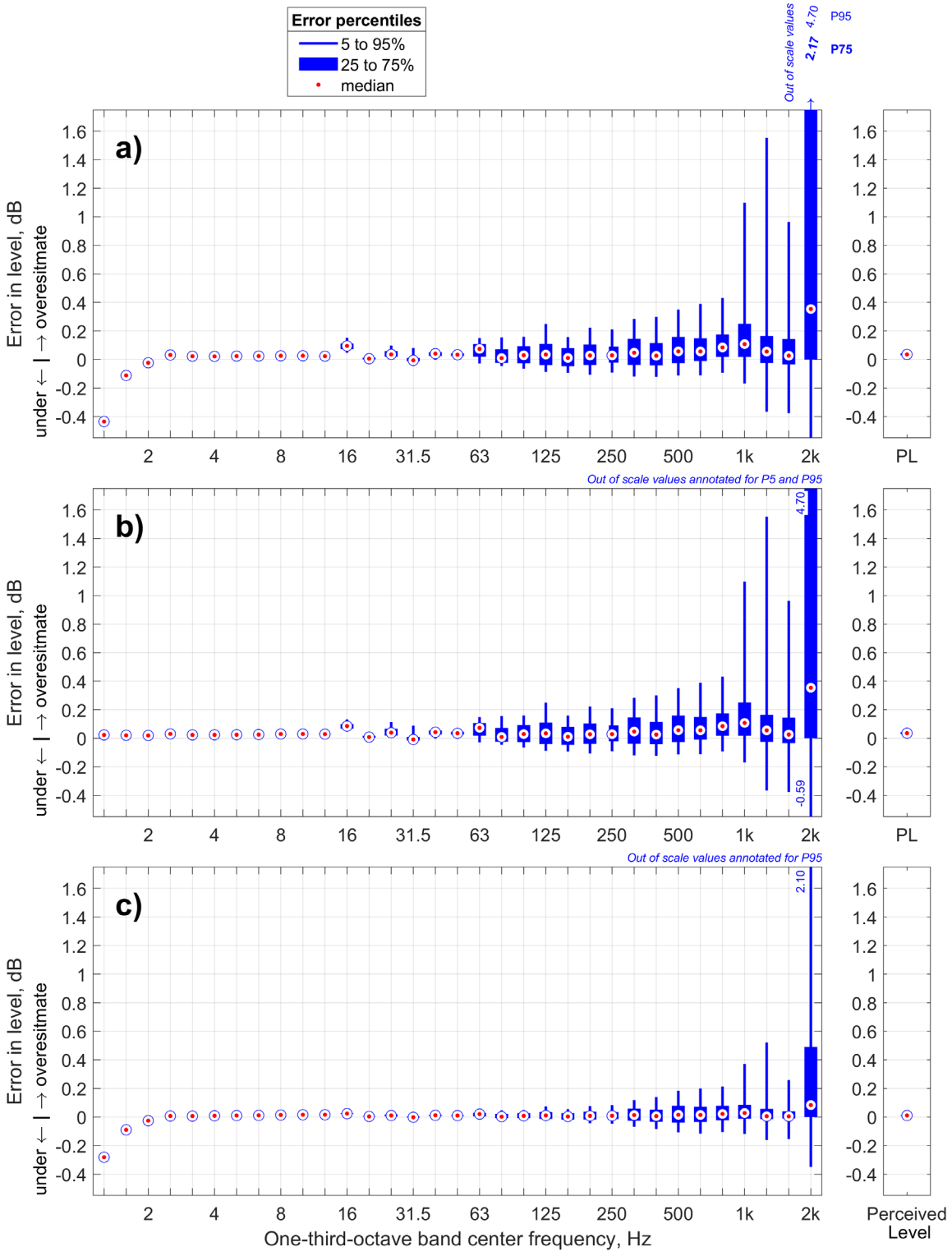

Figure 19: Spectral error (left) and error in PL (right) observed across 3,000 X-59 sonic boom waveforms using discrete-time filters to compute OTOB levels as compared to using narrow-band summation; where discrete-time filter are a) 18th order, b) 18th order with additional zero padding, and c) 34th order.

Table 11: Tabulated 5th, 50th, and 95th percentiles of error in PL for the data shown in Figures 18 to 19 (the right-hand subplots) when using discrete-time filters to compute one-third-octave band levels of 3,000 X-59 sonic booms.

Filter order	Total waveform duration, s (1.25 to 20 Hz)	Total waveform duration, s (25 Hz to 20 kHz)	5th percentile error PL, dB	50th percentile error PL, dB	95th percentile error PL, dB	Corresponds to error results from figure(s):
6	10.93	2.731	0.252	0.327	0.454	Figure 18a
10	10.93	2.731	0.0746	0.114	0.165	Figure 18b
18	10.93	2.731	0.0181	0.0352	0.0532	Figure 18c & Figure 19a
18	21.85	5.461	0.0187	0.0358	0.0540	Figure 19b
34	21.85	5.461	0.00414	0.0104	0.0169	Figure 19c

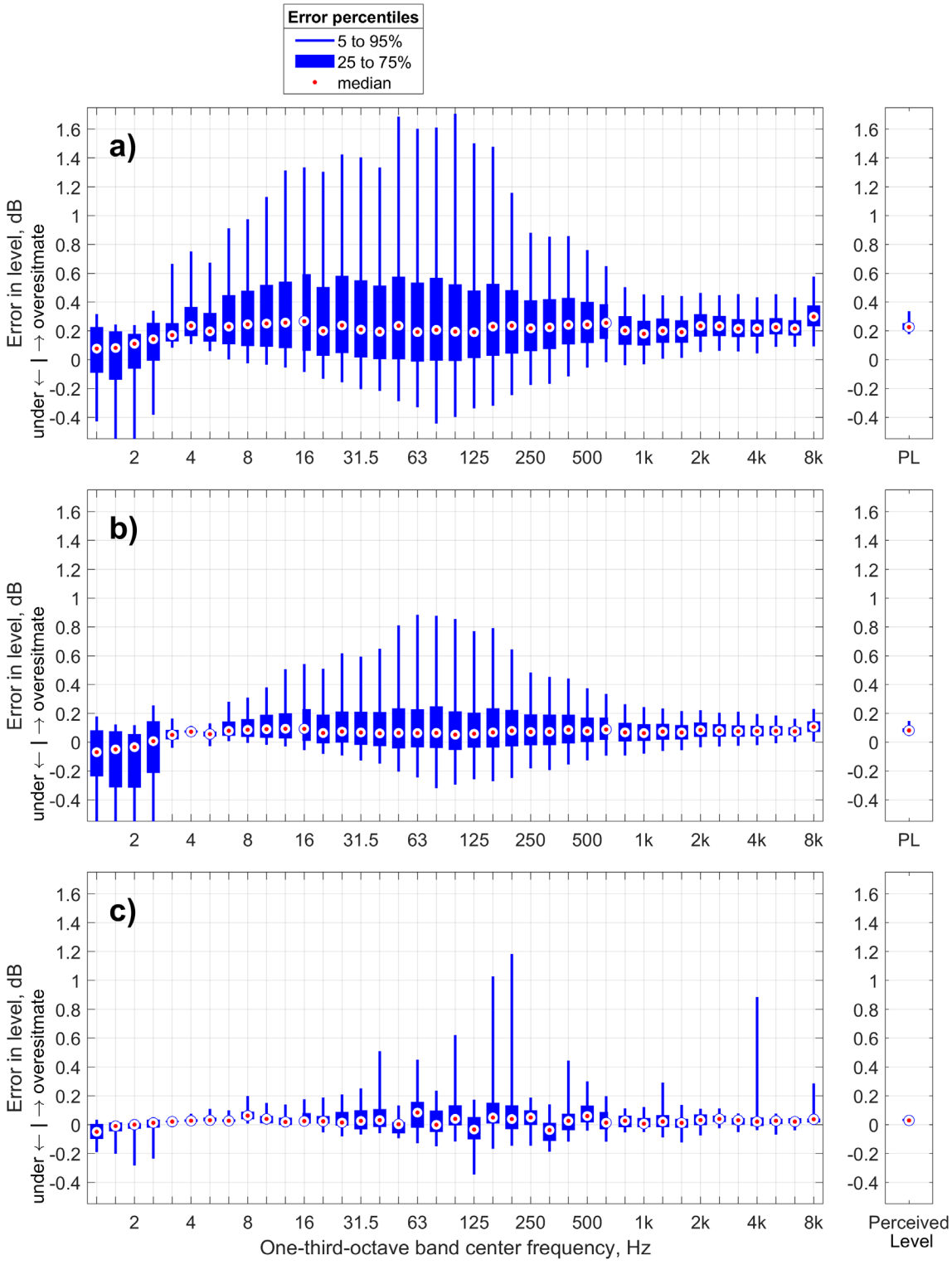

Figure 20: Spectral error (left) and error in PL (right) observed across 3,000 background noise waveforms using discrete-time filters to compute OTOB levels as compared to using narrow-band summation; where discrete-time filter are a) 6th order, b) 10th order, and c) 18th order.

Table 12: Tabulated 5th, 50th, and 95th percentiles of error in PL for the data shown in Figures 18 to 19 (the right-hand subplots) when using discrete-time filters to compute one-third-octave band levels of 3,000 background noise waveforms.

Filter order	Total waveform duration, s (1.25 to 20 Hz)	Total waveform duration, s (25 Hz to 20 kHz)	5th percentile error PL, dB	50th percentile error PL, dB	95th percentile error PL, dB	Corresponds to error results from figure:
6	10.93	2.731	0.177	0.226	0.336	Figure 20a
10	10.93	2.731	0.0520	0.0812	0.147	Figure 20b
18	21.85	5.461	0.0151	0.0290	0.0638	Figure 20c

5. Subsection summary

The narrow band summation method is documented in Appendices 1 and 2 and Section IV.A.2. This method avoids the complications identified above that are associated with choice of filter order and signal duration. It was shown in Section IV.A.2 and Appendix 2 that the narrow band summation method gives well converged results when using zero-padded signal durations as low as about 2 seconds. For example, one-third-octave band level errors were only a few hundredths of a dB at most when comparing the levels computed across 3,000 shaped sonic boom waveforms padded to a 2.7 second duration to those same waveforms padded to a 22 second duration (e.g., Section IV.A.2: Figure 13 and Appendix 2: Figure A2.5). Additionally, the errors in PL when computing levels using narrow band summation with short duration as compared to long duration shaped sonic boom waveforms were about a thousandth of a dB at most (Section IV.A.2: Table 7 and Appendix 2: Table A2.1). Results when using discrete-time filters of orders up to 34 are not that well converged (e.g., Figure 19c). Additionally, lower order discrete time filters overestimate, on average, the Perceived Level values of both shaped sonic booms and background noise by a few tenths of a dB (e.g., Tables 11 and 12). Finally, the computational time when using the narrow band summation method is significantly faster than when using high order discrete-time filters – typically an order of magnitude or better. For these reasons, narrow band summation is recommended.

B. Errors resulting from algorithm used to compute loudness spectrum

1. Subsection overview

The algorithm used to compute the loudness spectrum is studied in this subsection. Table 13 summarizes the algorithms used for each of the four main computational steps when computing both the true levels and the inexact levels (see also Table 3). In all cases in this subsection, the narrow band summation method is used to find the one-third-octave band levels in the initial step of the computation of Perceived Level (Table 13 and Figure 1). Then, the loudness spectra for true levels are computed using the methods recommended by Jackson and Leventhall [7], while the loudness spectra for inexact levels are approximated using interpolation between the equal loudness contours derived from information in Ref [2]. Importantly, the first and the last two computational steps use the recommended algorithms when computing the true and inexact levels.

Table 13: Algorithms used to compute true levels and inexact levels in subsection IV.B.

	True levels:		***Inexact levels:***	
Computational step	**Rec. algorithm**	**Non-rec. algorithm**	**Rec. algorithm**	**Non-rec. algorithm**
1: OTOB sound pressures	✓		✓	
2: Loudness spectrum	✓			✓
3: Level-amplitude conversions	✓		✓	
4: F(S) table values	✓		✓	

The interpolant values and the interpolation algorithm for the second computational step of inexact levels were adapted from a deprecated PCBoom software routine[8] that computed Perceived Level. The interpolant is formed for the twenty-seven unique sone values in Table 14. The PCBoom algorithms, and the associated data tables, were transcribed into a MATLAB® function for the evaluations presented here. Within the routine, an equal loudness contour is constructed for each of the twenty-seven sone values in Table 14, where each contour spans one-third-octave bands from 1.00 Hz to 12.5 kHz. A plot of the resulting interpolant is shown in Figure 21 (solid lines), which is similar to Fig. 1 in Ref. [2]. The sone value for each equal loudness contour are annotated along the right-hand side of the figure. For example, the lowest solid line (purple color) corresponds to the 0.3 sone equal loudness contour. Erroneous results when using this original interpolant (Figure 21, solid lines) are discussed in Subsection IV.B.2.

Table 14: List of loudness values, sone, that are used to form the interpolant that is used to compute the loudness spectrum of inexact levels.

Sone	0.3	0.4	0.6	1	1.5	2	3	4	6
Sone	8	10	15	20	30	40	60	80	100
Sone	150	200	300	400	600	800	1000	1500	2000

[8] The source of the software routine for the interpolation algorithm is PCBoom version 7.1. Versions of PCBoom after 7.1 use an updated PL computation routine that implements all recommended algorithms listed in Table 3. Those updated include using the Jackson and Leventhall method [7] instead of interpolation.

Also plotted in Figure 21 is an example shaped sonic boom spectrum. The one-third-octave levels are indicated as dots. Frequency bands with levels below the 0.3 sone equal loudness contour (Figure 21, points annotated in red text) were excluded from the interpolation result and assigned a loudness value of 0 sone. Because the deprecated routine did not consider contours below the 0.3 sone contours, the error in PL may increase for quiet sounds like shaped sonic booms since some of these points may have non-zero loudness values. Consequently, the effects of refining the interpolant using three additional equal loudness contours was also investigated here.

The refined interpolant included the contours for 0.07, 0.142, and 0.199 sone (dashed lines in Figure 21) in addition to those listed in Table 14 (Figure 21, solid lines). For the example spectrum in Figure 21, two additional points (red arrow annotations) will have loudness value estimates assigned when using the refined interpolant compared to the original interpolant. Thus, one might expect less error when using the refined interpolant compared to the original interpolant since residual loudness, the $(\sum S_i - S_m)$ term in Eq. (5), will be slightly larger when using the refined interpolant so should better match the proper value. Error results using this refined interpolant (Figure 21, solid and dashed lines) are discussed in Subsection IV.B.3 below.

Linear interpolation is used to estimate the sone values corresponding to all the frequency-level pairs in a one-third-octave band SPL spectrum that fall between two equal loudness contours. For example, black arrows in Figure 21 indicate two example data points relating frequency, level, and loudness. Importantly, errors may be introduced by the interpolation algorithm due to non-linear behavior of the equal loudness contour interpolant. For example, the change in loudness with SPL is not linear below 400 Hz – as evident by the changing slopes of the equal loudness contours in this frequency range. Thus, using linear interpolation for the spectral points that fall between the contours in this frequency range is expected to introduce variable error in the estimated loudness value. Additionally, the values used for the interpolant are imprecise because they are only reported to three or four significant figures, which is also expected to introduce variable amounts of error in computed loudness values. Consequently, these first two types of error will have a variable (non-bias) effect on the computed PL value. Finally, all spectral points falling below the lowest contour are ignored when using this interpolation method since they are assigned a loudness value of 0 sone. This third type of error will cause the total loudness to be underestimated (a bias effect).

In contrast, those three types of error are not expected to be present when using the Jackson and Leventhall method since the method uses geometric constructions to compute the exact equal loudness contour that passes exactly through each unique frequency-level pairing in the SPL spectrum. For example, to find the loudness level for one of the example points annotated in Figure 21, the Jackson and Leventhall method would construct the equal loudness contour that passes through the point at 200 Hz and 51.4 dB using the known contour slopes and frequency break points. The method would then construct the equal loudness contour passing through 160 Hz and 60.7 dB to find the loudness of the second example point, repeating that process for all points in the spectrum. Consequently, the interpolation algorithm discussed above is not expected to be as accurate as the algorithm presented by Jackson and Leventhall [7], which is why the latter method is recommended and used to compute the true levels here.

To investigate whether further refinement to the interpolation algorithm may better match the Jackson and Leventhall method, a very fine interpolant was created from ninety equal loudness contours (Figure 22). The spacing for the equal contours in that figure are logarithmic and equally spaced in sone values, ranging from 0.005 to 2000 sone. This results in a much finer spacing than the coarse spacing for the interpolant in Figure 21. Less error is expected when using the fine spacing (Figure 22) as compared to the coarse spacing (Figure 21). Error results when using this finely spaced interpolant are discussed in Subsection IV.B.4 below.

Importantly, a computational bug was discovered in the PCBoom interpolation algorithm[8] during the evaluations here, which will affect PL values that are computed and reported by PCBoom version 7.1 and earlier. This bug was corrected when generating the error results discussed below (Subsections IV.B.2 to IV.B.4). The cause and effects of this bug are documented briefly in Subsection IV.B.5 below, which may be useful for users of prior versions of PCBoom. This bug does not affect PCBoom versions 7.2 and later since the affected routine was revised in these later versions to use all algorithms recommended herein. That update removed this interpolation algorithm from the software and replaced it with the Jackson and Leventhall method.

Summarizing, errors in PL when using interpolation algorithms to find the loudness spectrum are documented in Subsections IV.B.2 to IV.B.5 below. Errors are computed relative to loudness values computed using the Jackson and Leventhall method. Because the error is expected to vary based on implementation, several interpolants are evaluated in the next subsections:

- IV.B.2: Error when using original interpolant with 27 equal loudness contours,
- IV.B.3: Error when using refined interpolant with 30 equal loudness contours,
- IV.B.4: Error when using an interpolant with 90 equal loudness contours, and
- IV.B.5: Cause and effects of bug identified in PCBoom 7.1 Perceived Level algorithm.

In all cases, the precursor one-third-octave band sound pressure spectrum is computed using the narrow band summation method and the recommended algorithms are used for the final two computational steps.

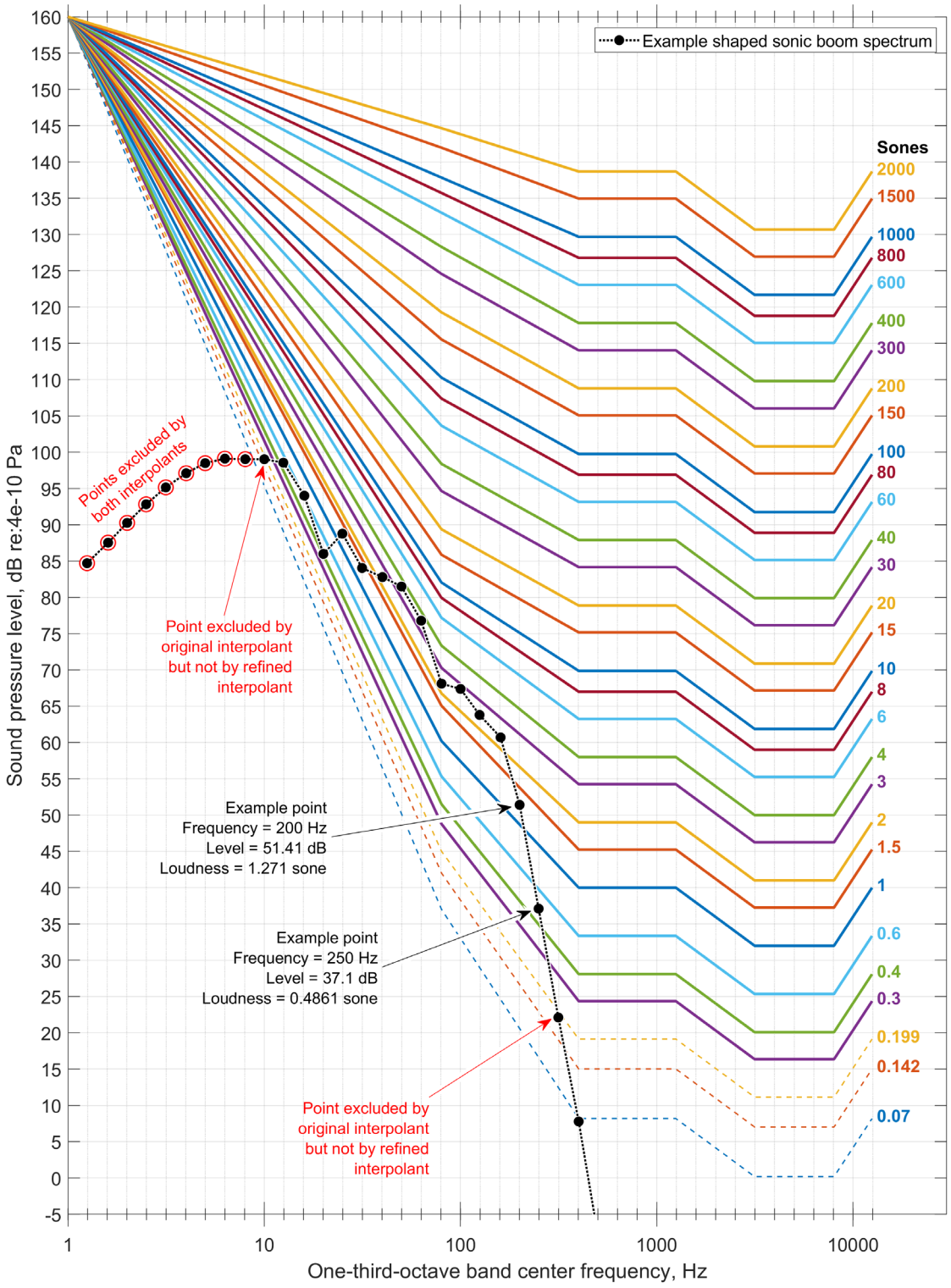

Figure 21: Equal loudness contours that form the interpolant (the non-recommended algorithm) that is used to estimate the loudness spectrum of inexact levels; where solid contours are original interpolant (Subsection IV.B.2), the three dashed contours are included in a refined interpolant (IV.B.3), and an example shaped sonic boom spectrum.

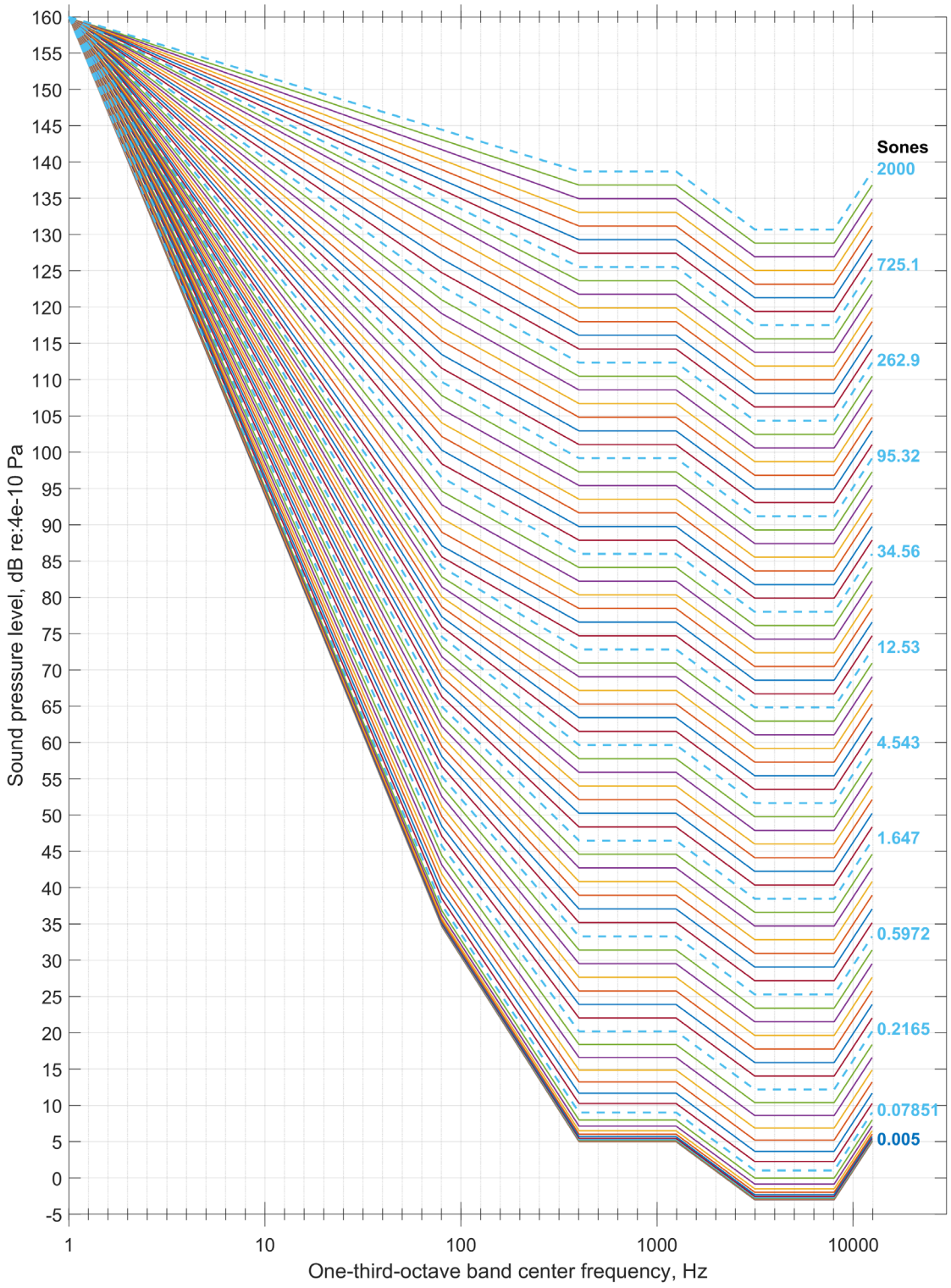

Figure 22: Ninety equally- and logarithmically-spaced equal loudness contours; used as a finely spaced interpolant for inexact levels in Subsection IV.B.4.

2. Error when using original interpolant with 27 equal loudness contours

Error results presented in this subsection are when using the original interpolant (Figure 21, solid lines only) to find inexact values. Additionally, the coding bug that was mentioned above was fixed for all data presented in this subsection.

Distributions of error in Perceived Level across the 3,000 X-59 shaped sonic booms (Subsection III.A.1) and the 3,000 background noise waveforms (Subsection III.A.2) are summarized as a histogram in Figures 23 and 24 below for that original interpolant. Additionally, the 5th, median, and 95th percentiles for PL error are identified in Figures 23 and 24 for the shaped sonic boom waveforms and the background noise waveforms, respectively. These percentiles are computed across the 3,000 waveforms in each set. The range between the 5th and 95th percentile, $\Delta_{P95\text{-}P5}$, is also annotated in those figures. Importantly, errors in level are always presented as the difference of the inexact levels minus the true levels, so a positive error indicates the non-recommended algorithm – interpolation within the equal loudness contours – overestimates the true level. Similar figures are included in IV.B.3 to IV.B.5 that document the error results for the other interpolants.

The error in PL is lower for shaped sonic booms than for background noise (Figure 23 versus 24). For example, the median error for shaped sonic booms when using interpolation to determine the loudness spectrum is about −0.061 dB and the range between the 5th and 95th percentile is about 0.122 dB (Figure 23). For comparison, the median and range for the background noise waveforms is −0.059 and 0.367 dB, respectively (Figure 24). Thus, the use of the original interpolation algorithm is expected to produce modest error in PL. These observed errors in PL are of the same order as, or slightly smaller than, those observed in the previous Section, e.g., Table 11 in IV.A, where the effects of using discrete-time filters to compute one-third-octave band levels were studied.

The error observed when using interpolation, as compared to the Jackson and Leventhall method, can be a few tenths of a dB in some cases. It may be possible to improve upon the interpolation algorithm used here by including contours below 0.3 sone or including more equal loudness contours in the interpolant. Behavior of error as those improvements to the interpolant are made is discussed in the next two subsections.

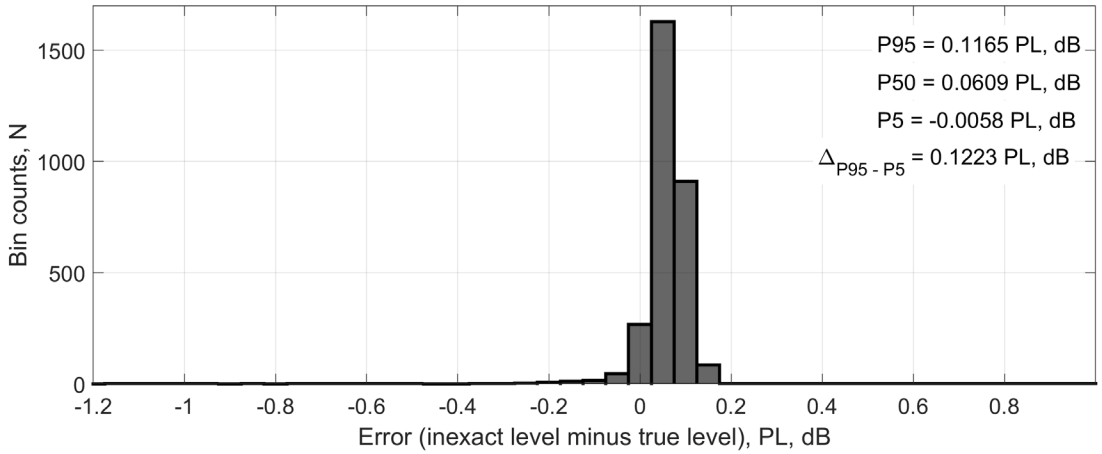

Figure 23: Error in PL across 3,000 X-59 sonic boom waveforms, loudness spectrum for inexact values computed when using the original interpolant (Figure 21, solid lines only).

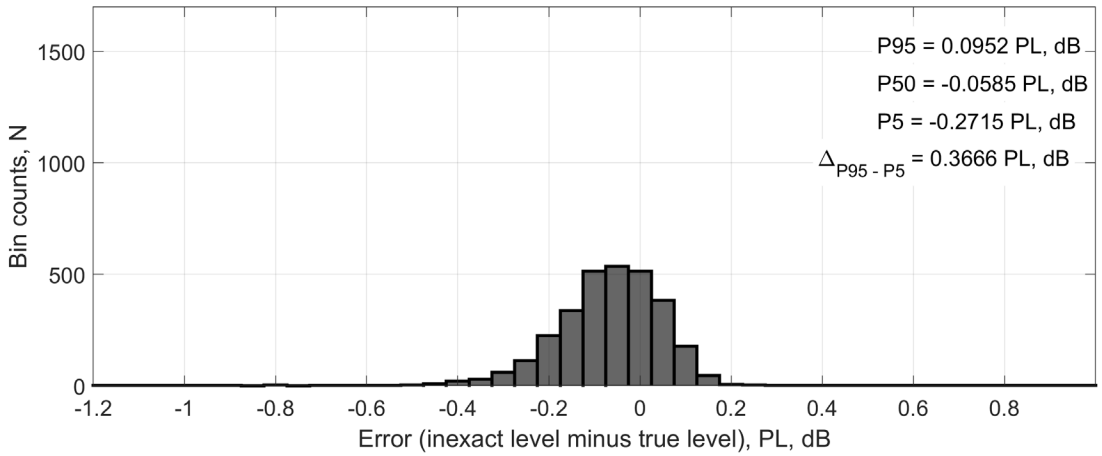

Figure 24: Error in PL across 3,000 background noise waveforms, loudness spectrum for inexact values computed when using the original interpolant (Figure 21, solid lines only).

3. Error when using refined interpolant with 30 equal loudness contours

Error results presented in this subsection are when using the refined interpolant (Figure 21, solid and dashed lines) to compute inexact values. This interpolant has additional equal loudness contours included at 0.07, 0.142, and 0.199 sone. The coding bug that was mentioned above was fixed for all data presented in this subsection.

Distributions of error in PL across the 3,000 X-59 shaped sonic booms (Subsection III.A.1) and the 3,000 background noise waveforms (Subsection III.A.2) are summarized as a histogram in Figures 25 and 26 below for the refined interpolant Figure 21 (solid and dashed lines). The error when considering the X-59 waveforms is mostly unchanged when using the refined interpolant (Figure 25) as compared to using the original interpolant (Figure 23). The median is slightly larger in this case, 0.124 versus 0.061 dB, but the range between the 5th and 95th percentile, $\Delta_{P95\text{-}P5}$, is about the same 0.123 dB. However, there is a modest reduction of error when considering the background noise waveforms – comparing Figure 26 to Figure 24. The range in error between the 5th and 95th percentile is reduced from 0.367 to 0.228 dB. This suggests that the loudness spectrum of background noise found using interpolation is more susceptible than that of shaped sonic booms to errors caused by omission of low-level equal loudness contours.

The modest error that is still observed in both histograms (Figures 25 and 26) may be caused by two effects: 1) the use of linear interpolation between the equal loudness contours, and 2) the precision of the table data that defines the coarse contours shown in Figure 21. For example, the data tables that were adapted from PCBoom 7.1 for use here were defined with only four significant digits. These two items are refined in the next subsection where error when using a finely spaced interpolant are documented.

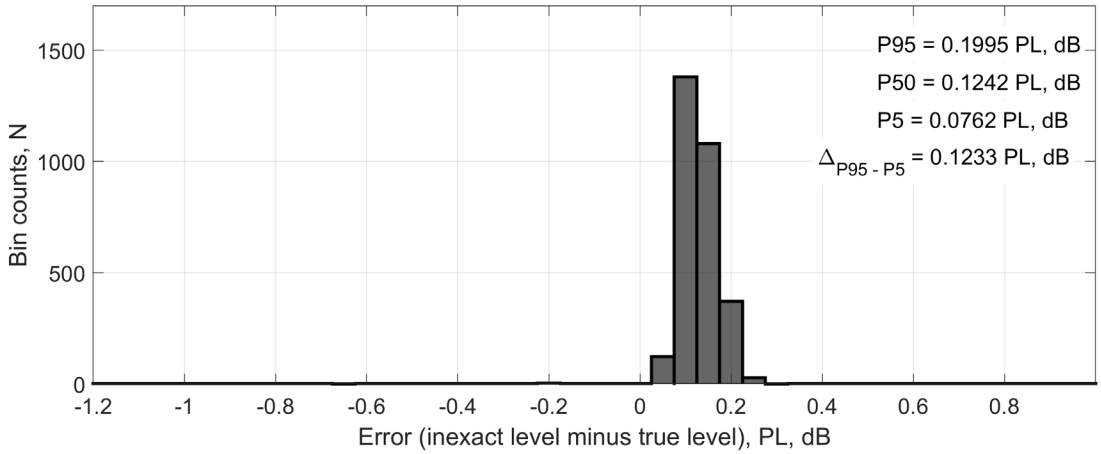

Figure 25: Error in PL across 3,000 X-59 sonic boom waveforms, loudness spectrum for inexact values computed when using the refined interpolant (Figure 21, solid and dashed lines).

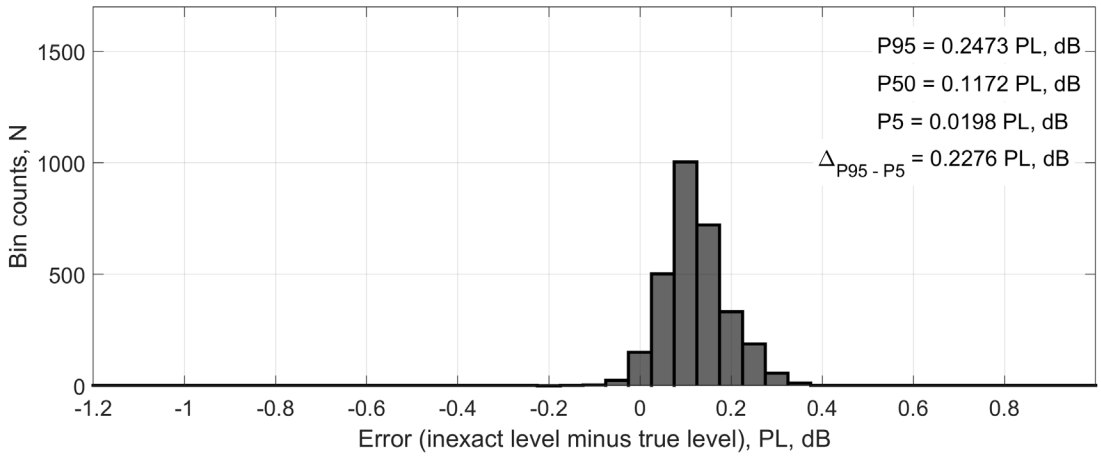

Figure 26: Error in PL across 3,000 background noise waveforms, loudness spectrum for inexact values computed when using the refined interpolant (Figure 21, solid and dashed lines).

4. Error when using an interpolant with 90 equal loudness contours

Error results presented in this subsection are when using the finely spaced interpolant (Figure 22) to compute inexact values. The values for those equal loudness contours were computed using the Jackson and Leventhall method and are defined using double precision values – as compared to only four significant digits for the contours shown in Figure 21 that were used in the prior two subsections. Thus, improved accuracy is expected due to both improved precision and a more finely spaced interpolant. Additionally, the coding bug that was mentioned above was fixed for all data presented in this subsection.

Distributions of error in PL across the 3,000 X-59 shaped sonic booms (Subsection III.A.1) and the 3,000 background noise waveforms (Subsection III.A.2) are summarized as a histogram in Figures 27 and 28 below for the finely spaced interpolant (Figure 22). The error is very small for this interpolant, where errors of only a few hundredths of a dB are observed for both the X-59 sonic booms and the background noise waveforms (Figures 27 and 28, respectively). Thus, interpolation can provide reasonably accurate results. However, the computational time tends to be much higher when using interpolation with a very finely spaced interpolant (e.g., Figure 22) to estimate the loudness spectrum as compared to using the closed-form Jackson and Leventhall method. Thus, interpolation is not recommended even if well converged results can be obtained with a finely spaced interpolant.

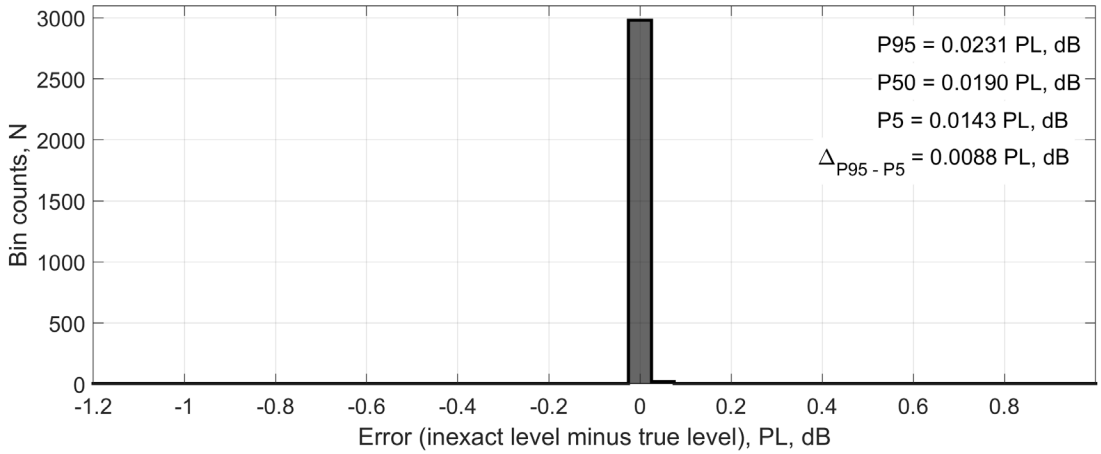

Figure 27: Error in PL across 3,000 X-59 sonic boom waveforms, loudness spectrum for inexact values computed when using the refined interpolant (Figure 22).

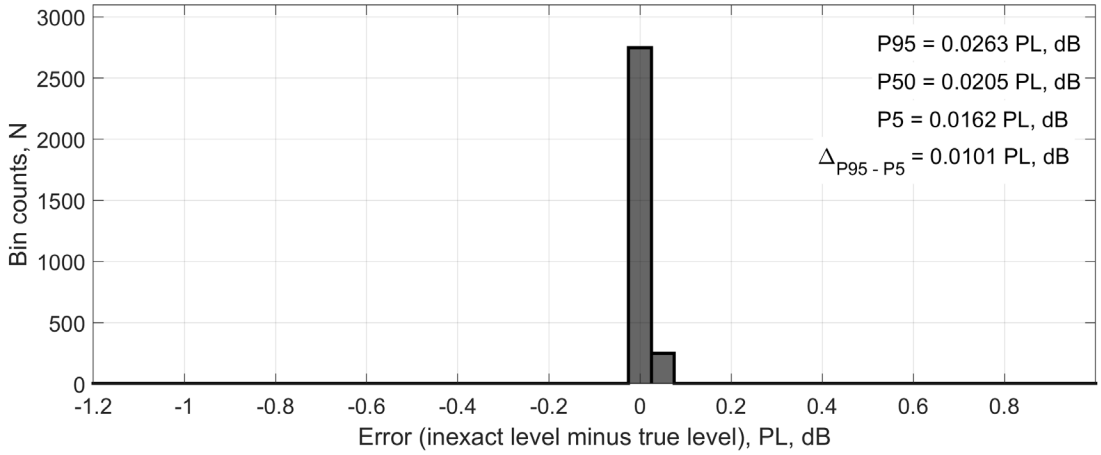

Figure 28: Error in PL across 3,000 background noise waveforms, loudness spectrum for inexact values computed when using the finely spaced interpolant (Figure 22).

5. Cause and effects of bug identified in PCBoom 7.1 Perceived Level algorithm

During the evaluations documented above, a minor "off-by-one" bug was discovered in the software routine that implemented the interpolation algorithm, which was taken from PCBoom version 7.1[8]. The bug was related to the indexing of one-third-octave band numbers, where a band index of 1 (the 1.25 Hz band) was incorrectly used as the band where equal loudness contours converge to a point at 160 dB when computing the interpolant. The proper band index is 0 (the 1.00 Hz band) for that convergence point (e.g., see Figures 21 and 22). The error caused the slopes of the equal loudness contours below 80 Hz to be incorrect, resulting in an underestimate in the loudness spectrum in that frequency range when the bug was present. The purpose of this subsection is to document the bug and provide data to show its effect. The proper interpolant for results presented in this subsection are shown in Figure 21 (solid lines only); the bug caused the convergence point at 160 dB to fall at 1.25 instead of 1.00 Hz.

Importantly, errors in level are always presented as the difference of the inexact levels minus the true levels, where true levels are when the Jackson and Leventhall method is used to compute the loudness spectrum. A positive error indicates the non-recommended algorithm – interpolation within the equal loudness contours – overestimates the true level. Error results are shown when inexact levels are computed both with the bug fixed and with the bug present.

Distributions of error in Perceived Level across the 3,000 X-59 shaped sonic booms (Subsection III.A.1) and the 3,000 background noise waveforms (Subsection III.A.2) are summarized as a histogram in Figures 29 and 30 below for analysis cases both with the bug fixed (subplot a) and with the bug present (subplot b). For the shaped sonic booms, the error is increased when the bug is present. For example, the median error changes from about +0.061 to −0.416 dB and the range between the 5th and 95th percentile, $\Delta_{P95\text{-}P5}$, changes from 0.122 to 0.579 dB (Figure 29). Inspecting the tail of the distribution in Figure 29, errors can be quite high, where the 5th percentile error is −0.828 dB and errors over 1.0 dB are occasionally observed. Consequently, the effect of this bug on the PL of shaped sonic boom noise is not minor and could be of consequence for users of PCBoom versions 7.1 and earlier, which motivated inclusion of these results here.

Interestingly, the effect of the bug on PL values of background noise is not as impactful. For example, the two error distributions shown in Figure 30 are very similar. Thus, the bug is expected to primarily affect sonic boom noise.

Additionally, the bug only affects the loudness spectrum in bands below 80 Hz. Consequently, it is expected that PL values of traditional N-wave sonic booms will not be as affected as shaped sonic booms (e.g., Figure 29) because higher frequency bands will be more dominant for N-waves than shaped booms. Characterizing the error in PL of N-wave due to this software bug was not done here and is left to future work, if desired.

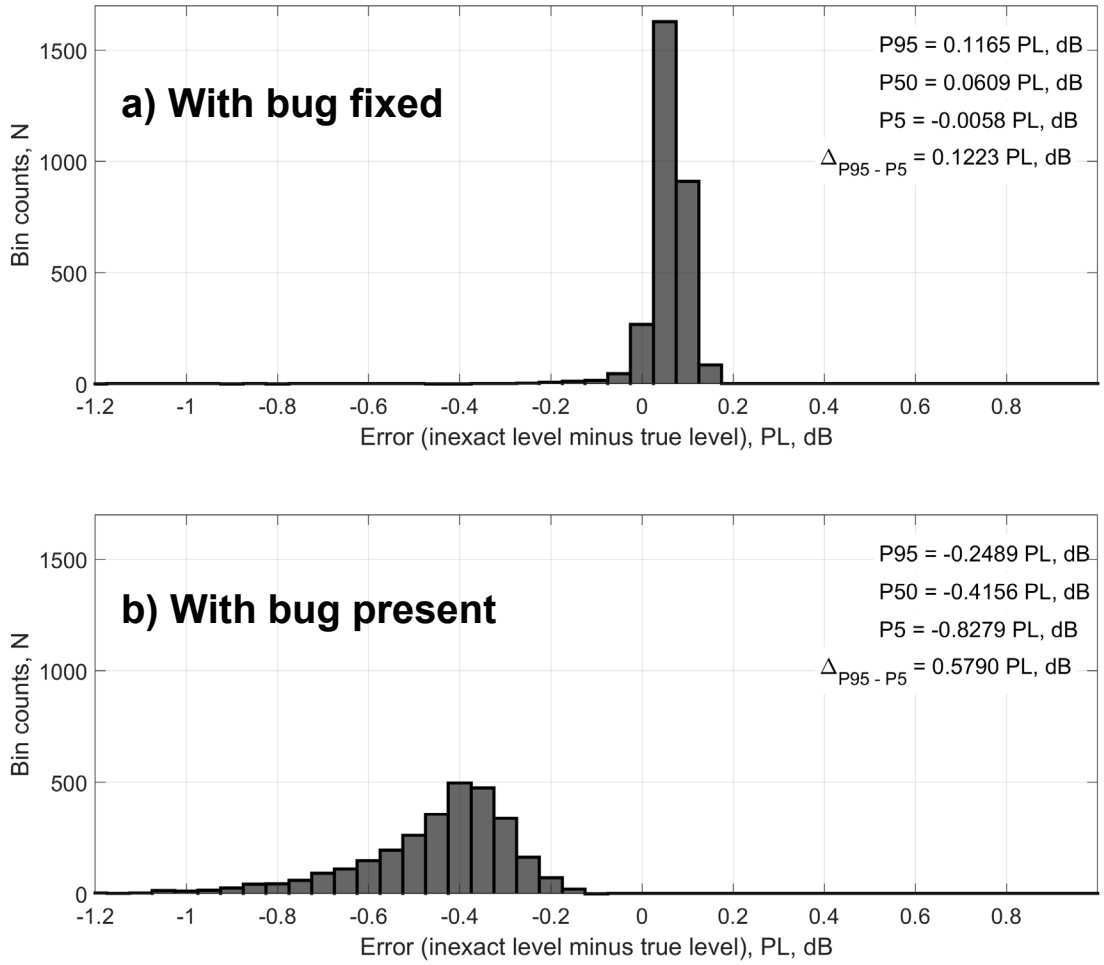

Figure 29: Error in PL across 3,000 X-59 sonic boom waveforms showing the effects of fixing the bug in the PCBoom version 7.1 PL software routine; where a) is identical to Figure 23.

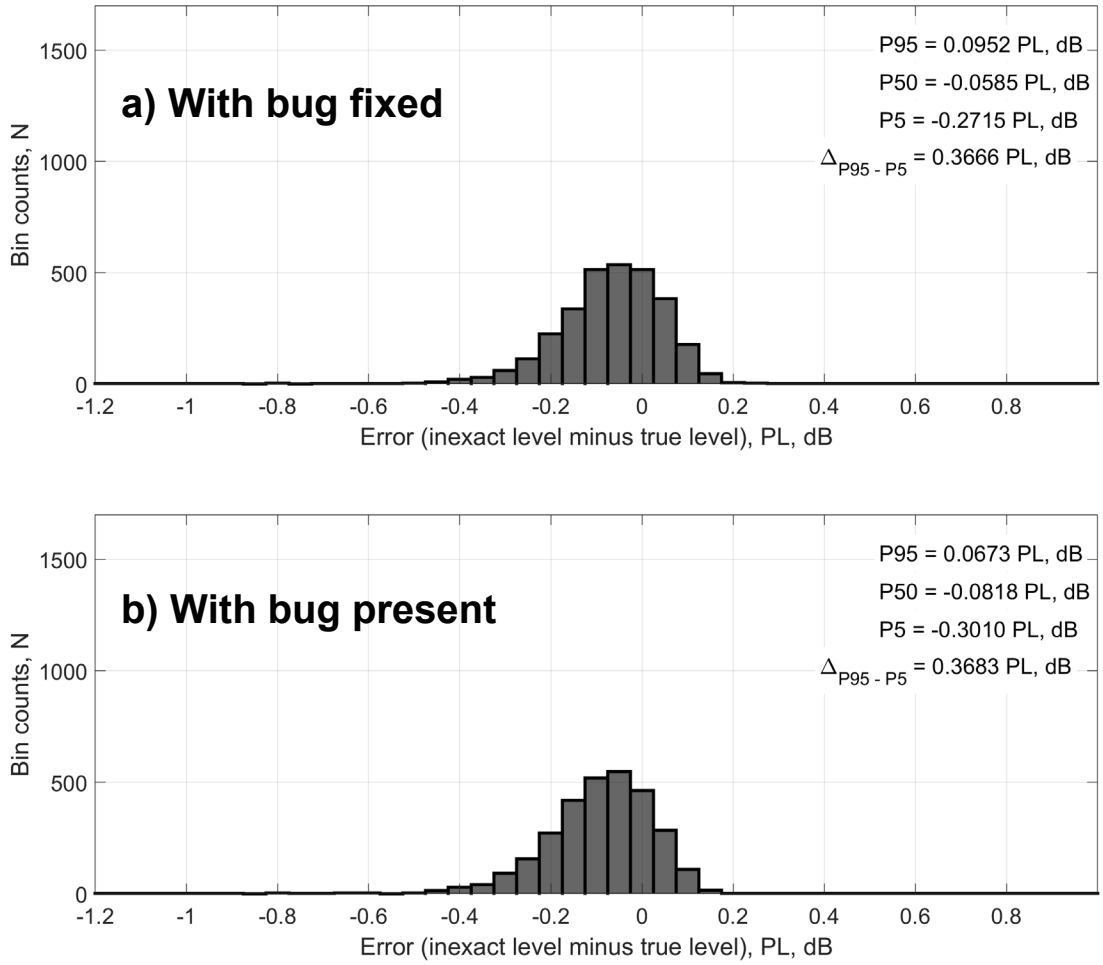

Figure 30: Error in PL across 3,000 background noise waveforms showing the effects of fixing the bug in the PCBoom version 7.1 PL software routine; where a) is identical to Figure 24.

6. Subsection summary

The error observed when comparing the non-recommended algorithm–interpolation – for finding the loudness spectrum is sensitive to the interpolant that is used. Initially, the interpolant from PCBoom 7.1 and earlier was evaluated, where modest error was observed for sonic booms and background noise (Subsection IV.B.2). This is due to the coarse spacing of the equal loudness contours and the limited precision to which the interpolant table was defined in that subsection. Refinements to the interpolant will improve error (Subsections IV.B.3 and IV.B.4). For example, error is reduced from a few tenths of a dB when using the original interpolant (IV.B.2) to a few hundredths of a dB when using the finely spaced interpolant (IV.B.4).

Importantly, the closed form Jackson and Leventhall method avoids these choice-based inaccuracies. Additionally, NASA has found that the Jackson and Leventhall method is more computationally efficient than interpolation. Consequently, interpolation is not recommended, and the method proposed by Jackson and Leventhall is recommended for use when converting an input SPL spectrum to a loudness spectrum.

C. Attenuation of the waveforms used for error evaluations

1. Motivation

In the next two subsections, the errors in Perceived Level associated with the following computational steps are investigated:

- IV.D: Errors related to the equations used to convert between level and amplitude, and
- IV.E: Errors related to the weighting table used to compute total loudness.

These are related to the algorithm choices discussed in Sections II.C and II.D, respectively. Using the non-recommended algorithms for these two computational steps was not found to produce large error when computing loudness levels of X-59 shaped sonic booms that are expected within the primary sonic boom carpet[9]. For reference, the primary carpet is the area underneath the aircraft where shock waves propagating away from the bottom of the aircraft reach the ground directly. However, the algorithmic changes discussed in Sections II.C and II.D are expected to produce errors in loudness level when noises are very low in level. Thus, these changes may become important when computing loudness levels of secondary noises associated with supersonic overflight.

For example, sounds much quieter than X-59 carpet booms may be observed in the shadow region that occurs beyond Mach cutoff[9], where evanescent waves can reach the ground several 10s of miles to the side of the aircraft trajectory. Very quiet sounds may also occur with "over-the-top" sonic booms, where the shock waves that propagate upward from the top of the aircraft eventually refract downward and impact the ground possibly hundreds of miles away from the aircraft trajectory[9]. It might be useful for analysts to record these, or similar, very quiet sounds and then quantify the noise levels using the PL calculation since people will experience, and may react to, these noises. Consequently, it is useful to quantify the algorithm-induced error in PL that may be expected in these use cases.

To assess the errors when sound levels are very low, the 3,000 predicted on-design X-59 waveforms that were documented earlier in Section III.A.1 are artificially attenuated to approximate the quieter sounds that might be expected in the propagation cases discussed in the previous paragraph. A scale factor of either 0.100 or 0.0316, corresponding to gains of either −20 or −30 dB, respectively, is applied to the waveforms before computing loudness levels and the associated errors. The attenuation value used will be documented alongside error results in Sections IV.D and IV.E. Those two attenuation values were chosen arbitrarily, so they only demonstrate the effect on error of noises with a reduced sound level. Importantly, the on-design X-59 waveforms from Section III.A.1 are carpet boom waveforms, so this is only a crude approximation of the error associated with quiet sounds that may occur either in the Mach cutoff region or from over-the-top sonic booms. Results associated with the attenuated waveforms cannot be attributed to any real-world propagation scenario.

Additionally, it is not known how representative the noise levels observed during the QSF18 dataset – discussed in Section III.A.2 – are to those of future field tests. Future field tests conducted by NASA or others in the supersonics community may have lower

[9] See Chapter 1 and Figures 1.2 and 1.3 and Chapter 2 in Ref. [15] for a discussion of the primary versus secondary boom carpet, Mach cutoff, and over-the-top sonic booms.

background noise levels than were observed in the QSF18 test, which may affect error levels when computing the PL of background noise. Consequently, error in PL is studied while also scaling the background noise levels from Section III.A.2 by 0.100, a gain of −20 dB.

2. Loudness levels of unattenuated versus attenuated waveforms

The distribution of true loudness levels is compared for the unattenuated waveforms versus the attenuated waveforms for the X-59 sonic booms and the background noise waveforms in Figures 31 and 32, respectively. The distribution of loudness levels is both lower in level and wider in range for the attenuated cases (e.g., Figure 31b and c) than the unattenuated cases (e.g., Figure 31a). Importantly, the shift is not exactly proportional to the gain that was applied to the waveforms, −20 or −30 dB in the case of the shaped booms. This is because the weightings that are used to compute Perceived Level are not linear so scaling the waveforms by −20 dB, for example, does not reduce the loudness level by exactly that amount. Reductions depend on both the spectral content and the scaling factor. In many instances, the reduction in PL will be larger than the attenuation applied to the waveforms, which causes the attenuated distributions to be wider than the unattenuated distributions (e.g., Figure 31a versus 31c).

Loudness level error results will be discussed in the next two subsections for both the unattenuated and attenuated waveform cases.

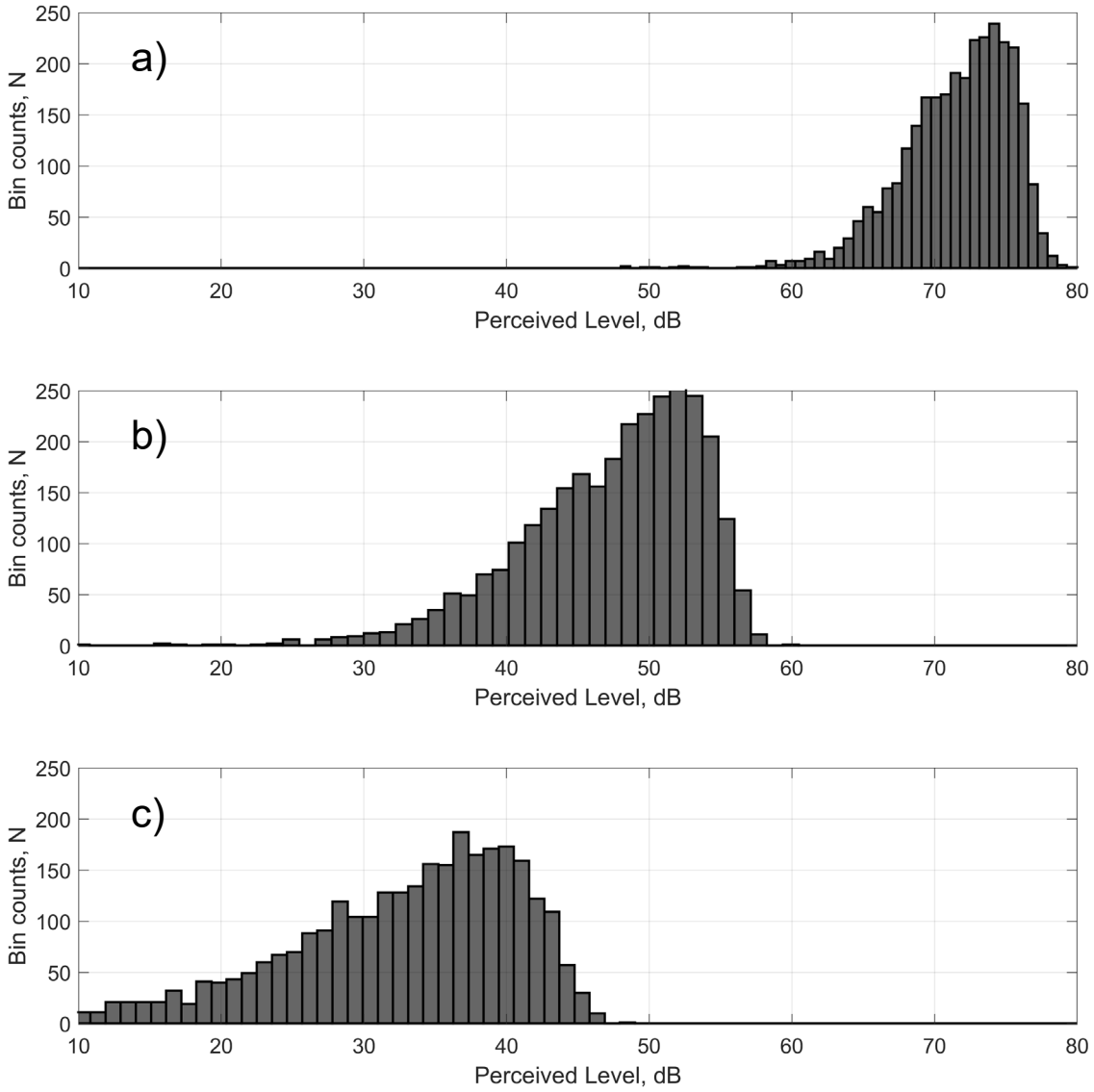

Figure 31: Distribution of PL across 3,000 X-59 sonic boom waveforms when the waveform amplitude is: a) unattenuated (same as Figure 6 in Section III.A.1), b) scaled by factor of 0.100 (−20 dB gain), and b) scaled by 0.0316 (−30 dB gain).

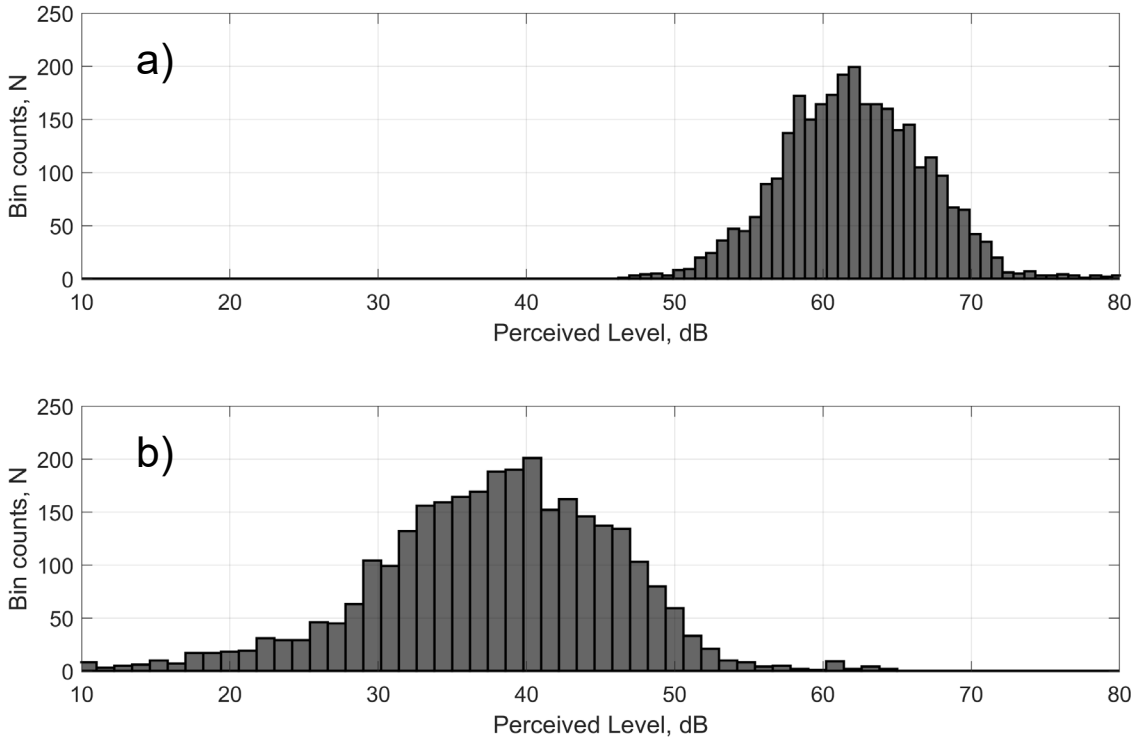

Figure 32: Distribution of PL across 3,000 background noise waveforms when the waveform amplitude is: a) unattenuated (same as Figure 10 in Section III.A.2), and b) scaled by a factor of 0.100 (−20 dB gain).

D. Errors related to the equations used to convert between level and amplitude

1. Subsection overview

This subsection examines errors in perceived level when Eqs. (1) and (2) are used to convert between level and amplitude across all levels versus the usage of Eqs. (3) and (4) to convert levels below 32 dB (or loudness amplitudes below 1 sone), as discussed in Section II.C. Table 15 summarizes the algorithms that are used in this subsection for each of the four main computational steps when computing both the true levels and the inexact levels (see also Table 3). Importantly, the first two and the final computational steps use the recommended algorithms when computing both the true and inexact levels. The non-recommended algorithm is only used for level-amplitude conversion for inexact levels. In all cases in this subsection, for example, the initial two steps in the computation of PL use the recommended methods: step 1) the narrow band summation method is used to find the one-third-octave band levels, and step 2) the Jackson and Leventhall algorithm is used to compute the loudness spectrum. Then, the recommended algorithms (for true levels) or non-recommended algorithms (for inexact levels) are used to convert between level and amplitude at different points in the computation (Table 15 and Figure 1). See Section II.C for a discussion of the level-amplitude conversion algorithms.

Table 15: Algorithms used to compute true levels and inexact levels in subsection IV.D.

	True levels:		***Inexact levels:***	
Computational step	**Rec. algorithm**	**Non-rec. algorithm**	**Rec. algorithm**	**Non-rec. algorithm**
1: OTOB sound pressures	✓		✓	
2: Loudness spectrum	✓		✓	
3: Level-amplitude conversions	✓			✓
4: F(S) table values	✓		✓	

2. Error results

The error distributions of PL when using the non-recommended algorithm to convert between level and amplitude are shown in Figures 33 and 34. The 5th, median, and 95th percentiles of the error distribution are identified in those figures and tabulated for five waveform cases in Table 16. The scale factor for the waveform case is identified in the second column of Table 16 and the captions of Figures 33 and 34. Three of those cases (Figure 33) are X-59 shaped sonic booms that are either unattenuated or attenuated by a gain of either −20 or −30 dB, like discussed in Subsection IV.C. The final two cases (Figure 34) are background noise waveforms that are unattenuated and attenuated by −20 dB (discussed in Subsection IV.C). The histograms in Subsection IV.C that show the range of true levels for each waveform case are referenced in parentheses in the first column of Table 16.

For the unattenuated waveforms, both shaped booms and background noise, the error in PL is always small, less than 0.10 dB (Table 16, first and fourth rows). However, the error increases as the waveforms are attenuated. For example, the 95th percentile error

changes from 0.07 dB to 1.47 dB when the shaped boom waveforms have a −30 dB gain applied. Likewise, the 95th percentile error for the background noise waveforms changes from 0.072 dB to 1.05 dB when they are scaled by a −20 dB gain. Thus, choices associated with this computational step are only expected to be impactful when the signals are very low in level. This may happen, for example, when analyzing noises that are recorded in the Mach cutoff region of the sonic boom carpet or in the secondary carpet[9].

Because the error in PL can be significant when analyzing very quiet sounds (e.g., Table 16), using Eqs. (1) and (2) above levels of 32 dB and Eqs. (3) and (4) below 32 dB is recommended, as discussed in Section II.C. This recommendation is consistent with Ref. [2]; although that reference recommends using a cutoff of 20 dB, not 32 dB. However, a cutoff of 32 dB is recommended here since Eqs. (3) and (4) are exact between 20 and 32 dB, whereas Eqs. (1) and (2) are only approximate in that range.

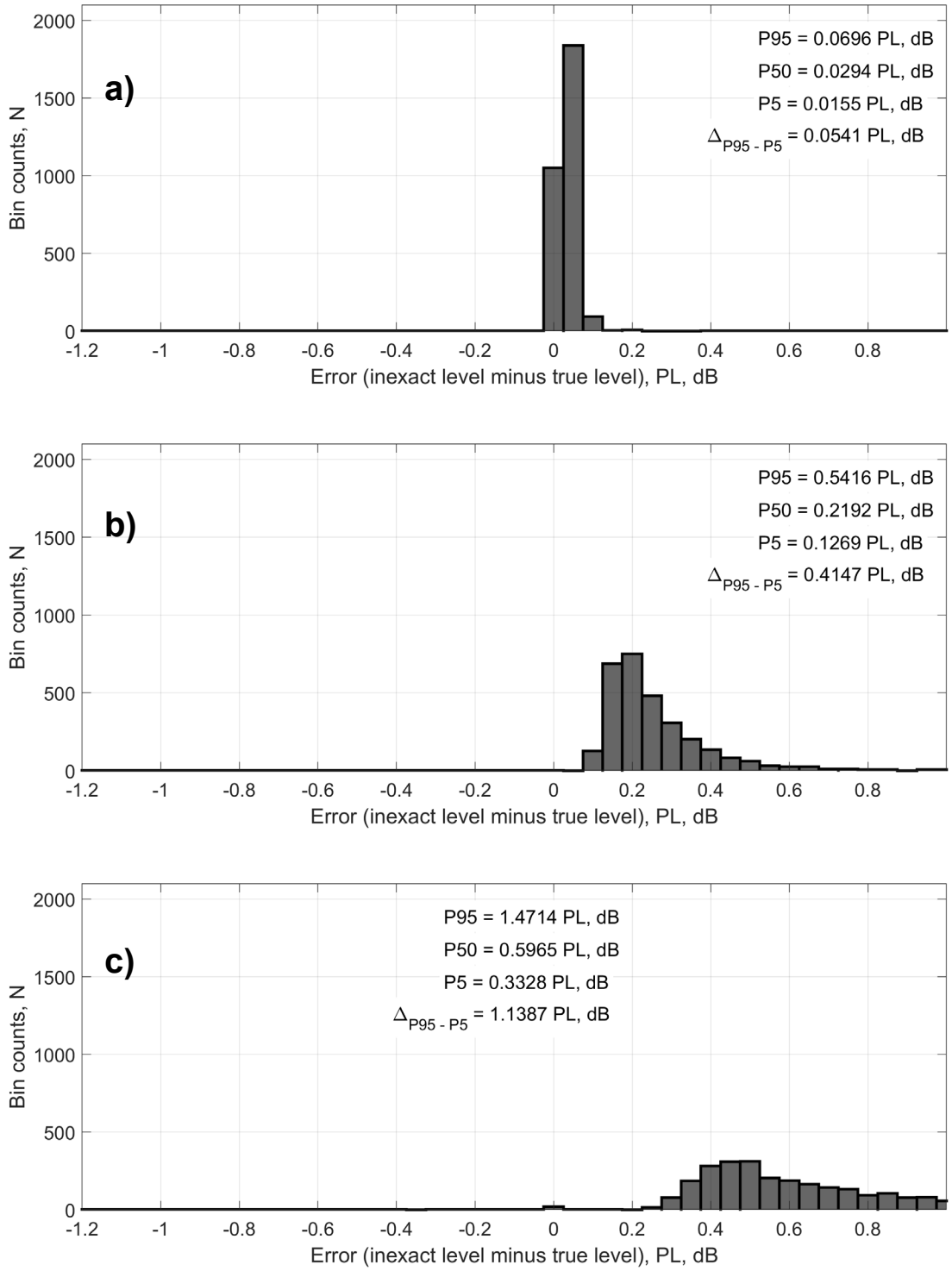

Figure 33: Error in PL across 3,000 X-59 sonic booms for inexact values computed when using Eqs. (1) and (2) only to convert between level and amplitude compared to using Eqs. (1) through (4); where a) is the unscaled waveform case, b) is the case where all waveforms are scaled by a factor of 0.100, and c) all waveforms are scaled by 0.0316.

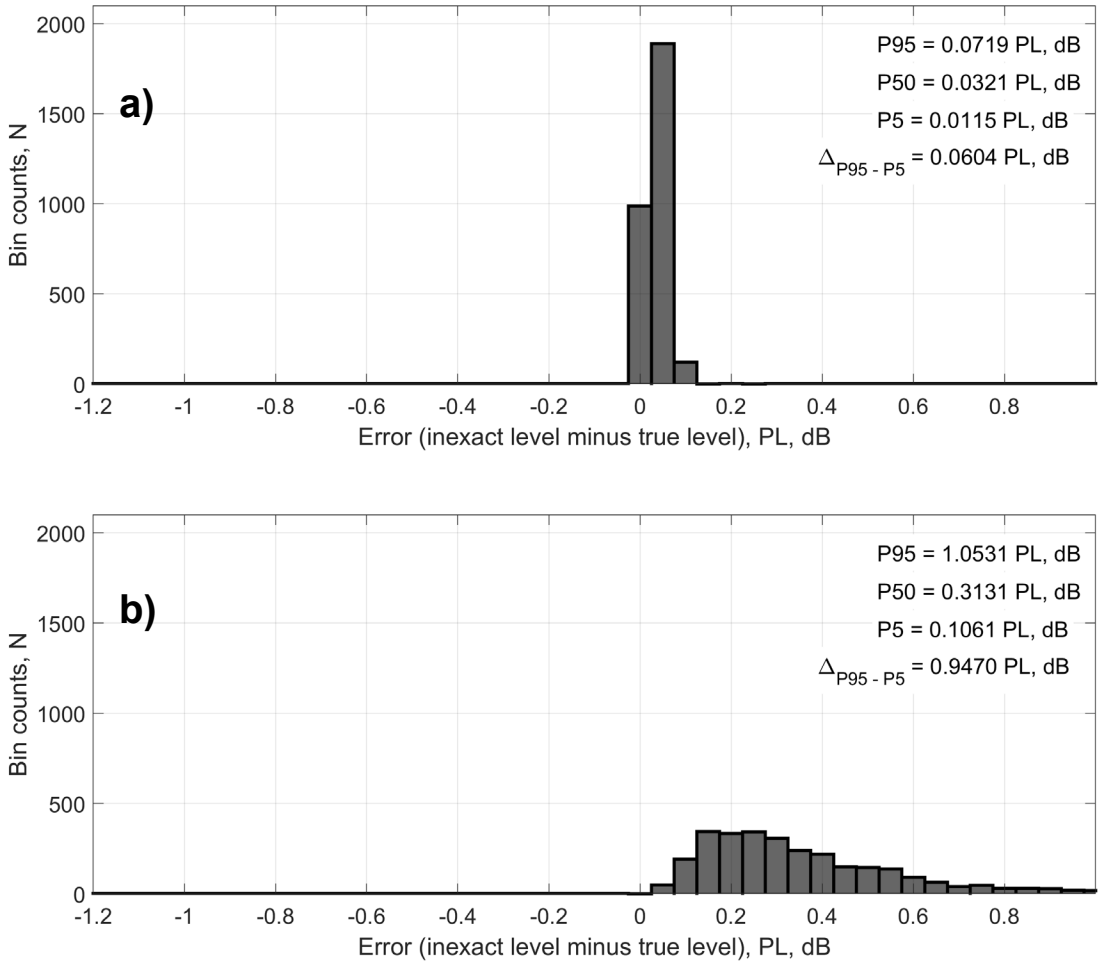

Figure 34: Error in PL across 3,000 background noise waveforms for inexact values computed when using Eqs. (1) and (2) only to convert between level and amplitude compared to using Eqs. (1) through (4); where a) is the unscaled waveform case, and b) is the case where all waveforms are scaled by a factor of 0.100.

Table 16: Tabulated 5th, 50th, and 95th percentiles of error in PL when using the inexact method to convert between level and magnitude for 3,000 waveforms of the type indicated in the first column.

Waveform type (Fig. with true PL)	**Amplitude scale factor**	**5th percentile error PL, dB**	**50th percentile error PL, dB**	**95th percentile error PL, dB**
X-59 boom (31a)	1.00 (Not scaled)	0.016	0.029	0.070
X-59 boom (31b)	0.100 (−20 dB)	0.127	0.219	0.542
X-59 boom (31c)	0.0316 (−30 dB)	0.333	0.597	1.471
Background (32a)	1.00 (Not scaled)	0.011	0.032	0.072
Background (32b)	0.100 (−20 dB)	0.106	0.313	1.053

E. Errors related to the weighting table used to compute total loudness

1. Subsection overview

For the fourth main computational step of Perceived Level, the loudness spectrum is summed to find total loudness. That sum is weighted, where the weighting factor F in Eq. (5) depends on the maximal value of the loudness spectrum. A closed form solution for F does not exist, so interpolation is required. A data table relating maximum loudness to F value is provided in Appendix B of Ref [2], from which the interpolant is formed. Two effects that are related to the determination of F are evaluated in this subsection: 1) the addition of two points to the data table to fill a gap at low sound levels (see Figure 35 and related discussion in Section II.D above), and 2) the interpolation method (e.g., linear versus cubic) used to interpolate between values in the data table.

Addressing the first effect, errors are evaluated by comparing the true loudness levels to the inexact loudness levels (Table 17). Inexact levels are computed without the two additional points but using the recommended algorithms for the first three computational steps (Table 17). For the second effect, differences in PL are presented when using linear interpolation versus cubic interpolation to compute F in Eq. (5). The two additional points are included in the interpolant when comparing output when using linear versus cubic interpolation by choosing the *pchip* option when using the *interp1* MATLAB® command.

Table 17: Algorithms used to compute true levels and inexact levels in subsection IV.E.

	True levels:		***Inexact levels:***	
Computational step	**Rec. algorithm**	**Non-rec. algorithm**	**Rec. algorithm**	**Non-rec. algorithm**
1: OTOB sound pressures	✓		✓	
2: Loudness spectrum	✓		✓	
3: Level-amplitude conversions	✓		✓	
4: F(S) table values	✓			✓

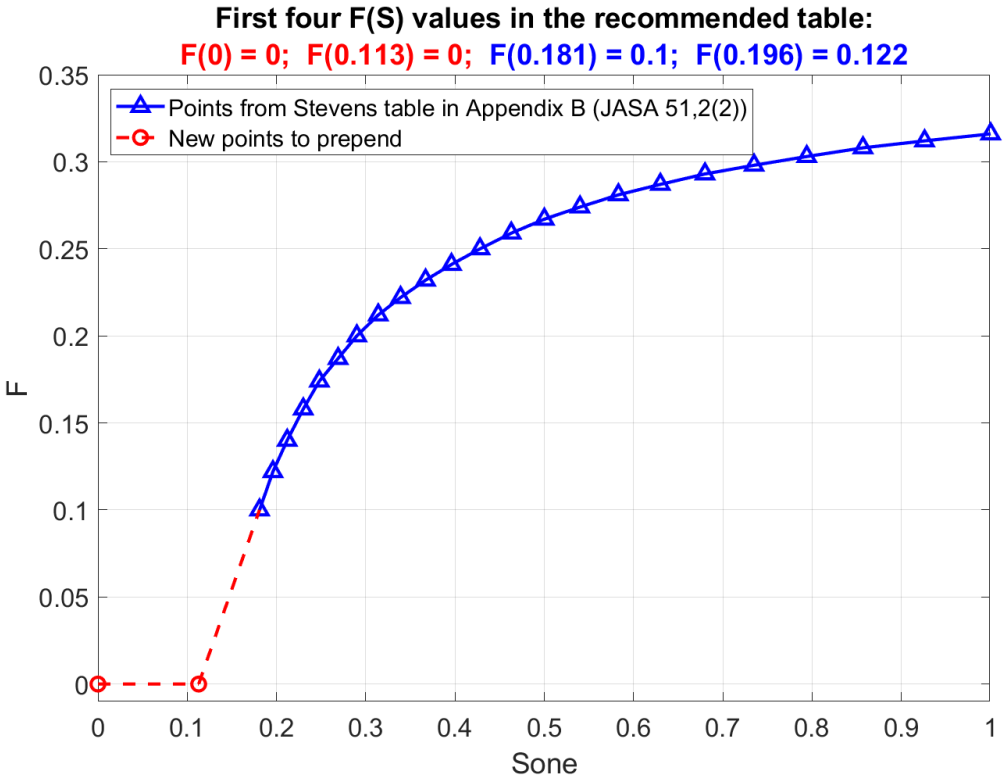

Figure 35: Two new interpolation points (circles) prepended to the table from Appendix B of Ref. [2] (reproduction of Figure 3 in Section II.D above).

2. Error results

The error when including the two new data points versus not including them – the first effect discussed above – is summarized in Table 18 for the five waveform cases identified in Section IV.C.

Table 18: Tabulated 5th, 50th, and 95th percentiles of error in PL when not using the two F(S) table points; across 3,000 waveforms of the type indicated in the first column and scaled by the factor in the second column.

Waveform case (Fig. with true PL)	**Amplitude scale factor**	**5th percentile error PL, dB**	**50th percentile error PL, dB**	**95th percentile error PL, dB**
X-59 booms (31a)	1.00 (Not scaled)	0.000	0.000	0.000
X-59 booms (31b)	0.100 (−20 dB)	0.000	0.000	0.000
X-59 booms (31c)	0.0316 (−30 dB)	0.000	0.000	0.000
Background (32a)	1.00 (Not scaled)	0.000	0.000	0.000
Background (32b)	0.100 (−20 dB)	0.000	0.000	0.000

The five waveform cases include both unattenuated and attenuated sets of X-59 sonic boom and background noise waveforms, where the scale factors for each case are identified in the second column of the table. The distributions of PL across the waveforms in each

waveform case are identified by the figure number in parentheses in the first column of Table 18. Finally, the 5th, median, and 95th percentile error in PL is tabulated in Table 18 (last three columns) across the 3,000 waveforms in each waveform case. The error is binned across the inexact minus the true loudness level of each waveform in each set of 3,000 waveforms.

Overall, the effect of prepending the two additional points to the data table from Appendix B of Ref. [2] very is small. The error is nearly zero across the 3,000 waveforms of both the X-59 sonic booms and the background noise (Table 18). Thus, the two new points are not expected to have a significant effect on the computed loudness level for most shaped sonic booms that will be experienced in the primary carpet of X-59. Likewise, the error observed for background noise is not expected to be impacted significantly by these additional points.

However, PL errors do occur occasionally for scaled waveforms when the two new points are omitted from the data table. For example, the properties of the outlier waveforms within each set of 3,000 waveforms that produce error is summarized in Table 19. The count, N, of waveforms with error is identified in the third column (Table 19) and the 5th and 95th percentile error for those N waveforms is summarized in the fourth and fifth columns (Table 19). While the occurrence of errors is rare, e.g., the number of waveforms that produce any error may only be about 100 out of 3,000 when noise levels are very low, the error in PL can be quite high when it does occur. For example, error between about −6 and −3 dB is observed in the subset of N=136 X-59 sonic boom waveforms that produced error when scaled by 0.0316 (Table 19, third row). Error can be even higher for very quiet background noise waveforms (Table 19, fifth row). This effect may become important when analyzing sounds that occur in the shadow region beyond Mach cutoff or from over-the-top sonic booms. Thus, including these two new points in the data table that is used to compute the factor F in Eq. (5) is recommended.

Table 19: Error summary for the subset of outlier waveforms that produce error in PL when not using the two F(S) table points; across N outlier waveforms of the type indicated in the first column, scaled by the factor in the second column, with count N identified in the third.

Waveform case (Fig. with true PL)	**Amplitude scale factor**	**Count of waveforms with error, N**	**5th percentile error in subset PL, dB**	**95th percentile error in subset PL, dB**
X-59 booms (31a)	1.00 (Not scaled)	0	—	—
X-59 booms (31b)	0.100 (−20 dB)	4	−2.499	−1.335
X-59 booms (31c)	0.0316 (−30 dB)	136	−5.921	−3.202
Background (32a)	1.00 (Not scaled)	0	—	—
Background (32b)	0.100 (−20 dB)	102	−10.844	−8.122

Finally, the difference in PL when using cubic interpolation instead of linear interpolation to compute the factor F in Eq. (5) is summarized in Table 7. The 5th, median, and 95th percentile difference in PL is tabulated in that table. Overall, differences are very small comparing the two methods, typically only a few thousandths of a dB (Table 7). Neither method has an obvious advantage when only considering the error in PL.

However, when considering the behavior of the table data that is used to find the factor F (e.g., Figure 35), linear interpolation is recommended for two reasons.

Firstly, the resolution of the existing table data is fine (see Figure 35, blue line segments), so changes in slope between neighboring points is relatively small. Thus, errors should be well behaved when using linear interpolation to find F values instead of cubic interpolation within the existing data points (the blue portion of Figure 35). Large differences between the two methods are not expected within that blue portion of the interpolant.

Secondly, the two new points that are recommended (see Figure 35, red circles) introduce a slope discontinuity at the point (0.113, 0.000). Estimates of F values between these two new points and the first existing point at (0.118, 0.100) will be better behaved when using linear interpolation than when using cubic interpolation. Specifically, linear interpolation will follow exactly the dashed red lines in Figure 35 while cubic interpolation will oscillate about the dashed red lines due to the polynomial formulation. Such oscillations may result in nonsensical values of F. For example, negative values for F may be possible around the two new points when using cubic interpolation. This possibility is demonstrated in Figure 36 where linear interpolation is compared to cubic interpolation using both the *spline* and the *pchip* options. Using the *spline* option does give nonsensical negative values, but *pchip* appears to be better behaved. Additionally, there is little difference between the cubic interpolation results and the linear interpolation results between the existing table points (blue lines). Thus, linear interpolation is recommended when finding F in Eq. (5) since it performs well around the two new points and gives very similar results to the cubic interpolation results at higher sone values.

Table 20: Tabulated 5th, 50th, and 95th percentiles of difference in PL when using linear versus cubic interpolation to find weight factor F in Eq. (5); across 3,000 waveforms of the type indicated in the first column and scaled by the factor in the second column.

Waveform case (Fig. with true PL)	**Amplitude scale factor**	**5th percentile difference PL, dB**	**50th percentile difference PL, dB**	**95th percentile difference PL, dB**
X-59 booms (31a)	1.00 (Not scaled)	−0.0042	−0.0005	0.0014
X-59 booms (31b)	0.100 (−20 dB)	−0.0009	0.0014	0.0063
X-59 booms (31c)	0.0316 (−30 dB)	0.0000	0.0029	0.0112
Background (32a)	1.00 (Not scaled)	−0.0023	−0.0001	0.0049
Background (32b)	0.100 (−20 dB)	0.0000	0.0037	0.0157

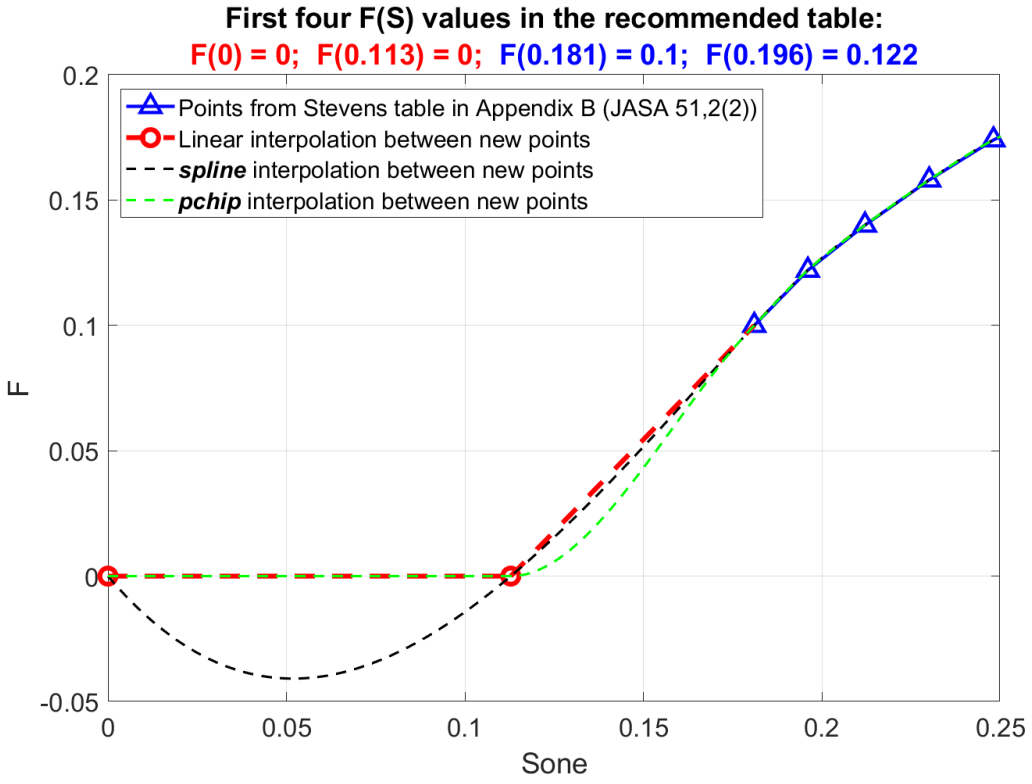

Figure 36: Comparison of linear versus two cubic interpolation methods for points falling between the tabulated weighting factor, F, points.

F. Errors when combining all non-recommended algorithms

1. Subsection overview

In previous subsections, inexact levels were computed when using only one of the non-recommended algorithms – for only one of the computational steps – while using the recommended algorithms for the other three computational steps. In this subsection, error in Perceived Level is documented when the non-recommended algorithms are used for all four computational steps (Table 21) to demonstrate the combined effects of all error sources. True levels are still computed using all recommended algorithms (Table 21), and error is the difference of inexact levels minus true levels, so a positive error corresponds to overestimation of true levels.

Specifically, inexact levels are computed using discrete-time filter orders of 6, 10, and 18 for the first computational step. Error results will be summarized separately for the three filter orders to demonstrate effects of that choice. The original interpolant (Figure 21, solid lines) is used for the second computational step. Then, only Eqs. (1) and (2) when converting between level and amplitude. Finally, the weighting table that is used to find the scalar term, F, in Eq. (5) did not include the additional two points (Section II.D) when finding inexact levels.

Table 21: Algorithms used to compute true levels and inexact levels in subsection IV.F.

	True levels:		***Inexact levels:***	
Computational step	**Rec. algorithm**	**Non-rec. algorithm**	**Rec. algorithm**	**Non-rec. algorithm**
1: OTOB sound pressures	✓			✓
2: Loudness spectrum	✓			✓
3: Level-amplitude conversions	✓			✓
4: F(S) table values	✓			✓

2. Error results

The error distributions of PL when using the non-recommended algorithms for all computational steps are shown in Figures 37 and 38 for the set of X-59 sonic booms and background noise waveforms, respectively. Unlike the prior two subsections, the waveforms were not attenuated prior to computing loudness levels. The 5th, median, and 95th percentiles of the error distribution are identified in those figures for each analysis case. Separate subplots are included for the three different discrete-time filter orders that were used in the first computational step: orders 6, 10, and 18.

Error is modest when using 6th order filters. For example, the median error for X-59 sonic booms is 0.381 dB and the 95th percentile is 0.519 dB (Figure 37a). That error is slightly larger than was observed in Section IV.A, where the effects of only the discrete-time filters was documented – as compared to this subsection where non-recommended algorithms are used for all computational steps. Specifically, the median and 95th percentile errors from Section IV.A when using 6th order filters only are 0.327 and 0.454 dB,

respectively (Table 11 in Section IV.A). This is because the different non-recommended methods tend to overestimate the level, so combining them leads to a larger overestimate. As filter order increases, the error is reduced – comparing Figure 37a to 37b and 37c – and the error introduced by the other computational steps becomes more impactful. For example, median and 95th percentile errors from Section IV.A when using 18th order filters was 0.036 and 0.054 dB, respectively (Table 11 in Section IV.A). That increases to 0.095 and 0.155 dB here (Figure 37a). Thus, the primary source of error for X-59 shaped sonic booms when using all the non-recommended algorithms is the discrete-time filter model when filter order is low. The other computational steps become more impactful as filter order increases and the one-third-octave band sound pressure levels are more accurately estimated by the discrete-time filters. In all cases here, true levels tend to be overestimated (Figure 37) by up to a few tenths of a dB.

Similar behaviors are observed for the background noise waveforms (Figure 38). For example, the median (bias) error improves as filter order increases. However, the width of the distribution remains about the same as filter order increases – comparing Figure 38a to 38b and 38c. This is because the interpolant used for computational step two to convert the SPL spectrum into a loudness spectrum is like that of Subsection IV.B.2. The error distributions from that subsection indicated that the error for background noise waveforms tends to be wider than for X-59 shaped booms (see Figures 23 and 24 in IV.B.2). Consequently, the random error observed in Figure 38 is caused by using the non-recommended interpolation method to compute the loudness spectrum while the bias in Figure 38a is introduced by the 6th order discrete-time filters that are used to find the SPL spectrum. That bias error improves as filter order increases.

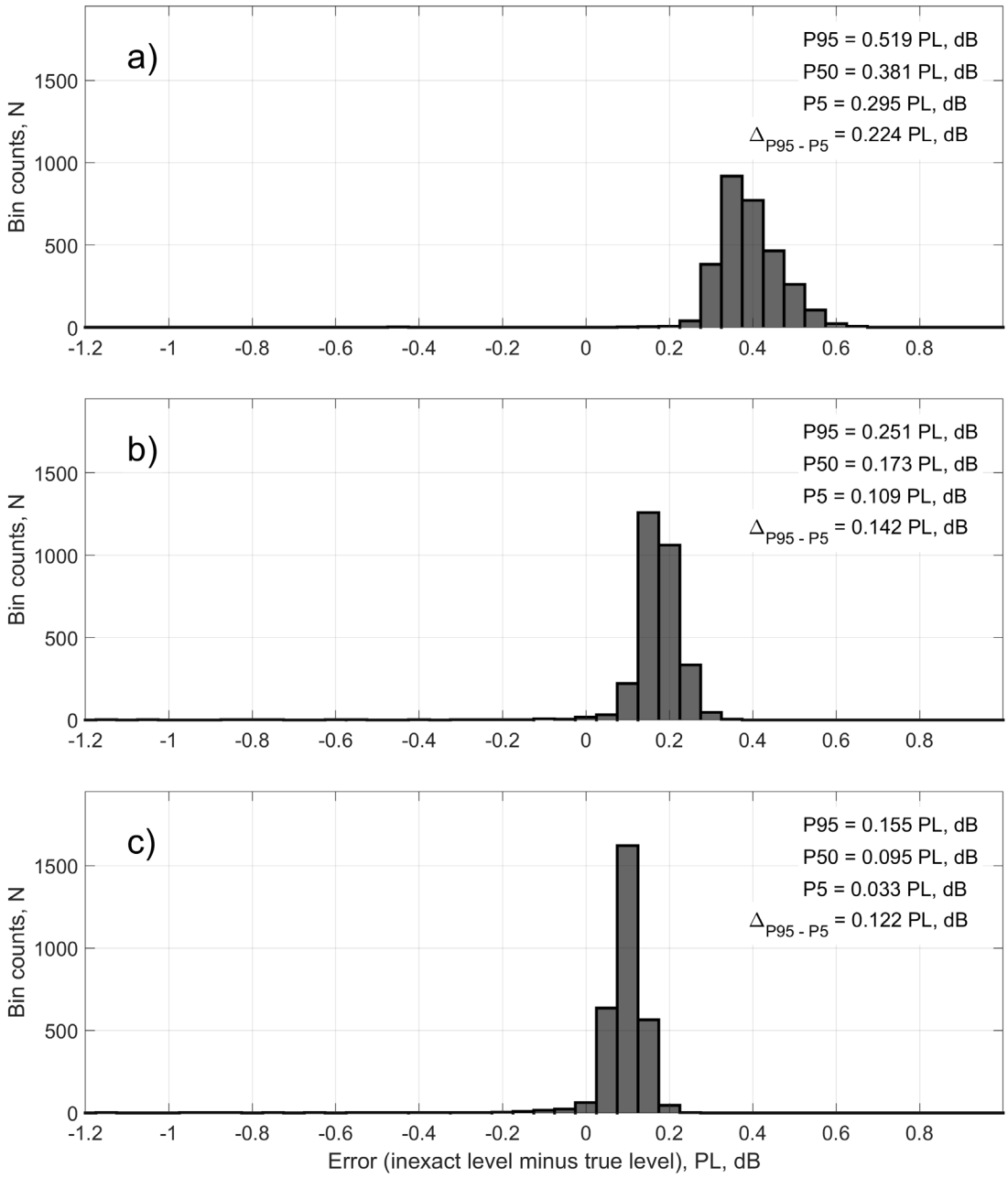

Figure 37: Error in PL across 3,000 X-59 sonic booms for inexact values computed when using non-recommended method for all four computational steps; where a) is the case when using 6th order discrete-time filters for the first step, b) is the case when using 10th order filters for that step instead, and c) is when using 18th order filters.

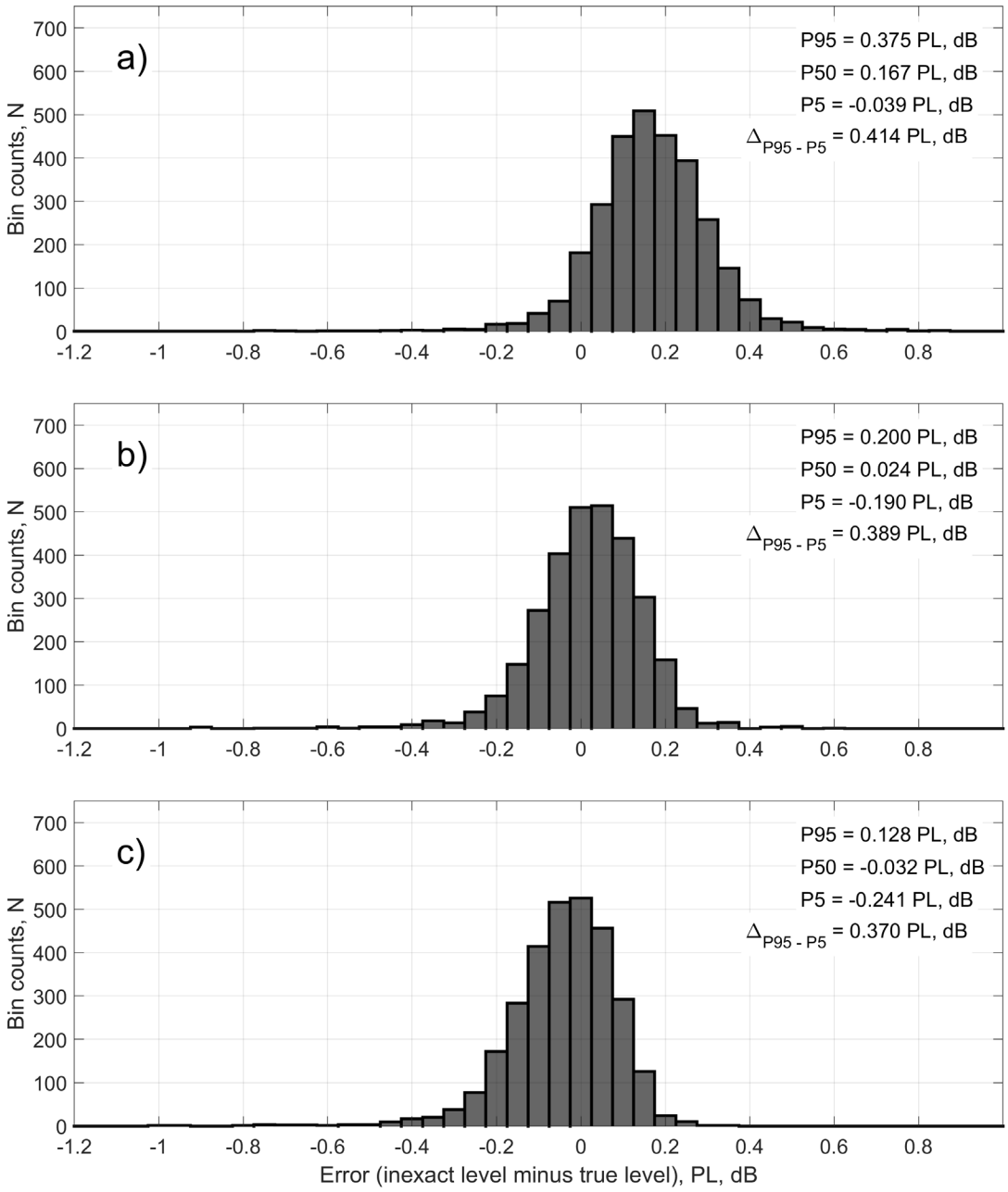

Figure 38: Error in PL across 3,000 background noise waveforms for inexact values computed when using non-recommended method for all four computational steps; where a) is the case when using 6th order discrete-time filters for the first step, b) is the case when using 10th order filters for that step instead, and c) is when using 18th order filters.

V. SUMMARY

Readers are referred to Figure 1 in the introduction for a flow chart of the Perceived Level computation. An Algorithm was recommended in Section II for each of the four main computational steps of Perceived Level:

- *Step 1, One-third-octave band sound pressure levels*: narrow band summation (see Appendices 1 and 2),
- *Step 2, Loudness spectrum*: the Jackson and Leventhall method (see Ref. [7]),
- *Step 3, Converting between level and amplitude*: Eqs. (1) and (2) above 32 dB and Eqs. (3) and (4) below 32 dB, and
- *Step 4, Weighting factor in Eq. (5) computed using*: table Appendix B of Ref. [2] with points at (0.0, 0.0) and (0.113, 0.0) prepended while using linear interpolation between tabulated points.

Also discussed in that section were alternative, non-recommended algorithms that an analyst could choose to implement the steps. The alternative algorithms are expected to be less accurate than the recommended algorithms. Error in level was studied in Section IV by comparing output of the non-recommended versus the recommended algorithms. These errors were documented for both simulated shaped sonic boom waveforms from the X-59 aircraft and background noise waveforms recorded during the NASA QSF18 community response test. These waveforms were documented in Section III and IV.C. Discussions were provided in Sections II and IV and Appendix 1 that document why the recommended algorithms are expected to be more accurate than the non-recommended algorithms.

A. Summary of error behaviors

The various combinations of recommended and non-recommended algorithms that were used when computing levels and related errors are summarized in Section III.B. The error results discussed in Section IV demonstrate that modest errors in PL may be observed when analyzing both shaped sonic boom waveforms and background noise waveforms. Errors on the order of a few tenths of a dB are often observed, relative to the recommended algorithms, and those error can change based on choices analysts might make when implementing the non-recommended algorithms. Errors of this magnitude – a few tenths of a dB – may be unacceptable if Perceived Level is to be used to define a noise-based certification standard.

Non-recommended algorithms are more error prone for some computational steps. For example, using discrete-time filters to find one-third-octave band sound pressure levels (for step 1) and using interpolation to estimate the loudness spectrum (for step 2) can lead to modest error relative to the recommended algorithms. Specifically, choices of discrete-time filter order and zero-padding length can have a modest effect on error when using filters for the first computational step. Error is relatively minor for choices related to the equations used for level-to-amplitude conversion (for step 3) and the points that are included and the interpolation method used to find the weighting values, F, in Eq. (5) (for step 4). The choices made for computational steps 3 and 4 only become important at very low noise levels, which may occur in the Mach cutoff shadow region or in the secondary boom carpet.

For the two most impactful non-recommended algorithms – steps 1 and 2 – error can be mitigated by refining the choices used for those algorithms. For example, applying

high order discrete-time filters to waveforms with significant zero-padding will give results for step 1 that converge to those when using the recommended narrow band summation algorithm (e.g., see Subsection IV.A.4, Tables 11 and 12). Similarly, using an interpolant with finely spaced, high-precision equal loudness contours for step 2 will converge to the recommended Jackson and Leventhall method [7] (e.g., see results in Subsection IV.B.4). Importantly, the recommended methods tend to be more computationally efficient than the non-recommended algorithms with settings that provide good convergence. Also, the recommended algorithms generally do not suffer from choice-based errors like the non-recommended algorithms. For example, the one-third-octave band SPL and the PL values are well converged when using narrow band summation even when using short duration waveforms (Appendix 2). This is because the narrow band summation method approximates the response of one-third-octave bands with rectangular skirts due to the way in which narrow-band bins are apportioned (Appendix 1). Discrete-time filters require much longer signals and high filter orders to obtain results that are still less well converged than when the narrow band summation method is applied to short duration signals (e.g., Subsection IV.A.4, Tables 11 and 12 versus Appendix 2). Similarly, the Jackson and Leventhall method is closed form so does not suffer from choice-based errors or precision-based errors.

There are no identified disadvantages with the recommended algorithms. Thus, the algorithms listed in the first paragraph above are recommended for calculating Perceived Level of shaped sonic booms and background noise.

B. Notes regarding NASA software

Recently, the Applied Acoustics branch at NASA Langley Research Center has updated two computer codes – NOM[1] and PCBoom [9] – that are actively maintained and used within the branch to compute noise metrics. They now compute PL in the same way and use the recommendations provided herein. As discussed in Section IV.B.5, prior versions of PCBoom (version 7.1 and earlier) likely had a programming bug that would return slightly lower than expected PL values for shaped sonic boom noise. Users of older versions of PCBoom are encouraged to review the discussion in Section IV.B.5.

NASA has released as source code MATLAB®-based sonic boom noise metrics software named NOM[1]. This code also includes capabilities to mitigate effects of background noise [13]. Importantly, deprecated NASA software has not been updated to include all recommended algorithms since those codes are no longer actively used within NASA. This exclusion includes the publicly available LCASB[2] software. Consequently, readers are encouraged to obtain and use the newer NOM software instead of LCASB.

References

[1] K. P. Shepherd and B. M. Sullivan, "A loudness calculation procedure applied to shaped sonic booms," NASA, Technical Report, TP-3134, 1993.

[2] S. S. Stevens, "Perceived Level of Noise by Mark VII and Decibels," *J. Acoust. Soc. Am.,* vol. 51, no. 2B, pp. 575-601, 1972.

[3] A. Loubeau, Y. Naka, B. G. Cook, V. W. Sparrow and J. M. Morgenstern, "A new evaluation of noise metrics for sonic booms using existing data," *AIP Conference Proceedings,* vol. 1685, no. 1, 2015, https://doi.org/10.1063/1.4934481.

[4] J. Rathsam, P. Coen, A. Loubeau, L. Ozoroski and G. Shah, "Scope and goals of NASA's Quesst Community Test Campaign with the X-59 aircraft," in *14th ICBEN Congress on Noise as a Public Health Problem*, Belgrade, Serbia, June 2023, https://ntrs.nasa.gov/citations/20230004142.

[5] G. Shah, J. Rathsam and A. Loubeau, "Preparations for Quesst Mission Community Response Testing – Overview and Status," in *2023 AIAA SciTech Forum (presentation only)*, National Harbor, MD, 2023, https://ntrs.nasa.gov/citations/20220018319.

[6] N. B. Cruze, "Overview of Community Response Testing Campaign with NASA's X-59 Aircraft," in *UC Davis Aircraft Noise and Emissions Symposium*, Davis, CA, May 2023, https://ntrs.nasa.gov/citations/20230006133.

[7] G. M. J. a. H. G. Leventhall, "Calculation of the perceived level of noise (Pldb) using Stevens' method (Mark VII)," *Applied Acoustics,* vol. 6, no. 1, pp. 23-34, 1973.

[8] *IEC 1260:1995-07, Electroacoustics - Octave-band and fractional-octave-band filters,* 1995.

[9] J. A. Page, J. B. Lonzaga, M. J. Shumway, S. R. Son, R. S. Downs, A. Loubeau and W. J. Doebler, "PCBoom Version 7.3 User's Guide," NASA/TM–20220016207, 2023, https://ntrs.nasa.gov/citations/20220016207.

[10] C. R. Bolander, D. F. Hunsaker, H. Shen and F. L. Carpenter, "Procedure for the Calculation of the Perceived Loudness of Sonic Booms," in *AIAA SciTech 2019 Forum*, San Diego, California, 2019, https://doi.org/10.2514/6.2019-2091.

[11] W. J. Doebler, S. R. Wilson, A. Loubeau and V. W. Sparrow, "Simulation and Regression Modeling of NASA's X-59 Low-Boom Carpets Across America," *Journal of Aircraft,* vol. 60, no. 2, March 2023, https://doi.org/10.2514/1.C036876.

[12] W. J. Doebler and A. Loubeau, "Estimating the noise dose range of the NASA X-59 aircraft in supersonic cruise using PCBoom propagation simulations," *JASA Express Letters,* vol. 3, no. 5, May 2023, https://doi.org/10.1121/10.0019501.

[13] J. Klos, "An Adaptation of ISO 11204 using Customized Correction Grades to Mitigate Ambient Noise Effects when Computing Sonic Boom Loudness Levels," NASA/TM–20220010779, Hampton, VA, 2022, https://ntrs.nasa.gov/citations/20220010779.

[14] *ANSI/ASA S1.42-2020, Design Response of Weighting Networks for Acoustical Measurements,* 2020.

[15] D. J. Maglieri, P. J. Bobbitt, K. J. Plotkin, K. P. Shepherd, P. G. Coen and D. M. Richwine, Sonic Boom: Six Decades of Research, Hampton, VA: NASA Special Publication , 2014, https://ntrs.nasa.gov/citations/20150006843.

Acknowledgements

The author would like to thank the X-59 community response contractor team led by Harris Miller Miller & Hansen Inc., specifically the subcontractor team at Blue Ridge Research and Consulting, LLC, for identifying bugs in the NOM software and deriving Eqs. (3) and (4), which led to updates to that software and the related discussions found in Sections II.C and II.D of this report.

Appendix 1: Description of the narrow band summation method

The narrow-band summation method that is used in NOM to compute a one-third-octave band spectrum of a sonic boom waveform is summarized in this appendix. The rules for apportionment of narrow band bin energies are as follows:

- The energies of narrow-band bins that fall wholly within a one-third-octave band are summed,
- The energies of narrow-band bins that overlap a one-third-octave band edge are apportioned proportional to the amount of overlap, and
- The relationship between bin energy, e_i in units of Pa^2, and bin level, L_i in decibel units, for the i^{th} narrow band bin are:
    - $L_i = 10 \times \log10(e_i / P_{ref})$, so
    - $e_i = P_{ref} \times (10\text{^}(L_i / 10))$.

The decibel reference constant, P_{ref}, is 4E-10 Pa^2. The method is illustrated below using example data.

Consider the one-sided, narrow band energy spectrum of a zero padded, discrete-time waveform of length NFFT. The centers of the i^{th} narrow-band bins are located at frequencies points $f_i = i \times \Delta f$ for i = [0, 1, 2, …, (NFFT/2)], where $\Delta f = f_s/\text{NFFT}$, f_s is the discrete-time sample rate in units of samples per second, and assuming NFFT is a power of two. The corresponding upper and lower edges of the i^{th} narrow band bin are at points $f_{i,edges} = f_i \pm {}^{\Delta f}/_2$. Small snippets of two example spectra are illustrated in Figure A1.1 (red and green curves), where data in the range from about 88 to 90 Hz only are shown. These two spectra were computed for the same sonic boom waveform but while using different zero padding lengths to highlight how such signal processing parameters might change the narrow band bin widths, bin energy levels, and their apportionment. The extent and decibel level of the narrow-band bins is illustrated by the solid line segments. The total number of samples, NFFT, was 65,536 in the case of the red spectrum, and twice that in the case of the green spectrum. That change results in narrow band bin widths that differ by a factor of two as annotated in the legend.

Also shown in Figure A1.1 is the lower edge frequency of the rectangular 100 Hz one-third-octave band (vertical magenta line at 89.125 Hz), which is also the upper edge of the 80 Hz one-third-octave band. For reference, the center frequencies for each o^{th} one-third-octave band from 1.25 Hz to 20 kHz are computed from $f_{o,c} = f_r \times G^{(⅓(o\text{-}30))}$, where constants f_r = 1000 and $G = 10^{(3/10)}$ and band indices are o = 1, 2, 3, …, 43. Then, the lower edge frequencies of the rectangular one-third-octave bands are $f_{o,l} = f_{o,c} \times G^{(-⅙)}$ and upper edge frequencies are $f_{o,u} = f_{o,c} \times G^{(+⅙)}$. Items inside parentheses above indicate powers of G. The lower edge frequency of the o^{th} band is equal to the upper edge frequency of the $(o-1)^{th}$ band. These edge frequencies, $f_{o,l}$ and $f_{o,u}$, are compared to the edges of the narrow-band bins, $f_{i,edges}$, to determine apportionment of bin energy.

Regarding apportionment of narrow-band bins in Figure A1.1 to the 80 and 100 Hz one-third-octave bands, many of the narrow-band bins shown in that figure fall wholly within one of those two one-third-octave bands. For example, bins 482 to 486 of the green spectrum in Figure A1.1 lie within the 80 Hz band since both the lower and upper bin edges (green lines) are below the band edge (vertical magenta line). Consequently, the energy in those bins would contribute only to the energy of the 80 Hz band. Likewise, bins 488 to 419 in Figure A1.1 fall completely within the 100 Hz band since both bin edges are above the band edge, so would contribute only to the 100 Hz band. Narrow band bin energies, e_i, that contribute to a one-third-octave band are added to compute the total band energy.

Similar behavior is identifiable for the red spectrum. While there are fewer, but wider bins in the case of the red spectrum, the energy level of each bin is higher than the green spectrum. Consequently, the summed energy should not be affected much by the choice of bin width (zero padding duration). The effect of zero padding duration on one-third-octave band levels is studied below in Appendix 2.

Importantly, for each spectrum there is one bin that overlaps the edge of these two one-third-octave bands: bin 487 in the case of the green spectrum and bin 243 for the red spectrum. The apportionment of bin energy in such cases is proportional to the amount of overlap, which is computed from the length of the line segment from the bin edge marked by the filled circular dots Figure A1.1 to the point of overlap identified by the black "x" mark, relative to the bin width, Δf. For the example datasets illustrated in Figure A1.1, apportionment of bin energy, e_i, to the lower, 80 Hz, one-third-octave band is

$$e_i \times (f_{o,u} - (f_i - {}^{\Delta f}/_2)) / \Delta f, \text{ for } o = 19$$

and to the upper, 100 Hz, band is

$$e_i \times ((f_i + {}^{\Delta f}/_2) - f_{o,l}) / \Delta f, \text{ for } o = 20$$

where:

- $e_i = P_{ref} \times (10\text{^}(36.39 / 10))$, $f_i = \Delta f \times 487$, $\Delta f \approx 0.1831$ Hz for the green spectrum,
- $e_i = P_{ref} \times (10\text{^}(38.93 / 10))$, $f_i = \Delta f \times 243$, $\Delta f \approx 0.3662$ Hz for the red spectrum, and
- $f_{19,u} = f_{20,l} \approx 89.125$ Hz.

Similar apportionment must be done for edge frequencies of all neighboring one-third-octave bands by considering different band indices, o. Additionally, if a narrow band bin overlaps more than one one-third-octave band, which might occur at very low frequencies if NFFT is small, then similar apportionment rules should apply to all segments of bin overlap. For example, it is possible that a narrow band bin could overlap the 1.00, 1.25, and 1.60 Hz one-third-octave bands if Δf is sufficiently large. Such occurrences should be eliminated to avoid inaccuracies when converting between narrow band and one-third-octave band spectra. This is done by zero padding signals to reduce the bin width, Δf. Zero padding should only be applied to waveforms that have a taper window applied.

The effects on one-third-octave band level accuracy of the total signal duration when using the narrow band summation method is documented in Appendix 2 below. NASA's metrics code, NOM[1], will always zero pad waveforms that are input to it so they are longer than 2 seconds in duration (and equal to a power of two in sample length) to mitigate low frequency inaccuracies when computing the one-third-octave band spectrum. NASA has found that most noise metrics returned by NOM are well converged when using a total signal duration of at least 2 seconds. However, Z-weighted sound exposure level (which is not the focus of this report) sometimes benefits from using additional zero padding, beyond the default 2 seconds used by NOM. Users of NOM are welcome to input waveforms that are longer than 2 seconds in duration to improve convergence of noise metric values or spectra that are output by NOM. Importantly, all waveforms passed as input to NOM must have a taper window applied to ensure the first and last sample in the discrete-time waveform are zero valued. The taper should be designed so the waveform of interest, the sonic boom for example, lies within a unity-valued portion of the window.

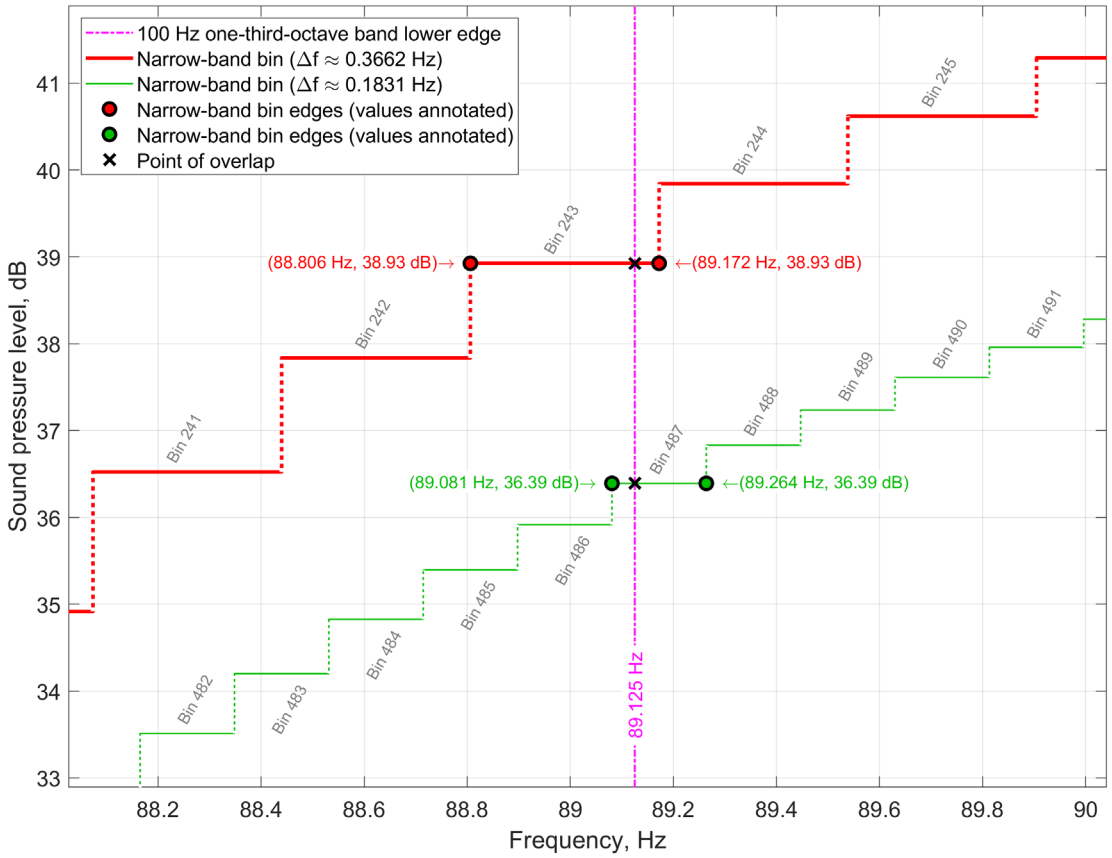

Figure A1.1: Illustration of narrow-band bins for two different bin widths with respect to the lower edge frequency of the 100 Hz one-third-octave band.

Appendix 2: Additional discussion of advantages of the narrow band summation method as compared to discrete-time filters to compute one-third-octave band levels

The error in one-third-octave band level and the Perceived Level noise metric is documented in this appendix while using the narrow band summation method to compute levels. NASA's metrics code NOM[1] was used for this study. Three thousand predicted X-59 on-design waveforms discussed in Section III.A were used as input to NOM while varying the total duration of the waveforms by changing the length of zero padding appended to them. All waveforms have an appropriate taper window applied to them.

The assumed true levels used a total waveform duration, including zero padding, of 21.85 seconds. That results in a narrow band bin width of about 0.0458 Hz, which provides for several narrow-band bins in the lowest one-third-octave band used by NOM (the 1.25 Hz band). For example, a typical narrow band spectrum with that bin width is compared to the edges of the four lowest one-third-octave bands in Figure A2.1 below. That spectrum corresponds to the waveform shown in Figure A2.2, but with zero padding applied so it has a total duration of 21.85 seconds. About 6 narrow-band bins lie in the 1.25 Hz octave band, which is expected to be well converged to the proper value when using the summation method outlined in Appendix 1 above.

Those true levels are differenced with levels computed when the waveform total duration is either 2.731, 5.461, or 10.92 seconds to identify how less zero padding affects the levels. To motivate this topic, the changes to the narrow band spectrum for the example waveform in Figure A2.2 are plotted in Figure A2.3 when those three different zero padding durations are used. Subplot a) is the case when the waveform is padded to 2.731 seconds in total duration. Subplot b) is a total duration of 5.461 seconds, and c) is 10.92 seconds. The coarseness of the narrow-band bins (blue lines), relative to the width of these low frequency one-third-octave band edges (vertical magenta lines), is much more evident in Figure A2.3 than Figure A2.1. For example, a full narrow band bin does not fall within the 1.25 Hz one-third-octave band when the total signal duration is only 2.731 seconds (Figure A2.3 subplot a). The issue investigated below is how such coarseness in the narrow band spectrum affects the one-third-octave band level accuracy and PL accuracy when using the narrow band summation method outlined in Appendix 1.

Importantly, errors in level are studied below when aggregated across 3,000 predicted X-59 waveforms. They are not computed for just the single waveform highlighted in Figures A2.1 to A2.3. There is significant diversity in the waveform characteristics – e.g., amplitude, duration, and rise time – across the set of 3,000 waveforms. For example, a subset of eight waveforms from the population is shown in Figure A2.4 to give readers a sense of the diversity within the population. A range of characteristics is visible in that figure.

Errors across the 3,000 shaped sonic boom waveforms are summarized visually as box plots in Figure A2.5. The percentiles associated with box plot features are identified in the legend. Errors in the one-third-octave band levels are shown in the left-hand subplots and the error in the PL noise metric is shown in the right-hand subplots. Results for three different waveform durations are shown in Figure A2.5: 2.731, 5.461, or 10.92 seconds as seen from top to bottom. These durations are the total length of the waveform including zero padding, where the same set of 3,000 waveforms was used in each analysis case. Again, these errors are presented relative to assumed true levels that were computed when using a total signal duration of 21.85 seconds. That duration is believed to be sufficiently long when computing the true levels since the median errors (red dots) in Figure A2.5 are converging to zero decibels and the ranges in error (blue boxes) are significantly reduced

across all box plots along the abscissa when moving from the top subplot to the bottom subplot. Use of additional zero padding beyond the 21.85 seconds used here is not expected to improve the convergence of true levels nor change the conclusions provided in this appendix.

Importantly, the range on the ordinate in Figure A2.5 is significantly smaller than that of similar figures in the main body (found in Section IV.A). This is because the one-third-octave band error observed here is only a few hundredths of a dB at most (Figure A2.5) while the error that was observed when using discrete-time filters to compute one-third-octave band levels was more than an order of magnitude higher (e.g., Figures 18 and 19). The largest one-third-octave band level error observed here when using narrow band summation is roughly −0.023 dB in the 2.5 Hz band for the analysis case with the shortest total signal duration (Figure A2.5a). All other one-third-octave bands produce less level error than that. For example, the one-third-octave band level error is only a few thousandths of a dB at frequencies above 50 Hz for all three total waveform duration cases (Figure A2.5, subplots a, b, and c).

The low error in one-third-octave band levels that is observed when using narrow band summation results in very small error in the PL noise metric in all three duration cases (Figure A2.5, right-most subplots). Again, the errors in PL are found relative to the assumed true levels, which are computed when waveforms are padded to be 21.85 seconds in total duration. For visual consistency, the same ordinate range is used for the PL error (right-most subplots) and the one-third-octave band level error (left-most subplots). As a result, only the median point (red dot) is visible in the box plots for Perceived Level, which is near zero decibel error in all three analysis cases. The other box plot features that illustrate the range of PL error are not visible on the chosen ordinate scale.

To convey the range in PL error, the percentiles of those errors are tabulated in Table A2.1, where the 5^{th}, 50^{th}, and 95^{th} percentiles are shown for all three signal duration cases. PL is well behaved in all three cases, where the largest median error is only 0.00034 dB, and the 95^{th} percentile is only 0.00107 dB for the case when the total signal duration is 2.731 seconds. Again, these errors are presented with respect to true levels at a total duration of 21.85 seconds. These errors are significantly smaller than the errors that were observed in Section IV.A when using discrete-time filters to compute the one-third-octave band levels input to the Perceived Level calculation. In Section IV.A, median errors in PL as high as 0.327 dB were observed when using 6^{th} order discrete-time filters (see Table 11). Error was still 0.036 dB when using 18^{th} order filters (see Table 11), which is two orders of magnitude higher than the median error for narrow band summation using the shortest signal duration (Table A2.1, the 2.731 second duration case).

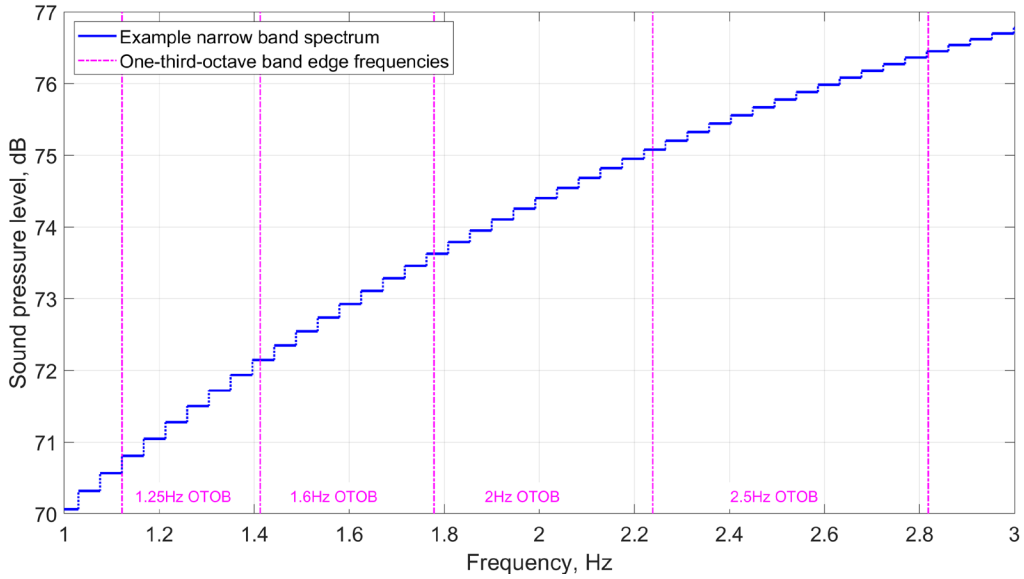

Figure A2.1: Example section of one narrow band spectrum (blue curves) for one zero padded waveform as compared to the low frequency one-third-octave band edges (vertical magenta lines); for a waveform total duration (zero padded) of 21.85 seconds.

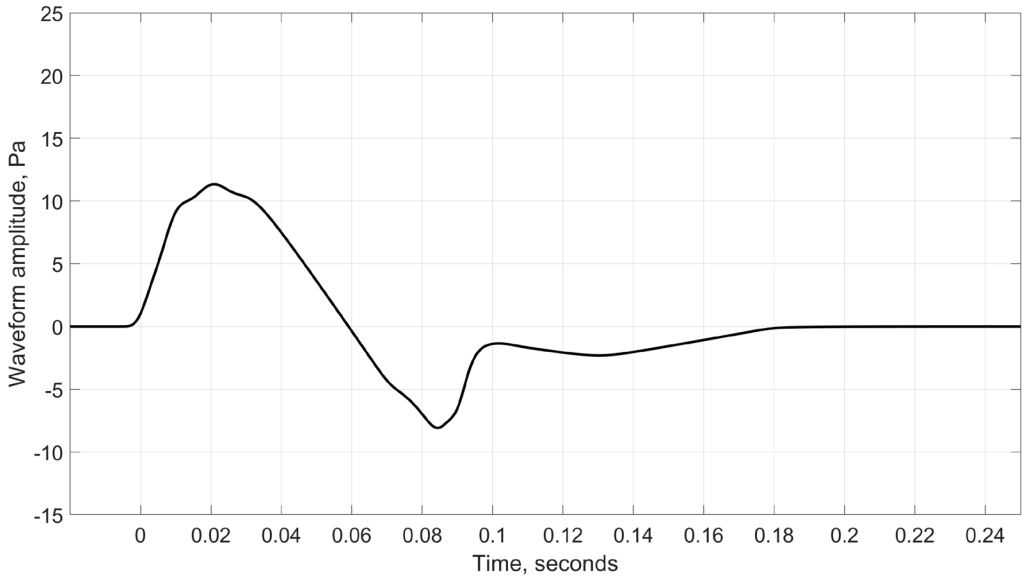

Figure A2.2: Example shaped sonic boom waveform corresponding to the spectrum shown in Figure A2.1 but prior to zero padding the waveform to 21.85 seconds.

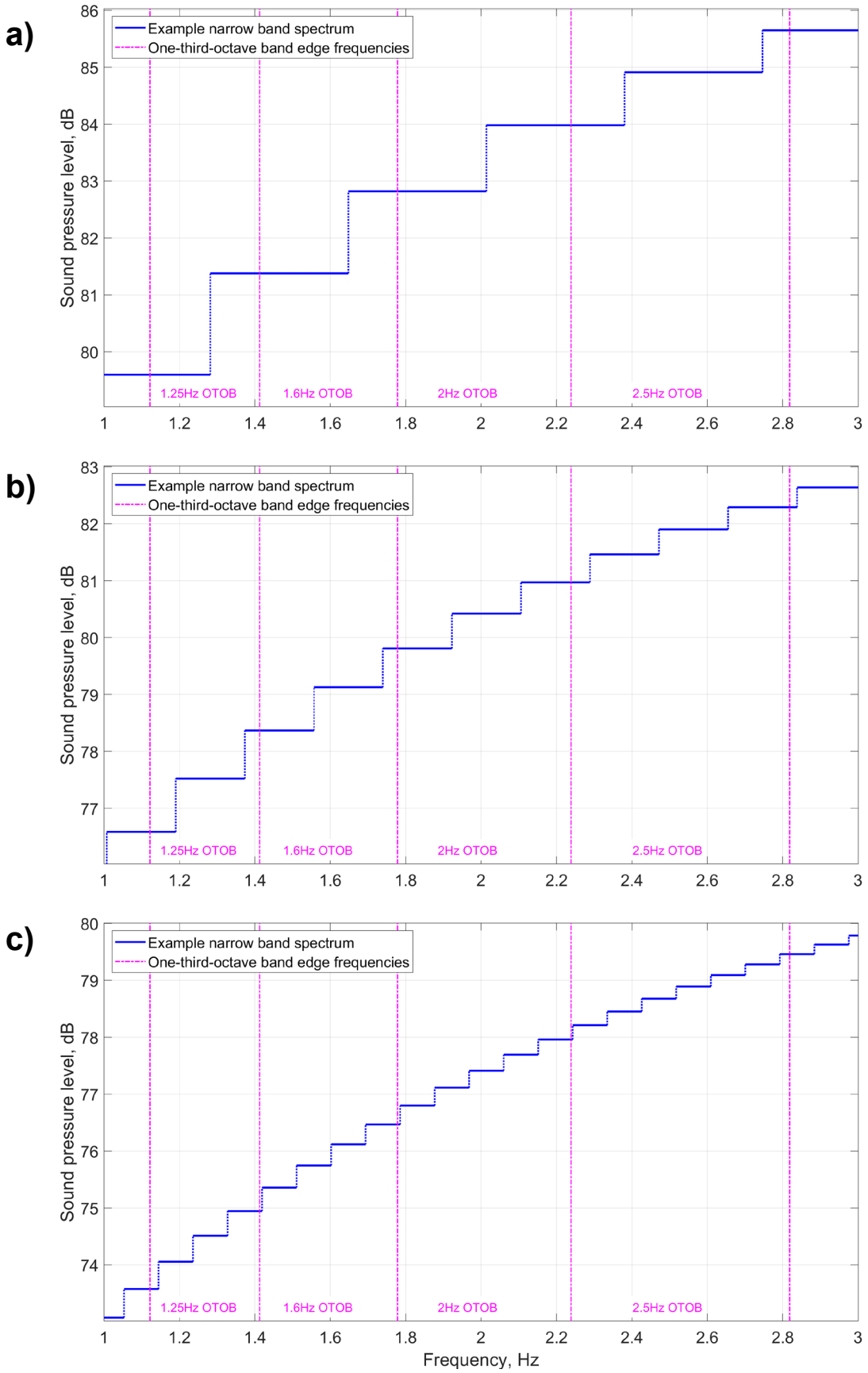

Figure A2.3: Example sections of narrow band spectra (blue curves) for different durations of zero padding as compared to the low frequency one-third-octave band edges (vertical magenta lines); for waveform total durations (zero padded) of a) 2.731 s, b) 5.461 s, and c) 10.92 s.

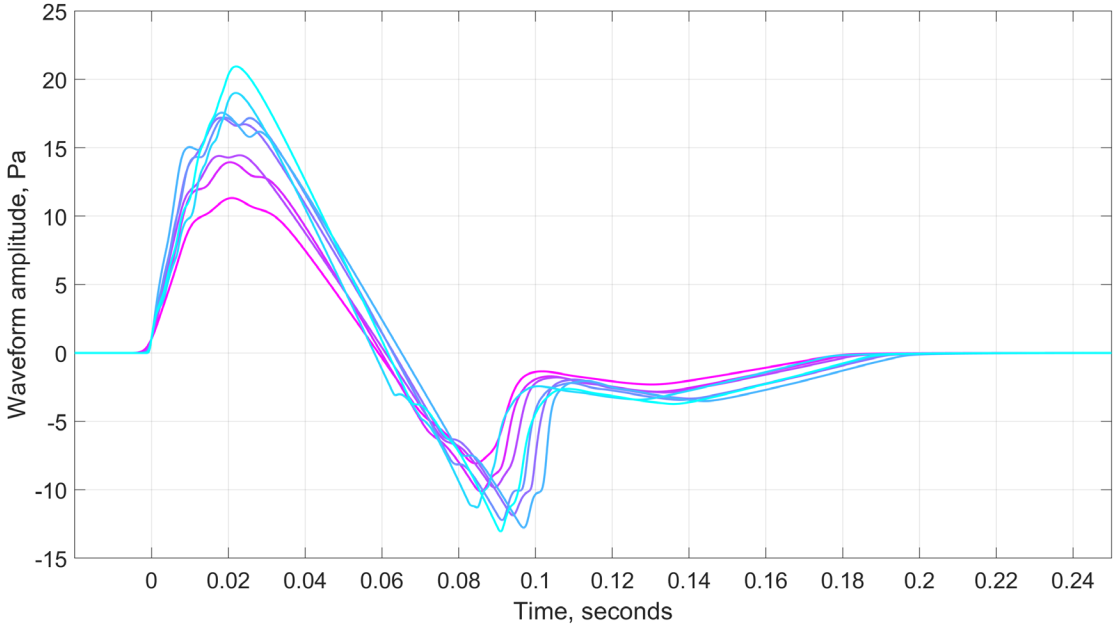

Figure A2.4: Eight example shaped sonic boom waveforms from the set of 3,000 waveforms that were used to study the effects on level error of zero padding duration.

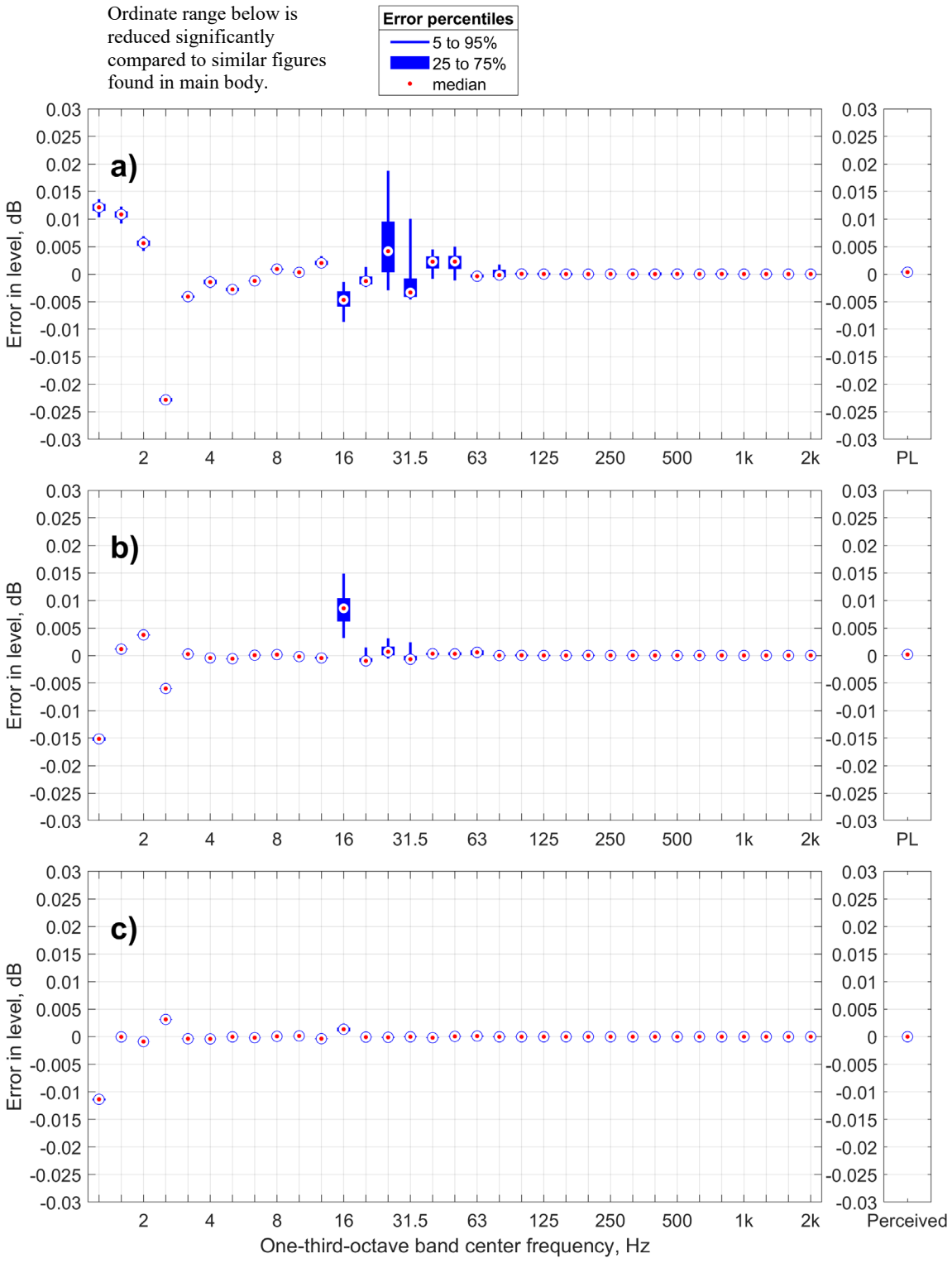

Figure A2.5: Error distributions for one-third-octave band levels (left-hand subplots) and the PL noise metric (right-hand subplots) across 3,000 X-59 waveforms when using the narrow band summation method; for waveform durations (zero padded) of a) 2.731 s, b) 5.461 s, and c) 10.92 s; and relative to values with a duration of 21.85 s.

Table A2.1: Tabulated 5th, 50th, and 95th percentiles of error in PL for the data shown in Figure A2.1 (the right-hand subplots) when using the narrow band summation method.

Total signal duration, s	**Number of signals**	**5th percentile error PL, dB**	**50th percentile error PL, dB**	**95th percentile error PL, dB**
2.731	3000	0.00017	0.00034	0.00107
5.461	3000	9.16E-05	0.00018	0.00040
10.92	3000	-3.05E-05	7.63E-06	3.81E-05

This page intentionally left blank.